

EVALUATION OF CRACKING RESISTANCE OF SUPERPAVE MIXTURES IN KANSAS

by

SYEDA RUBAIYAT AZIZ

B.S., Bangladesh University of Engineering and Technology, 2009

A THESIS

submitted in partial fulfillment of the requirements for the degree

MASTER OF SCIENCE

Department of Civil Engineering
College of Engineering

KANSAS STATE UNIVERSITY
Manhattan, Kansas

2013

Approved by:

Major Professor
Dr. Mustaque Hossain

Abstract

Reclaimed Asphalt Pavement (RAP) is a useful alternative to virgin aggregates in hot-mix asphalt (HMA) as it reduces cost, conserves energy, and enables reuse of existing asphalt pavement. However, use of higher percentage of RAP sometimes leads to drier mixes that are often susceptible to early cracking. In this study, cracking resistance of Superpave mixtures with varying asphalt and RAP contents were investigated. HMA specimens were prepared based on Superpave mix design criteria for 12.5-mm (1/2-inch) nominal maximum aggregate size (NMAS). Specimens were compacted using the Superpave gyratory compactor. Static and repeated semi-circular bending (SCB) tests and Texas overlay tests (OT) (TEX-248-F) were performed in order to evaluate cracking resistance of Superpave mixtures containing three different asphalt contents (5.2%, 4.9%, and 4.6%) and three RAP percentages (20%, 30%, and 40%) from two distinct sources. Results from both crack tests showed that, with decreased asphalt content, cracking propensity increases. In general, higher percentage of RAP decreases cracking resistance. Statistical analysis of the results indicated a strong positive correlation between the asphalt film thickness and the number of load cycles before failure. Comparison of mean test results suggested that the Texas overlay test could do better evaluation of cracking resistance than the R-SCB test. This study was limited to mixtures with two sources of RAP. Because of such limitations and conflicting results from these RAP sources, a general conclusion regarding the minimum binder and maximum RAP contents without compromising cracking resistance could not be made. However, separate conclusions were drawn depending upon the characteristics of the RAP source.

Table of Contents

List of Figures	v
List of Tables	vii
Acknowledgements	x
Dedication.....	xi
Chapter 1 - Introduction	1
1.1 Background.....	1
1.2 Problem Statement	2
1.3 Objectives	2
1.4 Organization of Thesis.....	3
Chapter 2 - Literature Review	4
2.1 Cracking Resistance Tests	4
2.1.1 Semi-Circular Bending (SCB) Test	4
2.1.1.1 Static Semi-Circular Bending (SCB) Test.....	5
2.1.1.2 Repeated SCB Test	6
2.1.2 Texas Overlay (OT) Test	9
2.1.3 Indirect Tension (IDT) Test	11
2.1.4 Direct Tension (DT) Test.....	14
2.1.5 Fénix Test.....	15
2.2 Superpave.....	16
2.3 Durability of HMA	17
2.4 Effects of Mixture Aging.....	18
2.5 Effects of Varying Asphalt Content	19
2.6 Voids in Mineral Aggregate (VMA)	19
2.7 Asphalt Film Thickness	20
2.8 Effect of Reclaimed Asphalt Pavement (RAP) in HMA.....	21
2.8.1 Obstacles in using High RAP contents in HMA	22
2.8.2 Mix Design Consideration for RAP.....	22
2.8.3 Performance of Mixtures with RAP	23
2.9 Summary.....	24

Chapter 3 - Methodology	26
3.1 Virgin Aggregates, RAP and Binder	26
3.2 Gradation and Aggregate Blending	26
3.3 Test Specimen Preparation for Cracking Resistance Tests	31
3.3.1 Mixing and Compaction.....	31
3.3.2 Determination of Air Void of Specimen by G_{mm} and G_{mb} Test	33
3.3.2.1 G_{mm} Test Procedure	33
3.3.2.2 G_{mb} Test Procedure	35
3.4 Cracking Resistance Test Procedures.....	36
3.4.1 Semi-Circular Bending (SCB) Test	36
3.4.1.1 Static SCB Test.....	37
3.4.1.2 Repeated SCB Test	38
3.4.2 Texas Overlay (OT) Test	40
Chapter 4 - Analysis and Results	44
4.1 SCB Test Results.....	44
4.1.1 Static SCB Test Results	44
4.1.2 Repetitive SCB Test Results	47
4.1.3 Crack Initiation and Propagation Investigation.....	54
4.2 Texas Overlay (OT) Test Results.....	60
4.3 Statistical Analysis	62
4.3.1 Correlation Analysis	62
4.3.2 Comparison between Means	82
Chapter 5 - Conclusions and Recommendations	90
5.1 Conclusions.....	90
5.2 Recommendations	91
References	93
Appendix A - Volumetric Properties and Cracking Test Results	99

List of Figures

Figure 1.1 (a) Typical RAP stockpile (www.pavementinteractive.org) (b) RAP (www.wjgraves.com).....	2
Figure 2.1 SCB test configuration	5
Figure 2.2 Texas overlay test specimen inside AMPT jig	10
Figure 2.3 IDT test setup (Wen, 2003).....	13
Figure 2.4 Demonstration of DT failure modes (Walubita et al., 2010).....	14
Figure 2.5 Test setup of Fénix test (Pérez et al., 2010).....	16
Figure 3.1 0.45 power gradation chart for SM-12.5A mixture.....	28
Figure 3.2 0.45 power gradation chart for SR-12.5A mixture with first source of RAP	30
Figure 3.3 0.45 power gradation chart for SR-12.5A mixture with second source of RAP	30
Figure 3.4 (a) Mixing of aggregates with binder in mixer; (b) HMA mixture undergoing short- term aging in oven.....	32
Figure 3.5 (a) SGC mold with loose HMA inside; (b) Specimen being compacted in SGC; (c) Final compacted specimen.....	33
Figure 3.6 (a) Loose HMA inside flask filled with water; (b) Trapped air taken out by vacuum application; (c) Weight of loose specimen in water being taken	34
Figure 3.7 (a) Weight of dry compacted specimen being taken; (b) Specimen submerged in water; (c) Wet specimen rolled out in damp towel	36
Figure 3.8 SCB test setup	37
Figure 3.9 A typical SCB specimen after fracture failure	38
Figure 3.10 R-SCB test process.....	39
Figure 3.11 SCB test setup with clip-on gauge	40
Figure 3.12 Trimming of OT specimen (Tex-248-F)	41
Figure 3.13 Glued OT specimen on metal base plates.....	42
Figure 3.14 Typical OT test setup within AMPT	42
Figure 3.15 OT testing process.....	43
Figure 4.1 Stress-displacement curve for SM-12.5A mixture.....	46
Figure 4.2 Stress-displacement curve for SR-12.5A mixture with first source of RAP	46
Figure 4.3 Stress-displacement curve for SR-12.5A mixture with second source of RAP.....	47

Figure 4.4 R-SCB percent load relationship curve for SM-12.5A	49
Figure 4.5 R-SCB percent load relationship curve for SR-12.5A with first source of RAP.....	51
Figure 4.6 R-SCB percent load relationship curve for SR-12.5A with second source of RAP	53
Figure 4.7 Crack length against number of load repetitions for SM-12.5A mixture.....	55
Figure 4.8 Crack length against number of load repetitions for SR-12.5A mixture (first source of RAP)	56
Figure 4.9 Crack length against number of load repetitions for SR-12.5A mixture (second source of RAP).....	57
Figure 4.10 Comparison of estimated N_i and predicted N_i	59
Figure 4.11 Scatter plot matrix for SM-12.5A mix (R-SCB test)	64
Figure 4.12 Scatter plot matrix for SR-12.5A mix with first source of RAP (R-SCB test).....	67
Figure 4.13 Scatter plot matrix for SR-12.5A mix for second source of RAP (R-SCB test).....	70
Figure 4.14 Scatter plot matrix for SM-12.5A mix (OT test)	72
Figure 4.15 Scatter plot matrix for SR-12.5A mix with first source of RAP (OT test).....	75
Figure 4.16 Scatter plot matrix for SR-12.5A mix with second source of RAP (OT test)	78
Figure 4.17 Normal probability plots for R-SCB test outputs.....	83
Figure 4.18 Normal probability plots for OT test outputs.....	84
Figure 4.19 R-SCB test results with 95% confidence intervals.....	87
Figure 4.20 OT test results with 95% confidence intervals.....	88

List of Tables

Table 2.1 Current VMA requirements given by KDOT	20
Table 3.1 Aggregate gradation	27
Table 3.2 Percentages of aggregates in SM-12.5A mixtures	27
Table 3.3 Aggregate blending for SM-12.5A mixture with KDOT requirements	28
Table 3.4 Percentages of aggregates and asphalt in SR-12.5A mixtures.....	29
Table 3.5 Aggregate blending for SR-12.5A mixture with KDOT requirements	29
Table 3.6 Compaction parameters for SGC	32
Table 4.1 Average static SCB test results	45
Table 4.2 R-SCB test results for SM-12.5A mixture.....	48
Table 4.3 Comparative cracking resistance improvement with increasing asphalt content.....	49
Table 4.4 R-SCB test results for SR-12.5A mixture with first source of RAP	50
Table 4.5 Comparative cracking resistance improvement with increasing RAP content (first RAP Source).....	51
Table 4.6 R-SCB test results for SR-12.5A mixture with second source of RAP.....	52
Table 4.7 Comparative cracking resistance improvement with increasing RAP content (second RAP Source)	53
Table 4.8 Crack lengths and stress intensity factors of mixtures	54
Table 4.9 Number of load repetitions for crack initiation.....	58
Table 4.10 Average OT test results for SM-12.5A mixture	60
Table 4.11 Average OT test results for SR-12.5A mixture for first source of RAP.....	61
Table 4.12 Average OT test results for SR-12.5A mixture for second source of RAP	61
Table 4.13 Interpretation of correlation (Mendenhall, and Sincich, 2003).....	62
Table 4.14 Correlation matrix for SM-12.5A mixture (R-SCB test).....	63
Table 4.15 Correlation matrix for SR-12.5A mixture with first RAP source (R-SCB test)	65
Table 4.16 Correlation matrix for SR-12.5A mixture with second RAP source (R-SCB test).....	68
Table 4.17 Correlation matrix for SM-12.5A mixture (OT test).....	71
Table 4.18 Correlation matrix for SR-12.5A mixture with first RAP source (OT test)	73
Table 4.19 Correlation matrix for SR-12.5A mixture with second RAP source (OT test).....	76
Table 4.20 Summary of correlation analysis of R-SCB test results (SM-12.5A mixture).....	79

Table 4.21 Summary of correlation analysis of OT test results (SM-12.5A mixture).....	79
Table 4.22 Summary of correlation analysis of R-SCB test results (SR-12.5A mixture)	80
Table 4.23 Summary of correlation analysis of OT test results (SR-12.5A mixture)	81
Table 4.24 Normality test results of R-SCB test outputs	82
Table 4.25 Summary of Tukey’s multiple comparisons (R-SCB test)	83
Table 4.26 Normality test results of OT test outputs	84
Table 4.27 Summary of Tukey’s multiple comparisons (OT Test)	85
Table 4.28 Summary of Bonferroni method comparisons (R-SCB test)	86
Table 4.29 Summary of Bonferroni method comparisons (OT test)	88
Table 4.30 Virgin asphalt as a percentage of total asphalt content for both sources of RAP	89
Table A.1 R-SCB test results for SM-12.5A (5.2% asphalt content)	99
Table A.2 R-SCB test results for SM-12.5A (4.9% asphalt content)	99
Table A.3 R-SCB test results for SM-12.5A (4.6% asphalt content)	100
Table A.4 R-SCB test results for SR-12.5A (20% RAP content from first RAP source)	100
Table A.5 R-SCB test results for SR-12.5A (30% RAP content from first RAP source)	101
Table A.6 R-SCB test results for SR-12.5A (40% RAP content from first RAP source)	101
Table A.7 R-SCB test results for SR-12.5A (20% RAP content from second RAP source)	102
Table A.8 R-SCB test results for SR-12.5A (30% RAP content from second RAP source)	102
Table A.9 R-SCB test results for SR-12.5A (40% RAP content from second RAP source)	103
Table A.10 Volumetric properties of R-SCB test specimens (SM-12.5A)	103
Table A.11 Volumetric properties of R-SCB test specimens (SR-12.5A, first source of RAP)	104
Table A.12 Volumetric properties of R-SCB test specimens (SR-12.5A, second source of RAP)	104
Table A.13 OT test results for SM-12.5A	105
Table A.14 Volumetric properties of OT test specimens (SM-12.5A)	105
Table A.15 OT test results for SR-12.5A (first source of RAP)	106
Table A.16 Volumetric properties of OT test specimens (SR-12.5A, first source of RAP)	106
Table A.17 OT test results for SR-12.5A (second source of RAP)	107
Table A.18 Volumetric properties of OT test specimens (SR-12.5A, second source of RAP)	107
Table A.19 Tukey's multiple comparison of R-SCB test results	108
Table A.20 Bonferroni's pairwise comparison of R-SCB test results	109

Table A.21 Tukey's multiple comparison of OT test results	110
Table A.22 Bonferroni's pairwise comparison of OT test results.....	111

Acknowledgements

First, I would like to pay my utmost respect to Almighty Allah for granting me this wonderful opportunity to work and to live.

I hereby acknowledge my sincere appreciation and due gratitude to my major professor Dr. Mustaque Hossain for academic guidance, mentorship, and continuous encouragement throughout my graduate studies.

I would like to thank Dr. Robert W. Stokes and Dr. Sunanda Dissanayake for being part of my thesis committee and for their encouragement.

I sincerely appreciate the financial support provided by the Kansas Department of Transportation (KDOT) for this unique research study.

I gratefully thank Ryan Benteman, Brandon Bortz, Nassim Sabahfar, Daniel Mealiff, Alex Wu, Andrew Brunner and Andrew Wiederholt for their help regarding specimen preparation and test set-up fabrication. I also appreciate on-time help provided by Mr. Adam O' Neill from Instrotek and Mr. Steve King (IPC Global- Australia) regarding the test process.

Finally, I wish to express my sincere respect and gratitude to my parents for their understanding, blessings, and love that helped me to be what I am today. I would like to especially thank my husband for his patience, support, and appreciation.

Dedication

This thesis is dedicated to my parents, Dr. Syed Azizul Haque and Dr. Nilufar Begum, my younger brother, Syed Reefat Aziz, and my husband, S M Shafiul Alam.

Chapter 1 - Introduction

1.1 Background

Durability of an asphalt mixture is a prerequisite for durable asphalt pavement. Asphalt durability is determined in terms of its performance in service life. Traffic and climate are two key factors determining the duration until when asphalt pavement can maintain a serviceable condition. Initially, the design of asphalt pavements was solely based on future traffic load; however, more emphasis is currently given to environment or climate.

Currently, approximately 94% of the highway network pavements in the United States are asphalt surfaced (flexible pavements), while the rest are either concrete or composite pavements (concrete pavements overlaid with asphalt) (FHWA, 2008). About 89% of the total paved-road network in Kansas is asphalt surfaced. Common pavement distresses on asphalt pavements can be partially mitigated by proper selection of construction materials and by developing suitable mix design. According to the National Asphalt Pavement Association (NAPA), approximately 4,000 asphalt plants exist in the United States, which produce 500 to 550 million tons of asphalt pavement materials worth more than \$30 billion annually (NAPA, 2013). These materials include large quantities of reclaimed asphalt pavement (RAP).

Recent rise in crude oil price, emphasis on sustainability, and limited virgin aggregate availability have increased RAP materials usage. Nationwide, approximately 100 million tons of RAP are produced each year. Approximately 80 million tons are reused in various aspects of pavement construction (MAPA, 2010). RAP contains long-term aged binder, thus asphalt mixes containing RAP could be a matter of concern, especially for durability and long-term pavement performance. Asphalt binder present in RAP is stiffer than the virgin binder. Stiffer mix has benefits, such as being less susceptible to permanent deformation or rutting. However, it decreases fatigue and thermal cracking resistance. There is a limitation to the maximum amount of RAP that could be used in surface layers, certain mixture types, and, in some instances, large or critical projects. Traditionally, the amount of RAP used has been limited to 15 percent or lower if no binder-grade changes are necessary. Current national guidelines indicate that a softer binder will be required if more than 15% RAP is used in the HMA mix (AASHTO M 323). Softer binders are expensive, however. Henceforth, it is necessary to come up with a certain

percentage of RAP which would be cost effective as well as provide sufficient cracking resistance.



(a)

(b)

Figure 1.1 (a) Typical RAP stockpile (www.pavementinteractive.org) (b) RAP (www.wjgraves.com)

1.2 Problem Statement

Some Superpave hot-mix asphalt (HMA) mixtures currently used in Kansas are found to be susceptible to moisture damage. Kansas standard test method, KT-56, measures this moisture susceptibility. Again, some mixtures are produced with asphalt content lower than the design asphalt content. As a result, relatively “drier” mixture is obtained, often leading to early cracking. This type of phenomena is severe for mixtures with recycled asphalt pavement (RAP). Recently, the Kansas Department of Transportation (KDOT) took some initiatives to ensure sufficient amount of asphalt in their mixtures. The contractors, however, instead of adding extra binder, introduced dust into the mixtures for lower N_{design} Superpave mixtures. The rutting and moisture susceptibility of mixtures with lower binder content have already been investigated, but cracking resistance is yet to be evaluated.

1.3 Objectives

The main objectives of this study were:

- a) Evaluate varying asphalt content on cracking resistance of Superpave mixtures;
- b) Evaluate the effect of varying RAP content on cracking resistance of Superpave mixtures;
- c) Evaluate the effect of RAP source on the cracking resistance; and

- d) Establish the minimum asphalt content and maximum RAP content while ensuring cracking resistance.

1.4 Organization of Thesis

This thesis consists of five chapters. Chapter 1 presents a brief introduction, problem statement, research objective, and thesis outline. Chapter 2 provides an overview of cracking resistance tests and related research work followed by a literature review on the relationship of the mixture durability with the voids in mineral aggregate (VMA) and asphalt film thickness. In addition, the effect of RAP on mixture performance has been discussed. Chapter 3 describes the materials used in this research as well as test procedures. Chapter 4 discusses the results obtained from the semi-circular bending (SCB) and Texas overlay (OT) tests, followed by statistical analysis. Chapter 5 presents conclusions from this project and recommendations for future research.

Chapter 2 - Literature Review

An extensive search was conducted to gather information about available cracking resistance tests for hot-mix asphalt (HMA) currently in use. In addition, a brief background on the Superpave mix design and aspects related to the durability of hot mix asphalt (HMA) are presented in the later part of this chapter.

2.1 Cracking Resistance Tests

In HMA pavements, cracking is considered as one of the prevailing distresses. Currently, no standardized laboratory cracking tests have been widely accepted for routine mix design or screening for HMA cracking potential (Walubita et al., 2010). Generally, durability and rutting are considered as the primary factors of any acceptable mix design. Still, a simple and practical cracking test is necessary, which could be frequently conducted in the laboratory and would identify whether the mixture is prone to early cracking. Indirect tension test (IDT), direct tension test (DT), Fénix test, semi-circular bending (SCB), and Texas overlay (OT) tests are the most commonly used cracking resistance tests.

In this study, semi-circular bending (SCB) and Texas overlay (OT) tests were selected to evaluate the cracking resistance of Superpave mixtures.

2.1.1 Semi-Circular Bending (SCB) Test

Chong and Kuruppu (1984) were the first group of researchers who used the SCB test for fracture testing of rock materials. For HMA, the test is conducted on a half disc-shaped specimen; typically 6 inches in diameter and 2 inches thick. The specimen is subjected to a three-point loading in compression. Using the Superpave gyratory compactor, 4-inch tall samples are prepared. The air void content of test specimen is $7 \pm 1\%$. Thus, from each sample, four SCB test specimens are obtained. The test configuration is shown in Figure 2.1. The SCB test specimen sits on two roller supports, spaced at a distance of 0.8 times the specimen diameter. Based on successful experimentation by various researchers, 0.05 inch/minute has been selected as the loading rate for statically or monotonically loaded SCB test.

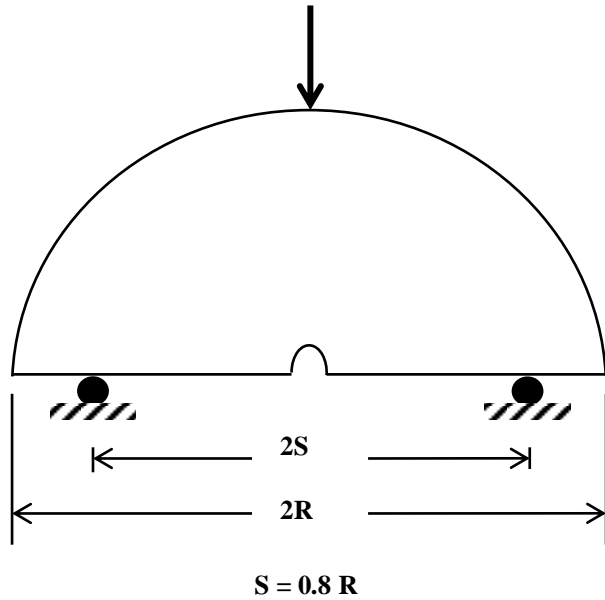


Figure 2.1 SCB test configuration

Specimen fabrication and preparation for the SCB test is simple and quick. A notch is cut at the base of the specimen to ensure that the crack initiates at the center of the specimen. Test temperatures considered for several SCB test studies typically range between 50°F (Huang et al., 2009) and 77°F (Walubita et al., 2010).

2.1.1.1 Static Semi-Circular Bending (SCB) Test

The loading configuration for static or monotonically loaded SCB test is straightforward. Static load at a rate of 0.05 inch/min is applied until the specimen fails at 77°F . SCB tensile stress is directly measured in the specimen. Vertical ram displacement and stress at the maximum load (failure point) are used as measures of HMA ductility and crack-resistance potential, respectively. From the test data, stress occurring in a notched specimen is determined as follows:

$$S_T = \frac{4.263 \times P}{D \times T} \quad (2.1)$$

Where, S_T = Tensile stress, (MPa);

P = Axial load, (N);

t = Specimen thickness, (mm); and

D = Specimen diameter, (mm).

2.1.1.2 Repeated SCB Test

Repeated SCB (R-SCB) Test is a two-step process involving the establishment of input loads via monotonic or static SCB testing and the use of a fraction of maximum SCB failure load as the R-SCB input load. Repeated load of 10 Hz frequency with no rest period is applied to the specimen at 77⁰ F. The cracking resistance potential of a mix under this test setup is characterized by the number of SCB load repetitions to cracking failure, where failure is tentatively considered as full crack propagation through the HMA specimen. R-SCB test shows greater potential for use than its monotonic counterpart, in characterizing the cracking resistance of HMA mixes.

The compressive load is applied vertically at the top of the specimen in such a manner as to produce constant crack mouth opening displacement (CMOD) rate. CMOD is measured at the bottom of the specimen using a clip-on gauge. Wells (1961) pioneered the introduction of CMOD. Crack extension takes place when material at the crack mouth attains maximum allowable strain. One limitation of this concept is that fracture strength cannot be calculated directly. Due to application of repeated loads, cracks will grow with time. As a crack becomes longer, higher stress concentration is induced, indicating that the crack propagation rate is dependent on time (Broek, 1987).

Load line displacement (LLD) is measured using a vertically-mounted extensometer attached to the bottom of the specimen, supported by a pair of metal blades. From the measured CMOD, crack length and stress intensity factor are calculated. Crack length is calculated from the relationship, shown in equation 2.2. This relationship was obtained by the finite element analysis method (FEM) conducted by van Rooijen and de Bondt (2008):

$$\left(\frac{c}{h}\right) = 0.1642 \times \log_e \left(\frac{CMOD_N}{CMOD_{(N=1)}}\right) + 0.1413 \quad (2.2)$$

Where, c = Length of crack, (mm);

h = Maximum length of crack (height of SCB specimen \approx 1/2 diameter);

$CMOD_{(N=1)}$ = CMOD at the beginning of the test; and

$CMOD_N$ = CMOD after N load cycles.

The stress intensity factor provides an estimate of the stress-strain scenario at the mouth of the crack. It is linearly dependent on the applied stress and is a function of the geometry of the structure and crack length (Mobasher et al., 1997). Stress intensity factor is related to available

energy for crack propagation by unit length and it is calculated from the relationship shown in equation 2.3 (CROW, 2006):

$$K_I = \sigma_{SCB} \times f\left(\frac{c}{h}\right) \quad (2.3)$$

The stress level σ_{SCB} is calculated by (CROW, 2006):

$$\sigma_{SCB} = \frac{4.263 \times F_{(SCB, N=1)}}{I_{SCB} \times t_{SCB}} \quad (2.4)$$

Where, $F_{(SCB, N=1)} = (F_{max} - F_{min})$ at the beginning of the test, (N);

I_{SCB} = Length of the specimen, (mm); and

t_{SCB} = Thickness of the specimen, (mm).

$f\left(\frac{c}{h}\right)$ is a geometry factor determined by the FEM analysis. For the SCB test, the geometry factor was found to be (CROW, 2006):

$$f\left(\frac{c}{h}\right) = 1398.6 \cdot \left(\frac{c}{h}\right)^5 - 2709.1 \cdot \left(\frac{c}{h}\right)^4 + 2141.9 \cdot \left(\frac{c}{h}\right)^3 - 799.94 \cdot \left(\frac{c}{h}\right)^2 + 155.58 \cdot \left(\frac{c}{h}\right) - 4.9965 \quad (2.5)$$

On the basis of micro-fracture model, the number of load repetitions required for crack initiation was determined by a past study conducted by Lytton et al. (1993). The relationship was derived using regression analysis and is given in equation 2.6 (Lytton et al., 1993).

$$\log_{10} N_i = b_0 + b_1 + b_2 \sigma_m + b_3 \{(\sigma_m)^2\} * E + (b_4 \log_{10} \sigma_m + b_5 \log_{10} E) (\% AC) \\ + \{[b_6 (\sigma_m)^2] / E + b_7 \log_{10} \sigma_m\} (\% Air) + \{b_8 (\sigma_m / E) + b_9 \log_{10} \sigma_m\} (\sigma_m / E) \quad (2.6)$$

Where, N_i = Number of load cycles to crack initiation;

σ_m = Mean stress, (psi);

E = Asphalt concrete modulus, (psi);

% AC = Asphalt content by weight percent, (%);

% Air = Air voids content, (%);

$b_0 = 4.415936$;

$b_1 = -5.421 \times 10^{-6}$;

$b_2 = 1.11 \times 10^{-7}$;

$b_3 = -8.51796 \times 10^{-11}$;

$$b_4 = -0.838837;$$

$$b_5 = 0.314813;$$

$$b_6 = 3.089278;$$

$$b_7 = -0.114846;$$

$$b_8 = 35,787,201; \text{ and}$$

$$b_9 = -12,144.$$

Among many factors affecting crack propagation, the most critical ones are thickness of the specimen, type of materials (aggregate and asphalt binder) used, temperature, topographic location, batch-to-batch variation, and environment. The influence of surrounding environment is the most unpredictable factor (Broek, 1987).

SCB test was investigated by many researchers. Li and Marasteanu (2004) studied SCB test as a candidate for low-temperature cracking. Based on the fracture energy, a split-plot analysis was performed and results showed that the binder type effect was significant.

Van Rooijan and de Bondt (2008) performed cyclic SCB on notched specimens at relatively low temperature. The duration of crack propagation was relatively short for different binders. The authors commented that crack propagation duration could be improved by a shorter notch length (approximately 5 mm). They could not obtain any correlation among parameters from the asphalt mixture testing. They recommended using a finer and more binder-rich asphalt mixture for comparing binder performance.

According to Wu et al. (2005), no fracture resistance parameter (vertical displacement or peak load) was able to correctly rank fracture resistance of various HMA mixes in a consistent order. However, the fracture resistance was consistent with that based on vertical displacement but was different from fracture resistance based on peak load.

Mull et al. (2002) investigated the fracture resistance of chemically modified crumb rubber asphalt (CMCRA) mixture. They used the J-integral concept and monotonic loaded SCB test procedure. Test specimens were 6 inches in diameter and 2.5 inches thick and had notches of various depths. Results were compared to crumb rubber asphalt (CRA) mixture and a control mixture. The study concluded that CMCRA had better cohesion to binder and strong adhesion to aggregates compared to other asphalt mixtures. CRA mixture showed a slightly higher fracture resistance than the control mixture. However, Scanning Electron Microscopic examination of the

fracture surface of each mixture proved that CMCRA mixture had significantly higher fracture resistance in comparison to the control mixture.

Krans et al. (1996) compared SCB test results to that of obtained from the bending beams test, indirect tensile test (IDT), and direct tensile test (DT). They described SCB test as an easy, simple test which also ensures stable crack growth. When compared to the IDT test, smaller loads can be chosen and undesirable effect or local failure near load was prevented by the SCB test. No gluing is needed and more stable crack propagation is ensured by the SCB test.

Walubita et al. (2010) concluded that repeated load SCB test shows the most promise among available surrogate cracking tests. They performed DT, OT, static, and repeated IDT and static and repeated SCB test. Among these tests, the repeated IDT and OT were considered second and third best, respectively. They suggested a few SCB test improvements, including the development of the repeated SCB test protocol, determination of appropriate failure criterion, and correlation of laboratory performance with field performance. The only drawback of the SCB test identified was the requirement of a Universal Testing Machine, which may be a hindrance, especially for large-scale application.

2.1.2 Texas Overlay (OT) Test

Texas Overlay Tester (OT) test pervasively has been used in many Texas Department of Transportation (TxDOT) mix designs for mix screening and as an indicator of cracking (reflective) resistance for HMA overlays. TEX-248-F is the standard test procedure for the OT test. Past research showed that OT test results indicated strong correlation with field performance (Von Holdt, and Scullion, 2005). Thus, OT test results were used as the standard for comparative evaluation of test duration, repeatability, and the ability to predict cracking resistance of other test methods.

Generally, the OT test is run at a fixed opening displacement of 0.025 inch and with a cyclic triangular loading rate of one cycle per 10 seconds (5 seconds to open, 5 seconds to close) and is typically run at 77⁰ F (Zhou et al., 2007). The specimen is 6 inches long, 3 inches wide and 1.5 inches thick. The specimen is prepared by cutting the Superpave gyratory compacted sample. Final air void content of the test specimen is $7 \pm 1\%$. This test can be performed in the Asphalt Mixture Performance Tester (AMPT), and load, displacement, and temperature are recorded automatically during the test. OT test specimens require gluing which is why a relatively long

time lag, approximately two days, exist between specimen fabrication and actual testing due to gluing and curing processes. This processing time makes the OT test unfavorable for routine application. Figure 2.2 illustrates OT test specimen inside the AMPT jig.



Figure 2.2 Texas overlay test specimen inside AMPT jig

In general, OT specimen is tested until the initial load decreases by 93 percent. The number of cycles to this load reduction constitutes the number of cycles to failure and is indicative of the HMA mix cracking resistance. Zhou et al. (2007) recommends tentative failure criterion of 300 cycles (minimum) for dense-graded mixes and 750 cycles (minimum) for the crack attenuating mixes (CAM). Therefore, a straightforward comparison can be made between a better and poor crack-resistant mixture by simply analyzing the number of cycles to OT failure. The test is terminated when 93% load reduction or 1,000 cycles, whichever occurs first. As a tentative mix screening criteria, mixes that last over 300 cycles are considered satisfactory with respect to laboratory cracking resistance. The sample molding height is 4.5 inches, while the

final OT test specimen is only 1.5 inches thick. Thus, larger mixing batches are required, which is material and labor intensive. Field cores can be tested without any difficulty using OT test. However, previous research indicated that this test had variability and repeatability issues (Walubita et al., 2010). Under these circumstances, the coefficient of variation (COV) of up to 30 percent is considered as an acceptable level of variability for the OT test.

Zhou et al. (2007) claimed that OT test correlates well with field performance. The test is simple, practical, and easy to test field cores. However, the variability and repeatability of OT is a matter of concern as the COV for the number of OT cycles of failure often exceeds the limiting value (less or equal 30%).

Hu et al. (2011) identified the most significant factors affecting cracking performance by performing OT and establishing corresponding cracking performance prediction models. The number of cycles to failure (N_{OT}) of each sample was determined from 93% reduction of maximum load recorded during the first cycle. They also prepared N_{OT} prediction models which yielded very high coefficient of determination ($R^2 \approx 0.9$). Using these models, the authors recommended minimum asphalt content during mix design.

In a recent study conducted by Walubita et al. (2013), fracture energy (FE) index was explored to characterize and differentiate the cracking resistance potential of HMA. They performed OT under monotonic tensile loading rate of 0.123 inch/min in the laboratory at room temperature. After evaluating a few commonly used HMA mixtures in Texas, it was concluded that FE index has the potential to be used as a fracture parameter. It also can be used to discriminate and rank the cracking resistance potential of HMAs in the laboratory. However, this concept requires further investigation with more mixes and validation with field data for subsequent consideration in routine use.

2.1.3 Indirect Tension (IDT) Test

The indirect tension test (IDT) has been used to characterize properties of HMA for more than 30 years and has shown the potential for accurately predicting cracking resistance properties of HMA mixes (Walubita et al., 2002). A typical IDT setup requires a servo-hydraulic closed-loop testing machine capable of axial compression (Huang et al., 2005). According to standard test specifications given in Tex-226-F, AASHTO T283, and ASTM D6931, the loading rate of 2 inch/min is typically used. Test temperatures range from -4° F to 77° F. According to Ruth et al.

(2002), the horizontal tensile strength at the center of the specimen is sensitive to aggregate gradation; however, tensile strength can be determined accurately only below 59⁰ F. The specimen is diametrically loaded in compression, thus indirectly inducing horizontal tensile stresses in the middle zone of the specimen which ultimately cause fracture. Figure 2.3 shows a typical IDT test setup. In order to evaluate the tensile properties of HMA mixes, the permanent deformation under the loading strip is undesirable (Kim and Wen, 2002). Therefore, the compressive load was distributed using loading strips which are curved at the interface to fit the radius of curvature of the specimen.

The fracture energy of the IDT specimen is calculated using the vertical strain at the center of the specimen, determined from the displacements with a 2-inch gauge length using linear viscoelastic solutions. However, past research indicated that the gauge length of the linear variable displacement transducers (LVDTs) used in IDT setup may cause some difficulties (Kim and Wen, 2002). If the length is too short, then it can affect displacement measurements between gauge points, specifically if large aggregates exist in the middle of the specimen (for coarse-graded mixes). Thus, special caution is required to avoid these potential problems and account for them in subsequent data analysis and interpretation of results. The IDT test data includes time, applied load, and horizontal and vertical specimen deformation.

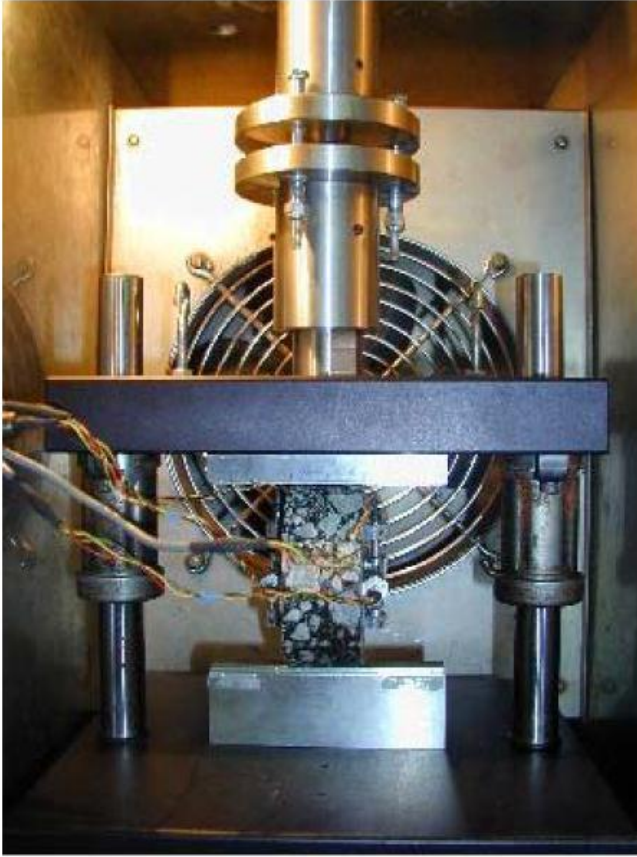


Figure 2.3 IDT test setup (Wen, 2003)

One disadvantage of the IDT test is the existence of a biaxial stress state (Matthews et al., 1993). The stress field in the IDT specimen is complex, and the failure mode of the IDT specimen is a combination of tension, compression, and shear. In fact, if the compressive strength of the tested mixture is less than three times its tensile strength, the crack may be initiated by compression rather than in tension (Matthews et al., 1993). Compressive failure is undesirable, because the tensile properties are commonly used to predict fracture resistance. Similarly, high stress concentration at the supports (upper and lower) may cause local and thus, total specimen failure. The combined effect of these stress complexities causes analysis problems and raises questions as to the accuracy of IDT results. Therefore, more accurate IDT analysis models still need to be developed. However, Texas Department of Transportation (TxDOT) continues to apply the IDT test for comparative HMA mixture evaluation and screening for fracture resistance. According to Walubita et al. (2002), this test can be used for developing a model for predicting remaining fatigue life of the surface layer of in-situ pavements.

2.1.4 Direct Tension (DT) Test

The direct tension test (DT) is the most recent addition to cracking resistance analysis. This test has the simplest analysis equation of all test methods as the specimen is tested in uniaxial tension. Variability in test results and test repeatability are also reasonable. The specimen is typically a cylinder 6 inches in height and 4 inches in diameter (Walubita et al., 2010). Test specimens are compacted to 6.9 inches in height using the Superpave gyratory compactor (SGC) and are cored afterwards. The loading rate during the test is typically 0.05 inch/min (Walubita et al., 2010). The specimen requires gluing of plates at the bottom of the specimen in order to attach it to a servo-hydraulic closed-loop testing system. This critical part of the test requires special caution to ensure accurate results. Gluing could be time-consuming, since the whole process, including curing, requires approximately 24 hours. Proper gluing techniques must be ensured, otherwise the specimen may fail around the glued area, indicating that the HMA may not have failed before the test termination and, thus, calculated stresses and strains will be inaccurate. Since the LVDTs are attached to the specimen, HMA stiffness determination is possible with this test. The DT test can be run at either 68⁰ F or room temperature (Walubita et al., 2002). The DT test data include the load, vertical displacement, and time.

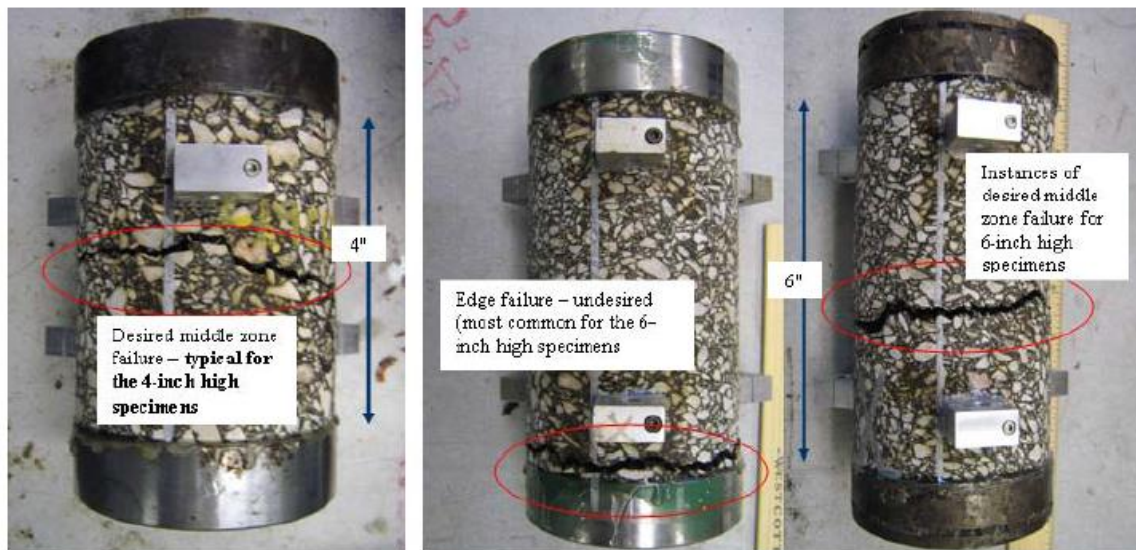


Figure 2.4 Demonstration of DT failure modes (Walubita et al., 2010)

DT fracture resistance parameters (tensile strength and axial strain) are highly sensitive to aging condition and binder type. Based on these factors, the 6-inch high DT test was recommended as a good surrogate mix screening test (Walubita et al., 2006). However, the specimen preparation and fabrication of test setup are tedious and comparatively prolonged processes requiring meticulous attention. In general, special guidance regarding specimen fabrication, gluing, and test setup is necessary, which at times may be costly. At the same time, these drawbacks may be an obstacle towards practical application and regular use of the DT test for HMA cracking resistance characterization. Research has shown that 6-inch high DT axial strain had difficulty differentiating between modified binders (Walubita et al., 2006). Additionally, the DT test is not readily applicable for testing field cores as fracture energy obtained from the DT test failed to show significant difference between fatigue performances of field mixtures (Walubita et al., 2006).

2.1.5 Fénix Test

The Road Research Laboratory of the Technical University of Catalonia, Barcelona, Spain has developed a new test to evaluate cracking resistance of asphalt concrete mixtures, named Fénix test (Pérez et al., 2010). They used dissipated energy during the cracking process, which is a combination of all the energies released during HMA deformation and cracking. The test procedure consisted of subjecting one-half of a 2.5 inches thick cylindrical specimen with a diameter of 4 inches, prepared by the Marshall or the Superpave gyratory compactor. The specimen underwent a constant displacement velocity of 0.04 inches/min. A 0.25 inch notch was cut at the midpoint of the bottom of specimen, similar to semi-circular bending test specimen and glued to steel plates with thixotropic adhesive mortar containing epoxy resins (Pérez et al., 2010). Fénix test provided evidence making it a practical and efficient method to characterize cracking behavior of HMA mixtures. This test gives an estimation of fatigue behavior of mixtures in terms of the relationships between parameters.



Figure 2.5 Test setup of Fénix test (Pérez et al., 2010)

2.2 Superpave

Superpave stands for *Superior Performing Asphalt Pavements*, and this mix design was originally intended to replace Hveem and Marshall methods (Roberts et al., 1996). The Hveem method was developed by California Division of Highways in the late 1920s, and the Marshall method was developed by the Mississippi Department of Transportation in the late 1930s. With rapid increase in asphalt usage and significant change in traffic volume, an increased demand arose for an improved asphalt mix design method which considered heavy-duty pavement load applications. Thus, in 1993, Superpave mix design was developed as a principal outcome of the \$50 million Strategic Highway Research Program (SHRP). The volumetric analysis of Superpave mix design is similar to the Hveem and Marshall methods of mix design and accounts for traffic loading and environmental conditions. Superpave mix design has gained considerable popularity among various states across the country, including Kansas, because it possesses distinct advantages when compared to traditional Hveem and Marshall Mix Design methods.

The advantages are:

- This method, by means of additional requirements, enables the selection of aggregates with relevant properties.
- Superpave gyratory compactor (SGC) provides replicate simulation of field compaction and traffic conditions.
- This method enables selection of asphalt binders which permit broader range of service temperatures.

Volumetric design procedure assumes that the number of gyrations applied by the Superpave gyratory compactor represents traffic conditions to which the mixture will be subjected. This method includes performance-based specifications. Though few differences are present in the Superpave mix design procedure, this method uses the same basic steps and strives for an optimum asphalt binder content that results in 4% design air void at the design number of gyrations, to that of Hveem and Marshall methods. (Asphalt Institute, 1995).

During compaction in the Superpave gyratory compactor, the mold is tilted at an internal angle of 1.16° at a constant speed of 30 revolutions per minute while being subjected to a compaction pressure of 87 ± 0.87 psi. Compacting effort in the SGC is expressed in terms of the number of gyrations (N) applied to the specimen. N_{ini} , N_{des} , and N_{max} are the three gyration levels considered in mix design. These levels of gyration represent the density of the mix at various stages of the pavement over the design life. The design number of gyration (N_{des}) is a function of the 20-year design ESALs. Mixtures subjected to heavy traffic condition require higher compaction effort. Maintaining accurate density is important as high density at N_{ini} may result in stability-related problems in the mixture, while high density at N_{max} can cause rutting and bleeding.

2.3 Durability of HMA

Durability is one of the important aspects of asphalt. When asphalt is mixed with aggregates or subjected to heating, durability resists the changes in properties and protects from hardening with time. Past research has shown that ensuring durability by incorporating minimum desirable asphalt content was the reason behind the minimum voids in mineral aggregate (VMA) requirements for a conventional asphalt mix (Kumar and Goetz, 1977). Film thickness has also proven to be closely related to durability. Thus, the basis of determining minimum VMA should

be minimum asphalt film thickness instead of minimum asphalt content (Kumar and Goetz, 1977).

Among several factors that control hardening, oxidation and volatilization appear to be the most crucial and require careful control. Lack of proper control during mixing operation can significantly reduce pavement life. In case higher mixing temperature is used, service life is decreased at the outset of the construction operation within a very short period. Therefore, during the construction phase, it is necessary to prevent damage of asphalt in order to extend pavement durability (Monismith et al., 1989). Specifications related to oven aging test and flash point test help control hardening. Oxidation and volatilization of asphalt is highly influenced by air void percentage, as lower air voids affect these properties.

Durability of asphalt mixture is enhanced by higher asphalt binder content, dense graded aggregate, and uniformly compacted mixtures. All these factors enable the mixtures to be protected against water, air, and water vapor. High asphalt content contributes to high average film thickness on mixtures and decreases gap sizes between aggregates, thus enabling the mixture to be impervious to air and water. Dense aggregate gradation, in combination with desired amount of asphalt and proper compaction, can provide low permeability to air and water (Monismith et al., 1989).

2.4 Effects of Mixture Aging

Brown and Scholz (2000) investigated the effect of oven-storage on the stiffness modulus of commonly used asphalt mixtures prior to compaction. This study considered mixtures commonly used in the United Kingdom. Their study concluded that storage of loose asphalt mixtures at 275⁰ F before compaction significantly increased stiffness of compacted asphalt mixtures. The results provided strong evidence to show that storing dense-graded loose mixtures for approximately 2 hours at 275⁰ F would represent the aging occurred from mixing, storage, and transportation in an actual construction site. Long-term aging was also addressed in this study and the conclusion was made that long-term aging protocol, involving a force-draft oven at 185⁰ F for 120 hours in absence of light, produces useful practical results.

2.5 Effects of Varying Asphalt Content

To obtain a durable mix, asphalt content must be monitored in HMA mixes. Insufficient amount of binder can lead to problems, such as cracking and raveling, while extra binder in HMA may lead to rutting or flushing (Kandhal and Cross, 1993).

2.6 Voids in Mineral Aggregate (VMA)

VMA are the volume of inter-granular void spaces between aggregate particles of a compacted paving mixture. This void space includes air voids and effective asphalt content, which is the total asphalt content minus the quantity of asphalt lost to absorption into aggregate pores (Asphalt Institute, 2007). VMA can be computed from the following equation:

$$\text{VMA} = 100 - \left(\frac{G_{mb} \times P_s}{G_{sb}} \right) \quad (2.7)$$

Where, G_{mb} = Bulk specific gravity of compacted mixture;

G_{sb} = Bulk specific gravity of aggregate; and

P_s = Percent of aggregate.

McLeod (1956) discussed the volumetric relationship between the binder content, aggregate air voids, and the total number of aggregates in a compacted paving mixture. He suggested restricting the VMA to a minimum of 15%, the percentage of air voids (within the VMA) to 3- 5%, which would consequently restrict binder volume in the compacted mixture to a permissible minimum of 10% by volume (4.5% by weight).

For the past few decades, no emphasis has been given to the adjustment of minimum VMA requirements based on air voids percentages. In 1993, VMA requirements corresponding to 3%, 4%, and 5% air void contents were established and incorporated into the Superpave mix design procedures. Though some older mix design methods had minimum VMA as a suggestion, Superpave included VMA as a requirement (Cross and Purcell, 2001). After an extensive analysis of data, Coree and Hislop (1999) suggested that the combination of air void between 3 - 5% and voids filled with asphalt (VFA) between 68-77% would be acceptable. Other researchers assumed a minimum film thickness and calculated VMA by considering gradation and volumetric properties (Hinrichsen and Heggen, 1996). Later, they stated that considering nominal maximum aggregate size (NMAS) of the mix as the basis for VMA criterion would eliminate percentages of aggregate gradations which otherwise would have resulted in satisfactory performance.

In Superpave mix design, the design binder content is determined using percent air voids. Air voids, VMA, and VFA are considered determining factors for mixture performance. Superpave design process adopted the minimum VMA requirement to ensure durability and avoid bleeding problems, by conforming to, required binder content as well as air voids.

Table 2.1 Current VMA requirements given by KDOT

Nominal Maximum Aggregate size (mm)	Minimum VMA (%)
9.5	15.0
12.5	14.0
19	13.0
25	12.0
37.5	11.0

2.7 Asphalt Film Thickness

The thickness of the asphalt cement film around a particular aggregate is a function of the diameter of the aggregate, absorption of the aggregate, and the percent of asphalt cement in the mixture. The current technique for calculating film thickness is based on surface area factors. Film thickness is indirectly administered by controlling the gradation (surface area) and minimum VMA (minimum asphalt content). Surface area of aggregates is dependent on gradation. For example, surface area of fine aggregates in per unit weight is higher than that of coarse aggregates (Brown et al., 2009). The asphalt cement film thickness is calculated using the following formula:

$$T_F = \frac{V_{asp}}{SA \times W} \times 1000 \quad (2.8)$$

Where, T_F = Average film thickness, (microns);

V_{asp} = Effective volume of asphalt cement, (liters), (total volume minus absorbed volume);

SA = Surface area of the aggregate, (m^2 per kg of aggregate); and

W = Weight of aggregate, (kg).

Calculated film thickness is the average film thickness that is generally correlated with durability. If the asphalt film is too thin, air enters into compacted HMA and rapidly oxidizes these films, causing HMA to become brittle and causing failure by cracking.

Extensive research has been conducted on the relationship of asphalt film thickness with durability of HMA mixtures. Campen et al. (1959) concluded that the asphalt content required for obtaining minimum air voids increases with an increase in surface area. However, the rate is significantly low to conclude it as a direct proportionality. Their recommendation is that 6 to 8 microns should comprise film thickness of most HMA mixes.

Kandhal and Chakraborty (1996) evaluated the impacts of asphalt film thickness on the aging of HMA mixes. They obtained a fair correlation between film thickness and the resilient modulus of aged HMA mix. Their results agreed with results obtained by Goode and Lufsey (1965).

Computation of film thickness involves inconsistency and inaccuracy because of variation among the researchers in calculating surface area. Hinrichsen and Heggen (1996) analyzed data from past few years and recommended a best-fit criterion for obtaining the surface area. Another study conducted by Li et al. (2009) computed the surface area by an index method in which aggregate shape is considered. They compared the results to that of conveniently-obtained surface area and concluded that shape of aggregate plays a considerable role in surface area calculation. In addition, they obtained a significant relationship between asphalt film thickness and rutting performance (Li et al. 2009).

It is recommended that minimum average asphalt film thickness be used to ensure mix durability instead of minimum VMA. An average minimum thickness of 8 microns is recommended (Kandhal et al., 1998).

2.8 Effect of Reclaimed Asphalt Pavement (RAP) in HMA

Reclaimed Asphalt Pavement (RAP) is the recycled asphalt pavement material containing aggregates and asphalt binder. RAP can be obtained from an existing asphalt pavement when it undergoes rehabilitation or reconstruction or when a cut is made on roadways to access underground utility lines. Removal of asphalt pavement is done either by full-depth removal or milling whenever an existing wearing course is removed. Full-depth removal is conducted by milling the HMA surface in several passes, depending on the depth, or ripping the surface with a bulldozer. Once broken, RAP is crushed, screened, and stock-piled (Copeland, 2011). The Federal Highway Administration (FHWA) estimated more than 90 million tons of asphalt pavements were rehabilitated in the early 1990s. RAP can be used as a replacement of new

aggregate along with asphalt cement in asphalt mixes as a stabilized base aggregate in sub-base or as filler material in an embankment.

Copeland (2011) stated the following advantages of using RAP in HMA:

- Preservation of environment
- Preservation of resources
- Conservation of energy
- Reduction in construction and transportation costs
- Reduction in the use of non-renewable resources (virgin aggregate and asphalt binder)

2.8.1 Obstacles in using High RAP contents in HMA

Currently, approximately half of the DOTs in the United States allow 20% RAP in HMA mixtures, although up to 30% RAP can be used in various layers of pavement (Copeland, 2011). A few obstacles exist that must be overcome in order to increase regular usage of a higher percentage of RAP. As reported by a survey performed by State DOTs, the most common obstacles to high RAP usage include limitation of RAP specifications, lack of RAP availability, and variability of RAP. Also, specifications assume that complete blending takes place between virgin and RAP binder. However, in reality, the blending occurs in an intermediate stage, somewhere between no blending and complete blending. Currently, research is being conducted to evaluate blended binder properties by means of dynamic modulus. Some DOTs are imposing constraints depending on past bad experience with RAP. Also, because of issues related to maintaining required dust and moisture content and strict prerequisites for quality control (QC), contractors are not willing to add higher percentages of RAP (Copeland, 2011).

2.8.2 Mix Design Consideration for RAP

One crucial factor related to RAP is knowledge of the exact amount of asphalt present in RAP. The aged binder in RAP is harder, which denotes higher PG grade. Mixtures with more than 20% RAP require consideration of the rheological and physical properties of the asphalt binder residue. In order to maintain a balance for the presence of hardened binder in RAP, a relatively softer virgin PG binder grade is selected, especially when more than 15% of RAP is used in the mixture.

Gradation of aggregates in RAP is an important characteristic and determined by Kansas test method KT-2 (AASHTO T27). After gradation, bulk specific gravity (G_{sb}) of RAP is required. In case G_{sb} is not available, effective specific gravity (G_{se}) can be used as a replacement. This substitution is valid as G_{se} is always greater than G_{sb} . In case none are available, the asphalt absorption is assumed based on past experiences from similar locations (Copeland, 2011).

Superpave mix design allows various additives into the HMA mixture while ensuring specified gradation. Requirements for mixtures with higher percentages of RAP are similar to those containing 100% virgin materials. After RAP has been characterized, it can be combined with virgin aggregates to form a uniform blend gradation for mix design purposes. The selected blend must pass between the control points in order to satisfy gradation requirements.

RAP usually contains significantly higher percentages of material passing a 0.075-mm (US No. 200) sieve. For this reason, the amount of RAP able to be used in a mix design while simultaneously satisfying volumetric specification is somewhat limited.

Asphalt binder content of the total mix comprises both virgin and reclaimed asphalt binder. Thus, careful attention is required when determining asphalt binder content. RAP material is usually heated separately at much lower temperatures (around 140⁰F) than needed for mixing and compaction (approximately 320⁰F). To balance the lower RAP temperature, virgin aggregates are heated at a higher temperature (around 350⁰F) so that the mix temperature remains within the required mixing temperature range after mixing. This step is essential, especially when a higher percentage of RAP is added to the mix. Since RAP contains aged binder, this is done to prevent additional aging of the existing binder in RAP. RAP should meet all test procedures and criteria as required for the virgin HMA (Brown et al., 2009).

2.8.3 Performance of Mixtures with RAP

In a study conducted by McDaniel (2002), laboratory mixtures from Indiana, Michigan, and Missouri were compared to the plant-produced mixtures with identical materials and RAP contents between 15% and 25%. In addition, a few mixtures were designed and tested in the laboratory in order to investigate the effect of recycled materials on mixture performance with RAP content up to 50%. Results showed that plant-produced mixes were similar in stiffness to the laboratory mixtures at the same RAP content for Michigan and Missouri samples. Mixtures

with up to 50% RAP could be designed with Superpave, provided RAP gradation and aggregate quality were sufficient. It was observed that increasing RAP content in a mixture increased stiffness and decreased shear strain, indicating an increased resistance to rutting. The conclusion was made that when RAP properties are appropriately accounted for in the material selection and mix design process, mixtures can perform very efficiently (McDaniel, 2002).

Carvalho et al. (2010) analyzed data of 18 projects from the long-term pavement performance (LTPP) program executed across North America to evaluate short- and long-term performance of RAP mixes. Results were compared with virgin HMA overlays over existing flexible pavements. The study considered roughness, rutting, and fatigue cracking. The structural performance of overlaid sections was also evaluated from deflection data. Analysis of variance (ANOVA) results indicated that the performance of RAP mixes and virgin HMA are not statistically different. Statistical similarity of deflections showed that RAP overlays can provide structural improvement equivalent to virgin HMA overlays.

Huang et al. (2011) conducted a study on laboratory cracking resistance of asphalt surface mixtures containing screened RAP. They used mixtures with 0, 10, 20, and 30 % RAP with two types of aggregates and three types of binder. After evaluating the cracking resistance through indirect tension test and semi-circular bending test, it was concluded that up to 20% RAP generally improves the stiffness and indirect tensile strength of the mixture, but decreased the cracking resistance. Mixture properties changed abruptly at 30% RAP content compared to those with 10% and 20% RAP.

2.9 Summary

Indirect tension test (IDT), direct tension test (DT), Fénix test, semi-circular Bending (SCB), and Texas overlay (OT) tests are the most commonly used cracking resistance tests. Repeated SCB test is the most promising surrogate cracking test while OT test results can correlate well with field performance. Ensuring durability enhances cracking resistance potential of HMA mixture. Durability of asphalt mixture is enhanced by higher asphalt binder content, dense graded aggregate, aging and uniformly compacted mixtures. Superpave mix design was developed in 1993 and it included voids in mineral aggregate (VMA) as a requirement. Studies recommended minimum average asphalt film thickness should be used to ensure mixture durability instead of minimum VMA. An average minimum asphalt film thickness of 6-8

microns is recommended. Using reclaimed asphalt pavement (RAP) is a recent practice in Superpave mixtures which affects durability significantly. The aged binder in RAP is harder, thus, mixtures with more than 20% RAP require consideration of the rheological and physical properties of the asphalt binder residue.

Chapter 3 - Methodology

3.1 Virgin Aggregates, RAP and Binder

In this study, 12.5-mm nominal maximum aggregate size (NMAS) Superpave mixtures were evaluated. The design binder content of the base SM-12.5A (no RAP mixture) is 5.2%. To investigate the effect of varying asphalt contents on cracking resistance, asphalt content was reduced by 0.3% and 0.6%. Thus, SM-12.5A mixtures with 4.9% and 4.6% asphalt content were also considered in this study. To investigate the effect of varying RAP content on cracking resistance, SR-12.5A mixture with three RAP contents, 20%, 30%, and 40%, were investigated. RAP used in SR-12.5A mixture was collected from two different sources to study the effect of RAP source on mixture cracking resistance. The first and second RAP sources were from Shilling Construction Co., located in Manhattan, Kansas, and Konza Construction Co., located in Junction City, Kansas. Mix designs for the SR-12.5A mixtures were developed in a previous study conducted by Sabahfar (2012).

Both SM-12.5A and SR-12.5A mixtures were prepared with identical virgin aggregates and virgin binder PG 70-28. Five different virgin aggregates obtained from Shilling Construction Company were coarse-crushed limestone (CS-1), fine-crushed limestone (CS-1A), manufactured sand (MSD-1), crushed gravel (CG-5), and natural/river sand (SSG). In order to meet the required dust-to-binder ratio specifications given by the Kansas Department of Transportation (KDOT), one percent limestone dust obtained from the Los Angeles Abrasion machine was added to the SM-12.5A mixtures with 4.9% and 4.6% asphalt contents. The PG grades of the first and second sources of RAP used in SR-12.5A were 84-16 and 90-10, respectively.

3.2 Gradation and Aggregate Blending

Superpave gradation requirements include use of the Federal Highway Administration (FHWA) 0.45- power chart, based on the Fuller gradation formula. Gradation performance is evaluated based on the maximum density line of the 0.45-power chart which is obtained by drawing a straight line from origin to the maximum aggregate size. Gradation of each aggregate and RAP are given in Table 3.1. Both sources of RAP contained significant amounts of dust. Percentages of individual aggregates in the aggregate blends and gradations for SM-12.5A are

shown in Table 3.2 and 3.3, respectively. Blending of SM-12.5A mixtures are shown in Figure 3.1. All mixture gradation passes over the maximum density line in the sand sizes.

Table 3.1 Aggregate gradation

Material	CS-1	CS-1A	MSD-1	CG-5	SSG	first RAP	second RAP
Sieve Size	% Passing						
¾	100	0	0	0	0	100	100
½	59	100	100	100	100	98	96
3/8	20	100	100	100	100	94	92
#4	2	29	99	96	95	80	78
#8	2	6	63	77	77	64	64
#16	2	2	36	49	53	47	48
#30	2	1	22	30	31	33	35
#50	2	1	13	18	12	20	21
#100	2	1	9	11	4	13	15
#200	2	1	8	9	4	10	12

Table 3.2 Percentages of aggregates in SM-12.5A mixtures

Asphalt Content (%)	CS-1 (%)	CS-1A (%)	MSD-1 (%)	CG-5 (%)	SSG (%)	Limestone Dust (%)
5.2	25	15	15	20	25	0
4.9	24	15	15	20	25	1
4.6	24	15	15	20	25	1

Table 3.3 Aggregate blending for SM-12.5A mixture with KDOT requirements

Sieve size (mm)	P _b = 5.2% (%)	P _b = 4.9% (%)	P _b = 4.6% (%)	KDOT Requirements (%)
19	0	0	0	0
12.5	10	10	10	0-10
9.5	20	19	19	10 Min
4.75	38	37	37	
2.36	55	54	54	42-61
1.18	71	70	70	
0.60	82	81	81	
0.30	91	90	90	
0.15	95	94	94	
0.075	96	95	95	90-98

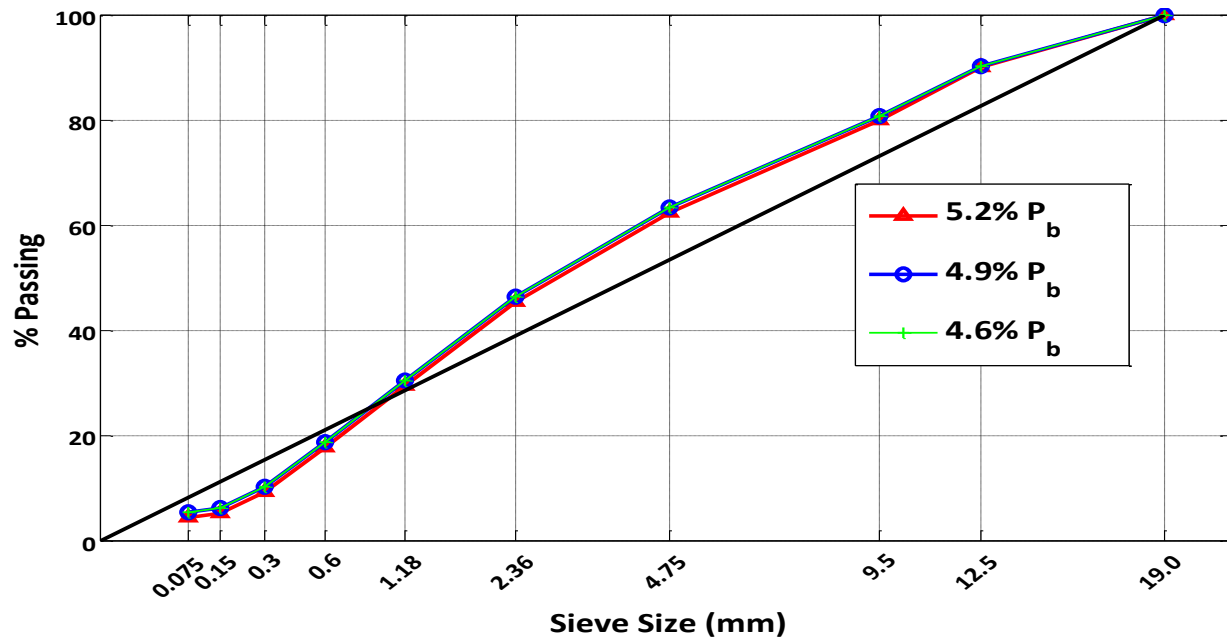


Figure 3.1 0.45 power gradation chart for SM-12.5A mixture

Percentages of individual aggregates in the aggregate blends and gradations for SR-12.5A mixtures are shown in Table 3.4 and 3.5, respectively. Blending of SR-12.5A mixtures with the first and second sources of RAP are shown in Figure 3.2 and 3.3, respectively. The blends are finer i.e. they have a predominance of fine or sand materials.

Table 3.4 Percentages of aggregates and asphalt in SR-12.5A mixtures

RAP Content (%)	Virgin Aggregates					Total Asphalt Content (%)			
	CS-1 (%)	CS-1A (%)	MSD-1 (%)	CG-5 (%)	SSG (%)	First RAP Source		Second RAP Source	
						Total Asphalt	Virgin Asphalt	Total Asphalt	Virgin Asphalt
20	20	12	12	16	20	4.7	3.6	4.3	3.5
30	16	15	13	12	14	4.8	3.1	4.4	3.2
40	12	13	13	12	10	4.3	2.1	4.1	2.5

Table 3.5 Aggregate blending for SR-12.5A mixture with KDOT requirements

Sieve size (mm)	20% RAP		30% RAP		40% RAP		KDOT Requirements
	First RAP (%)	Second RAP (%)	First RAP (%)	Second RAP (%)	First RAP (%)	Second RAP (%)	
19	0	0	0	0	0	0	0
12.5	8	7	6	9	8	6	0-10
9.5	17	15	12	18	15	13	10 Min
4.75	34	34	30	34	34	31	
2.36	51	51	48	51	51	48	42-61
1.18	67	67	65	67	67	64	
0.60	79	79	77	79	78	76	
0.30	89	88	87	88	88	86	
0.15	93	93	92	93	92	91	
0.075	95	94	93	94	93	92	90-98

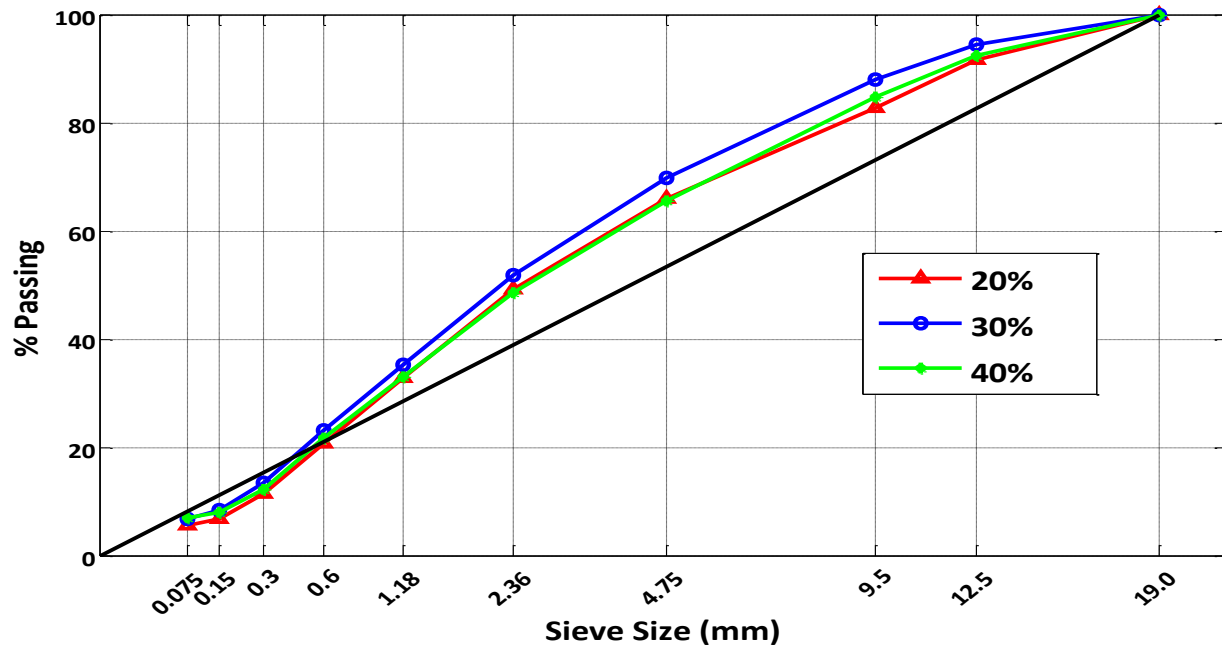


Figure 3.2 0.45 power gradation chart for SR-12.5A mixture with first source of RAP

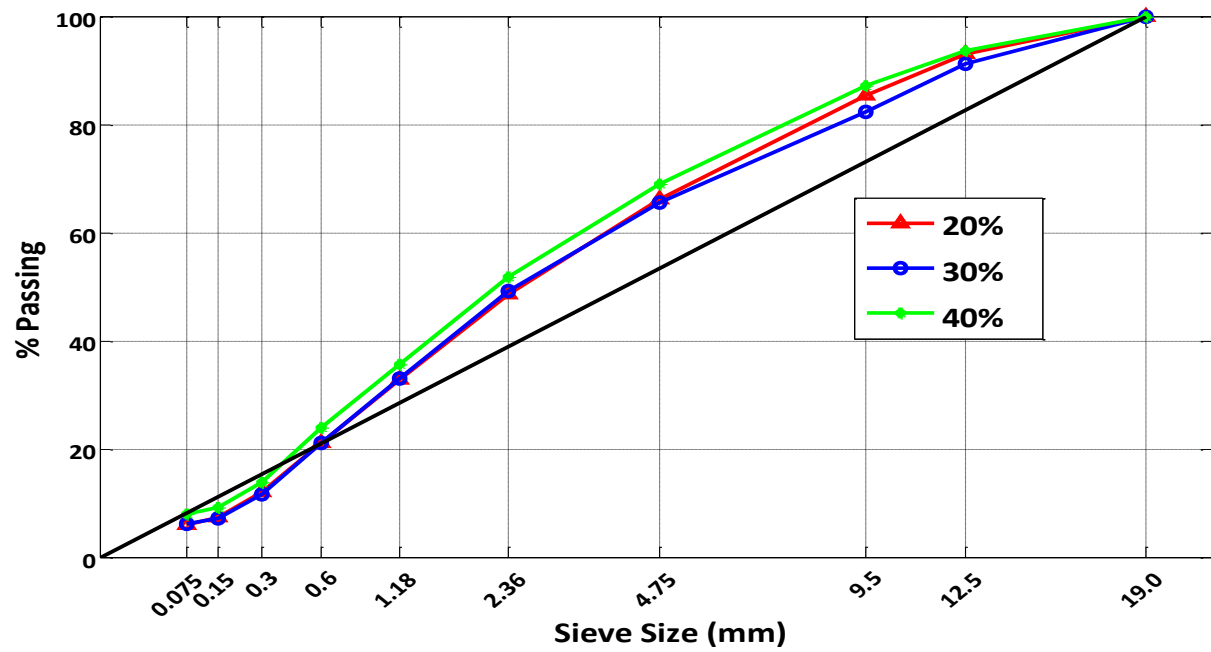


Figure 3.3 0.45 power gradation chart for SR-12.5A mixture with second source of RAP

3.3 Test Specimen Preparation for Cracking Resistance Tests

3.3.1 Mixing and Compaction

Samples were prepared following the Kansas Test Method KT-58 Procedure. The main steps involved in preparing SCB and OT test specimens include drying aggregates to constant weight, batching aggregates, heating the aggregates and binder to mixing temperature, mixing binder and aggregates, conditioning (short-term aging), and compacting specimens to appropriate percent air voids using the Superpave gyratory compactor (SGC). An illustration of mixing and short-term aging is given in Figure 3.4. Detailed steps involved in the preparation of specimens are described as follows:

1. All required aggregates were weighed in steel pans separately.
2. Aggregates and binder were heated in the oven to appropriate mixing temperature (309 – 320⁰ F). For mixtures containing RAP, the RAP was heated separately (approximately 122⁰ F), much lower than the mixing temperature to prevent additional hardening of RAP asphalt cement. In such case, the virgin aggregates were heated above the mixing temperature (350⁰ F) to compensate for the lower mixing temperature of RAP so that the temperature of the total mix was within the actual range of the mixing temperature.
3. After the aggregates and binder reach the mixing temperature, heated aggregates were transferred into a mechanical mixer and mixed thoroughly. The required amount of binder was added and mixing continued until every particle was uniformly coated. Dust was added at this step as required.
4. After mixing, the mixture was placed in a pan, spread evenly, and transferred to an oven at compaction temperature (270 – 281⁰ F) for approximately 2 hours ± 5 minutes for short-term aging. The mixture was stirred after 60 ± 5 minutes to maintain uniform aging. Afterwards, the mixture was ready to be compacted using the SGC.



(a)



(b)

Figure 3.4 (a) Mixing of aggregates with binder in mixer; (b) HMA mixture undergoing short-term aging in oven

For compaction, the molds, plates of SGC, and pouring pan were preheated to the compaction temperature for approximately 45-60 minutes before the start of compaction. The mold and base plate were removed from the oven and the mold was charged with the required amount of mixture using a pouring pan. The mixture was leveled with a spatula and the top plate was placed in the mold. To avoid the mixture sticking to the plates, paper disks were placed in between the plates and the mixture. The mold was then transferred into the SGC and the SGC was started. When the SGC reached the specified number of gyrations, it stopped automatically. The mold was then removed from the SGC; the sample was extruded from the mold, and cooled for 5 minutes in front of a fan. Figure 3.5 shows the compaction process. Inputs given to the SGC are summarized in Table 3.6.

Table 3.6 Compaction parameters for SGC

Parameter	SCB Test	OT Test
Specimen Height	100 mm	112.5 mm
Pressure	600 ± 18 kPa	600 ± 18 kPa
Angle of Gyration	$1.16^0 \pm 0.02^0$	$1.16^0 \pm 0.02^0$
Number of Gyration	$N_{\text{initial}}=7, N_{\text{design}}=75, N_{\text{max}}=115$	$N_{\text{initial}}=7, N_{\text{design}}=75, N_{\text{max}}=115$
Speed of Rotation	30 ± 0.5 gyrations per minute	30 ± 0.5 gyrations per minute



(a)

(b)

(c)

Figure 3.5 (a) SGC mold with loose HMA inside; (b) Specimen being compacted in SGC; (c) Final compacted specimen

3.3.2 Determination of Air Void of Specimen by G_{mm} and G_{mb} Test

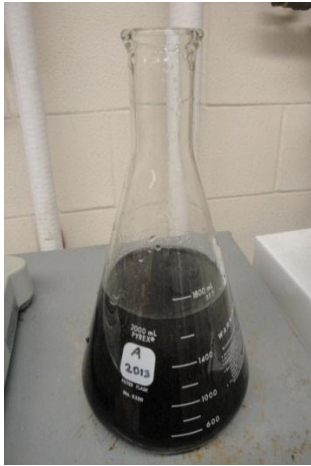
After compaction, the air voids in the test specimen were calculated using the bulk specific gravity of the compacted specimen (G_{mb}) and the theoretical maximum specific gravity of loose mixture (G_{mm}). G_{mb} and G_{mm} were determined by the Kansas Test method KT-15 (Procedure-III) and KT-39, respectively.

3.3.2.1 G_{mm} Test Procedure

Theoretical maximum specific gravity (G_{mm}) of asphalt paving mixtures was obtained using the Kansas Test Method KT-39 procedure. After loose HMA mixture was aged for 2 hours \pm 5 minutes, the required amount of mix is spread on a clean surface and allowed to cool completely. Afterwards, this test is conducted.

In this test, the sample size depends on the nominal maximum size of aggregates (NMA). Since this study considered 12.5-mm NMA mixtures, thus 3.31 lbs. were used. The sample was cooled to room temperature, broken into pieces not larger than 0.25 inches, and put inside a calibrated flask. The weight of the sample was recorded. Then, a sufficient amount of water at $77^{\circ} \pm 2^{\circ}$ F was added to the sample so that it was covered completely. Next, trapped air in the sample was removed by applying gradually increased vacuum until the residual pressure manometer reads 27 ± 3 mm of Hg. Full vacuum was applied for 30 seconds and residual pressure was maintained for 14 minutes \pm 0.5 minutes. The container and contents were agitated

during the vacuum period using a mechanical device. At the end of vacuum period, the pressure was released slowly and the container and contents were suspended in a water bath at $77^{\circ} \pm 2^{\circ} \text{F}$ for $10 \text{ minutes} \pm 1 \text{ minute}$. Finally, the mass of loose sample in water was recorded. G_{mm} was calculated using equation 3.1. Figure 3.6 shows graphical illustration of this test procedure.



(a)



(b)



(c)

Figure 3.6 (a) Loose HMA inside flask filled with water; (b) Trapped air taken out by vacuum application; (c) Weight of loose specimen in water being taken

$$G_{mm} = \frac{A}{(A-C)} \quad (3.1)$$

Where, A = Mass of dry sample in air, (gm); and

C = Mass of water displaced by sample at 25⁰ C, (gm).

3.3.2.2 *G_{mb} Test Procedure*

Several approaches exist for determining bulk specific gravity. In this study, Kansas Test Method KT-15, Procedure-III was used. After compaction with SGC, the specimens are allowed to cool to room temperature before performing this test. Usually, G_{mb} test is conducted approximately 24 hours after compaction. Steps of the test procedure are explained as follows:

First, dry mass of the HMA specimen was recorded. Then, the HMA specimen was soaked in a water bath at 77⁰ ± 2⁰ F for 4 ± 1 minutes and its submerged mass was recorded. Afterwards, it was removed from the water and rolled on a damp towel to remove excess water from the sample surface. Finally, the saturated surface dry (SSD) mass was recorded. Bulk specific gravity was calculated using equation 3.2. The test procedure is shown in Figure 3.7.

$$G_{mb} = \frac{A}{(B-C)} \quad (3.2)$$

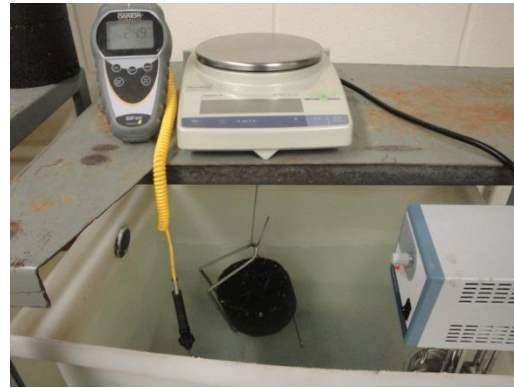
Where, A = Mass of dry specimen in air, (gm);

B = Mass of saturated surface dry specimen, (gm); and

C = Mass of water displaced by specimen at 77⁰ F, (gm).



(a)



(b)



(c)

Figure 3.7 (a) Weight of dry compacted specimen being taken; (b) Specimen submerged in water; (c) Wet specimen rolled out in damp towel

Once the G_{mm} and G_{mb} are calculated, the air void in a compacted specimen is determined by equation 3.3.

$$\% \text{ Air void} = \frac{G_{mm} - G_{mb}}{G_{mm}} \times 100 \quad (3.3)$$

3.4 Cracking Resistance Test Procedures

3.4.1 Semi-Circular Bending (SCB) Test

For this test, SGC compacted specimens were cut into 2-inch thick discs. Afterwards they were cut from middle and finally, semi-circular specimen with a dimension of 2 inch thickness and 6 inch diameter were obtained. A notch, 0.25 inch deep, was cut at the bottom of the

specimen to ensure that the crack initiated at the center of the specimen. For each type of mixture, three replicate samples were prepared and subjected to the SCB test. SCB specimens were compacted to a target air void of $7 \pm 1\%$.

3.4.1.1 Static SCB Test

The prepared specimen was placed inside the Universal Testing Machine (UTM-25), resting upon a custom-made support system which would ensure that three-point bending would occur. The specimen was aligned so that a notch in the middle of the bottom of the specimen is directly beneath the point of load application. The load cell applied a compressive load to the specimen at a rate of 0.05 inch/min until the specimen failed (full crack propagation through the specimen). The loading rate was determined from a previous study (Walubita et al., 2010). Failure was defined as the maximum load in the specimen. Once the peak load was achieved, the test was stopped manually. The average peak load of three replicates was considered for this analysis. Figure 3.8 illustrates the SCB test setup. Measurable parameters are the loading rate (0.05 inch/min), the axial load, time, and specimen deformation (measured by the machine's vertical ram displacement). This test was performed at a temperature of 77^o F to ensure consistency among the test methods.



Figure 3.8 SCB test setup



Figure 3.9 A typical SCB specimen after fracture failure

3.4.1.2 Repeated SCB Test

The repeated SCB test is a stress-controlled test performed with identical test setup as the static SCB but with a repeated load of 10 Hz and no rest period. This rate was used in a study conducted at the Texas Transportation Institute, to represent traffic loading patterns (Walubita et al., 2010). Four fractional peak load (static SCB) levels obtained at 30, 40, 50, and 60 percent were arbitrarily tried as the R-SCB input loads. The test continued until a crack propagated through the entire specimen. The final parameter for comparison was the number of load cycles to failure. The more the specimen could withstand cycles prior to fracture failure, the better cracking resistant it would possess. According to studies conducted by previous researchers (Walubita et al., 2013; van Rooijen and de Bondt, 2008), approximately 50% of static SCB peak load should be considered R-SCB input load. However, in this study, 30% and 50% of static SCB peak load were considered to investigate the effect of repeated load on the number of cycles to failure. The step-by-step process of R-SCB test is shown in Figure 3.10.

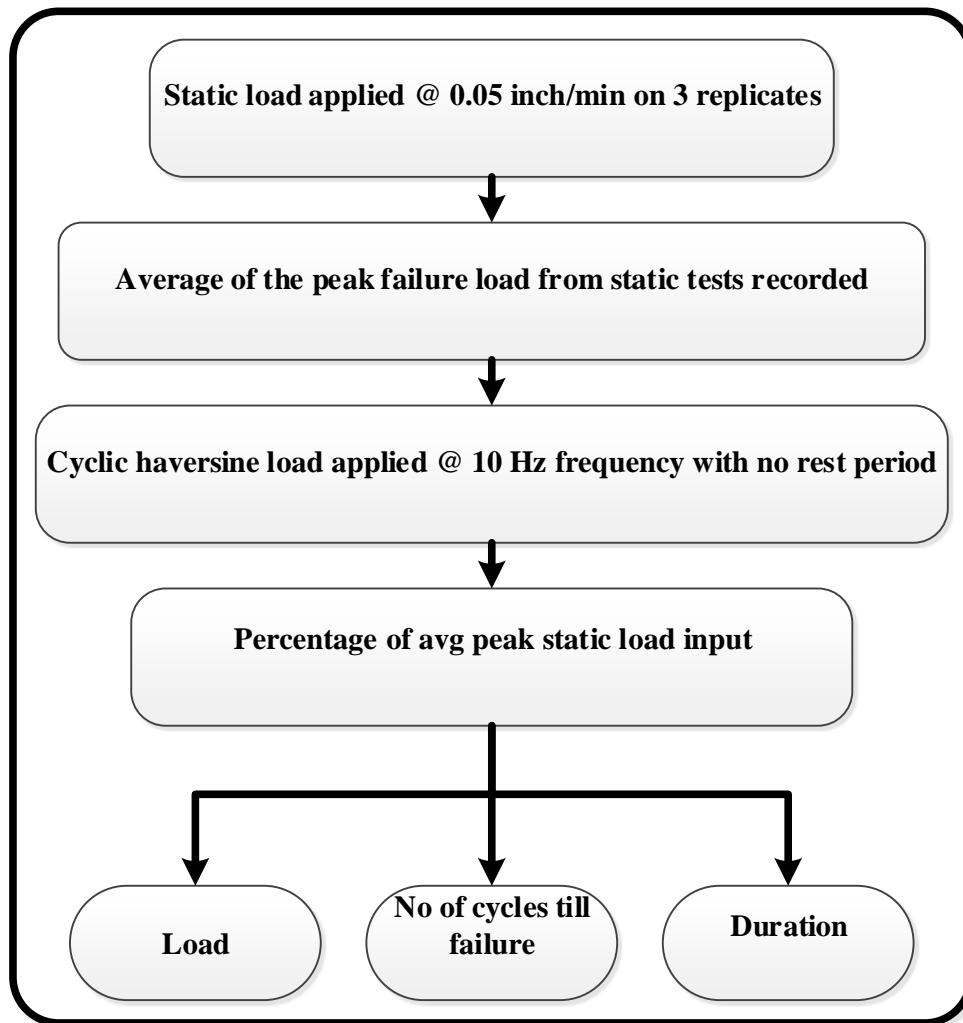


Figure 3.10 R-SCB test process

Additionally, crack propagation behavior and crack length of R-SCB loaded specimen were investigated. To perform this task, specimens were prepared from each Superpave mixture being studied and cut and notched as any other SCB specimen. An epsilon clip-on gauge was attached at the bottom of each specimen perpendicular to the notch with the help of bolt-on knife edges. This gauge was able to record the horizontal displacements around the crack. With the help of this deformation data, crack length was calculated. Results will be discussed in a later section. Figure 3.11 shows the SCB test setup with a clip-on gauge attached.

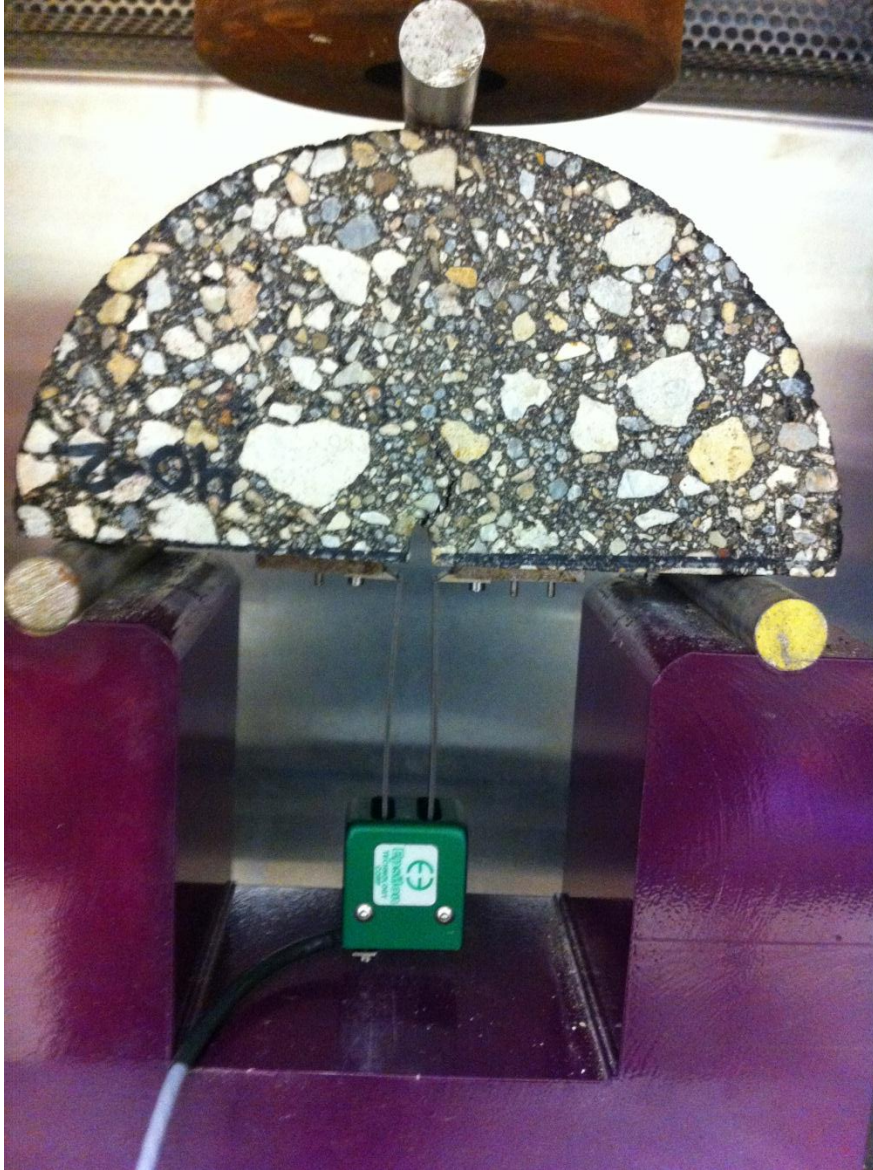


Figure 3.11 SCB test setup with clip-on gauge

3.4.2 Texas Overlay (OT) Test

The OT test is a performance test specified by Tex-248-F that quantifies the fatigue resistance potential of HMA in the laboratory. Each compacted specimen was cut to the dimensions shown in Figure 3.12 in order to achieve an OT specimen of 6 inches long, 3 inches wide and 1.5 inches thick. After cutting, the air void in the specimen was checked. IF the air void exceeded $7 \pm 1\%$, the specimen was discarded.

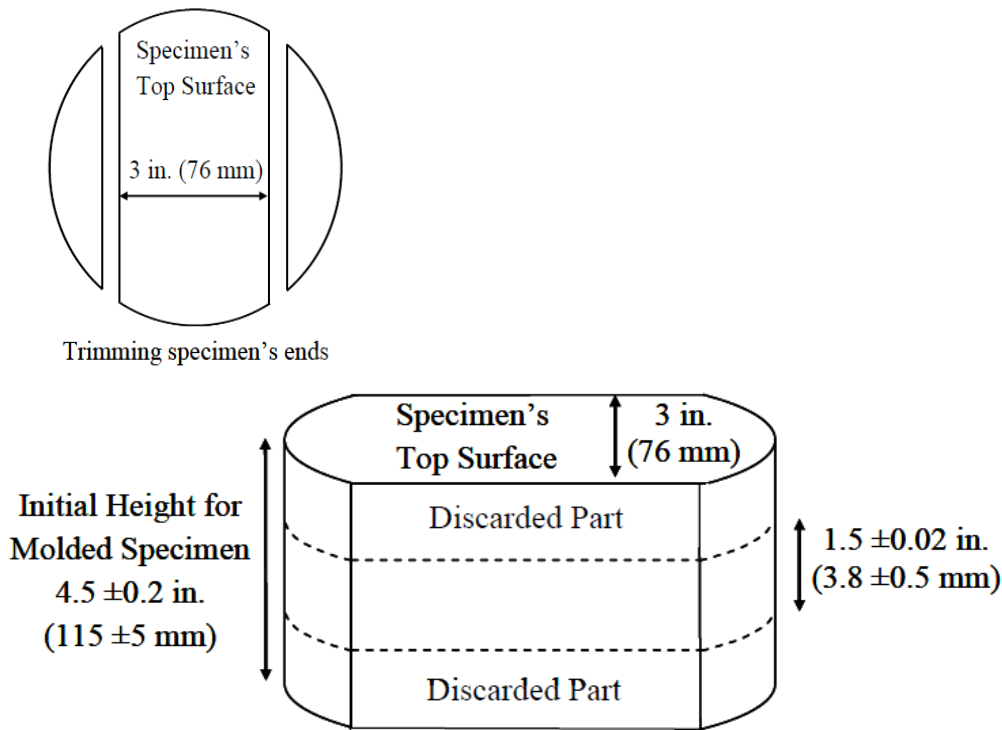


Figure 3.12 Trimming of OT specimen (Tex-248-F)

The cut specimen was then glued to two metal base plates using epoxy glue. The base plates were mounted on a metal frame to ensure the required gap between plates. A ten-pound weight was applied to the specimen, and the glue was allowed to set for 24 hours. Figure 3.13 shows an OT test specimen glued to the base plates. The test was conducted at a test temperature of 77⁰ F, consistent with the Tex-248-F test procedure. This test was conducted in the Asphalt Mixture Performance Tester (AMPT) machine. Loading configuration of this test consists of a cyclic triangular displacement-controlled waveform at a standard maximum opening displacement of 0.025 inch and a loading rate of 10 seconds per cycle (5 seconds of loading and 5 seconds of unloading). Figure 3.14 shows the typical test setup. The glued specimen along with the base plate was mounted inside the jig and an LVDT was attached at the back. During testing, one plate was held motionless while the other plate was pulled at the specified displacement and pushed to return to its original position. This load simulates the movement of the overlay and directly produces tensile stress in the center of the specimen. Measured parameters are the applied load (stress), displacement (fixed), time, number of load cycles, and test temperature. The test was terminated at either 1,000 cycles or at a load reduction of 93 percent, whichever

occurred first. For each type of mixture, three replicate specimens were tested. Figure 3.15 shows the step-by-step process of the OT test.

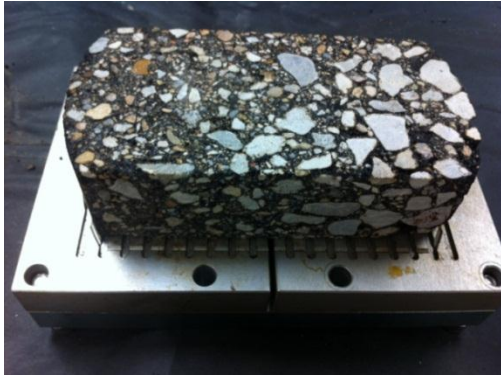


Figure 3.13 Glued OT specimen on metal base plates



Figure 3.14 Typical OT test setup within AMPT

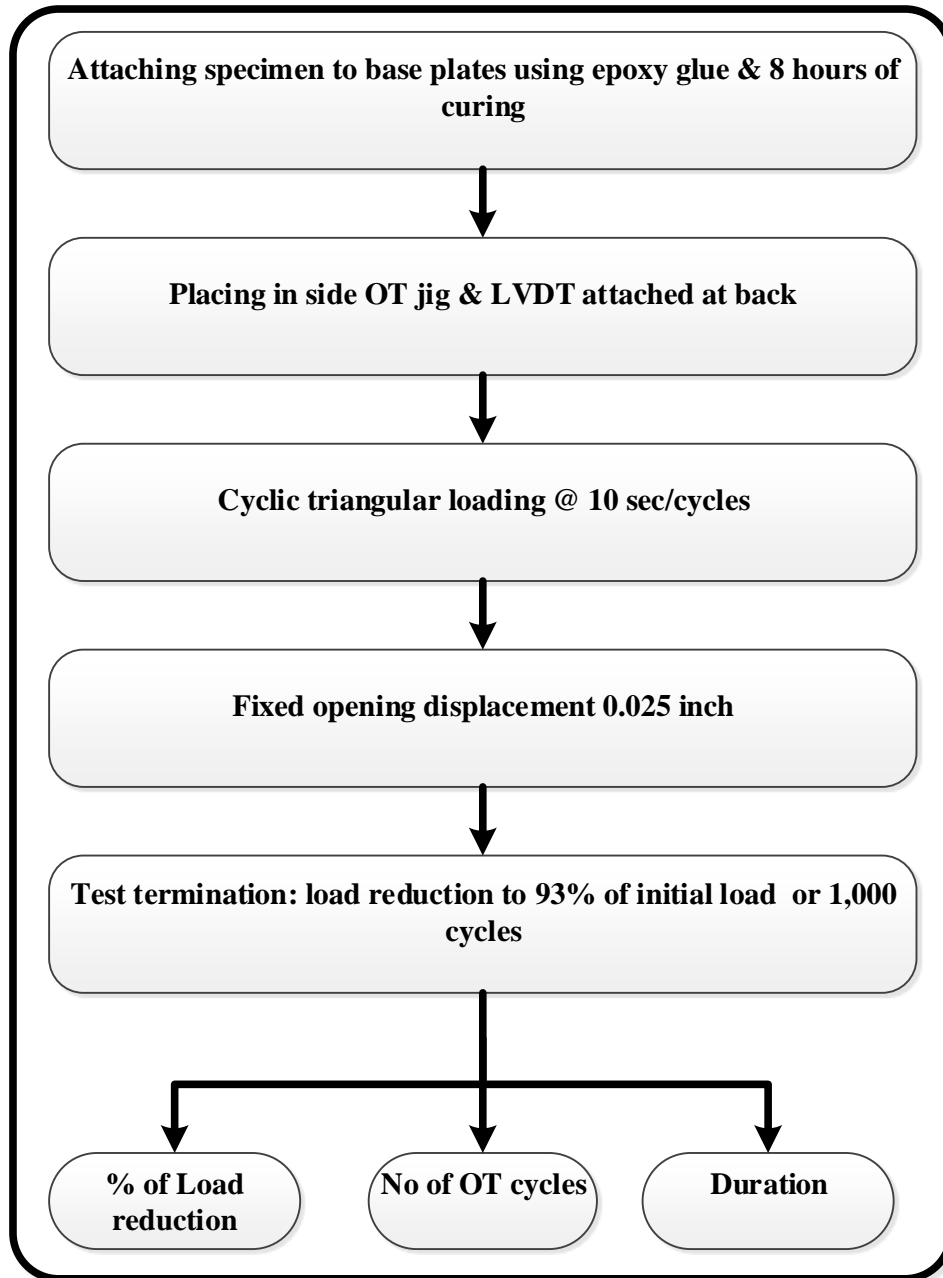


Figure 3.15 OT testing process

Chapter 4 - Analysis and Results

4.1 SCB Test Results

The SCB test was one laboratory test method investigated in this study for the characterization of cracking resistance of Superpave mixtures. Three replicate specimens for each mix design were tested in both static and repetitive SCB tests.

4.1.1 Static SCB Test Results

In the static SCB test, crack initiation and subsequent propagation was centrally localized using a 0.25-inch notching at the base of the specimen. Bending strain and stress at maximum load were used as the indicative measures of HMA ductility, tensile strength, and cracking resistance. Average static SCB test results are given in Table 4.1.

Results indicate that SM-12.5A mixture with 5.2% asphalt content, SR-12.5A mixture with 20% RAP content from the first source, and 40% RAP content from the second source demonstrate best cracking resistance among the SM and SR mixtures, respectively. This performance evaluation is based on bending displacement achieved at the peak tensile stress. These mixtures are considered to have the most potential to elongate prior to tensile cracking failure. Figure 4.1 shows that, with an increase in asphalt content, the displacement at maximum load or tensile stress increased. Though the mixture with 4.9% binder showed higher peak tensile stress, the displacement at the peak load was less than that of 5.2% binder. Thus, the latter can be considered to have the best cracking resistance among the “no RAP” mixtures. Results of SR-12.5A mixtures with the first and second sources of RAP are shown in Figures 4.2 and 4.3, respectively. For first source of RAP, performance deteriorated with an increase in RAP content. However, the second source of RAP performed differently and the highest displacement at peak load was observed at 40% RAP content. Although SR-12.5A mixture with 30% RAP from the second source showed maximum elongation, it had lower displacement at peak load. Thus, this mixture was unable to show good cracking resistance compared to the other two mixtures.

Table 4.1 Average static SCB test results

SM-12.5A Mixture				
Asphalt Content (%)	Air Void (%)	Maximum Load (KN)	Maximum Tensile Stress (MPa)*	Ram Displacement @ Maximum Load (mm)*
5.2	7.3	1.75	0.97 (7.3%)	1.94 (12.2%)
4.9	7.4	2.13	1.21 (5.2%)	1.50 (10.1%)
4.6	7.1	1.55	0.88 (6.1%)	1.34 (8.2%)
SR-12.5A Mixture (first RAP Source)				
RAP Content (%)	Air Void (%)	Maximum Load (KN)	Maximum Tensile Stress (MPa)*	Ram Displacement @ Maximum Load (mm)*
20	7.3	2.55	1.45 (9.4%)	1.97 (11.4%)
30	7.2	3.15	1.79 (6.9%)	1.33 (6.2%)
40	7.3	3.88	2.21 (8.8%)	0.87 (7.2%)
SR-12.5A Mixture (second RAP Source)				
RAP Content (%)	Air Void (%)	Maximum Load (KN)	Maximum Tensile Stress (MPa)*	Ram Displacement @ Maximum Load (mm)*
20	7.2	2.48	1.41 (5.5%)	1.32 (3.3%)
30	7.1	1.72	0.98 (2.3%)	0.95 (10.7%)
40	7.2	3.12	1.77 (4.3%)	1.57 (8.3%)

*COV shown in parenthesis; 1 KN = 224 lbf; 1 MPa = 145 psi

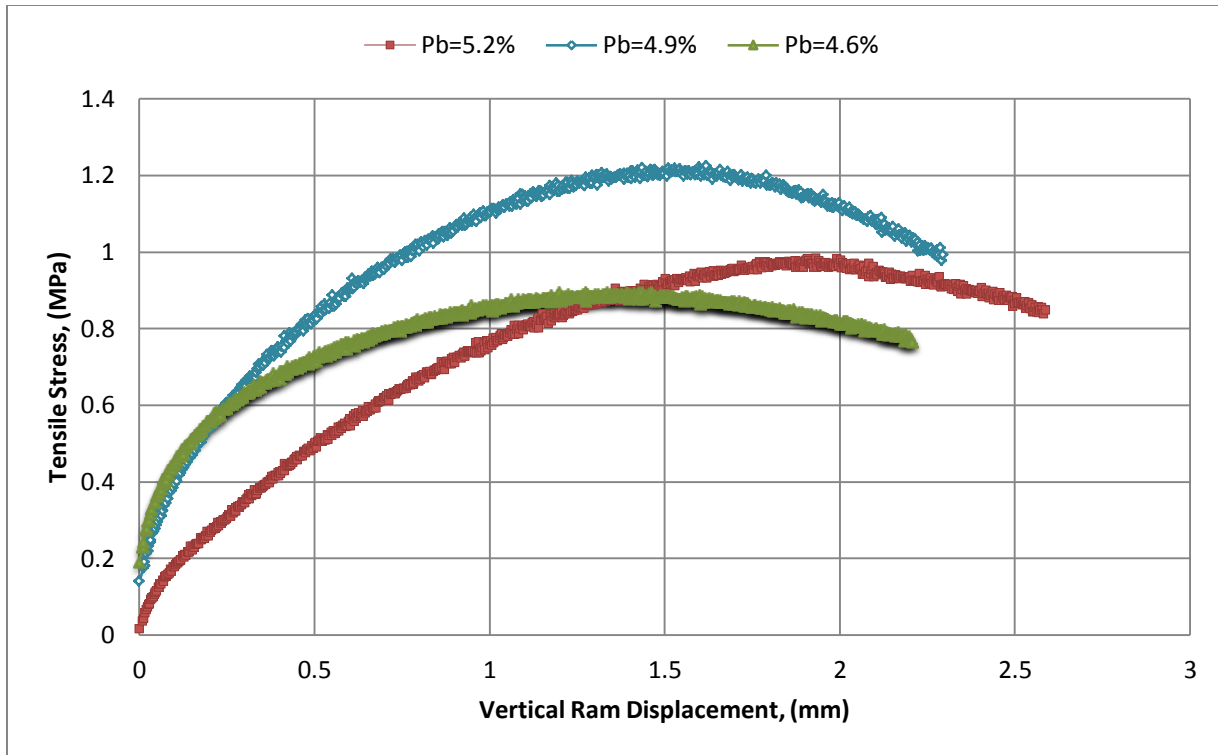


Figure 4.1 Stress-displacement curve for SM-12.5A mixture

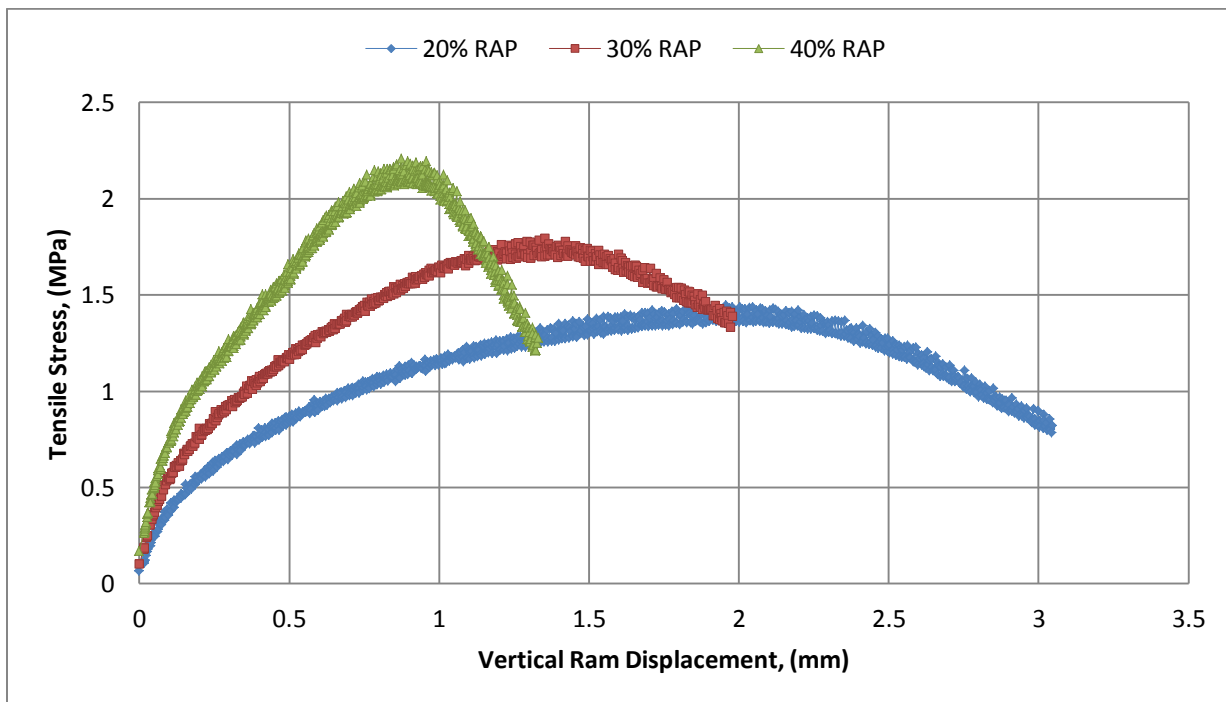


Figure 4.2 Stress-displacement curve for SR-12.5A mixture with first source of RAP

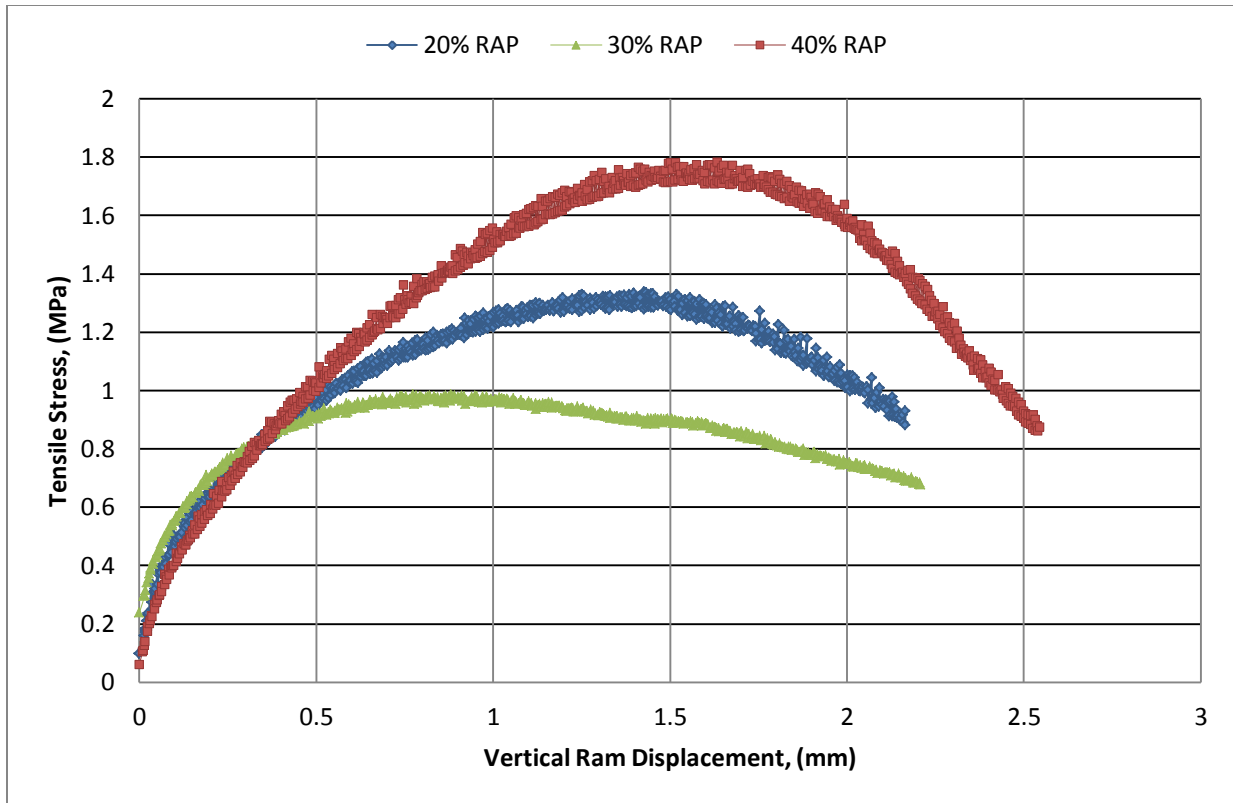


Figure 4.3 Stress-displacement curve for SR-12.5A mixture with second source of RAP

4.1.2 Repetitive SCB Test Results

R-SCB test was performed at 10 Hz (without any rest period) and 77⁰ F. Since R-SCB test requires an input of peak load from the static SCB test, initial tests were performed at each of 30%, 40%, 50%, and 60% of static SCB test peak failure load. After considering the loading parameters used and to avoid early specimen failure, 50% was selected as a reasonable R-SCB load input. In addition, results for 30% static peak load were also considered for correlation analysis to check for a different correlation pattern with the volumetric properties. Results are shown in Tables 4.2, 4.4, and 4.6, followed by Figures 4.4, 4.5 and 4.6. Results of R-SCB tests are explained by the number of load repetitions completed prior to the fracture failure. All results represent an average of at least three replicate specimens per mix type.

Table 4.2 R-SCB test results for SM-12.5A mixture

5.2% Asphalt					
% of Static SCB Peak Load	R-SCB Input Load (KN)	Average Time (min)	Average SCB Load Repetitions to crack Failure	Standard Deviation	COV (%)
30	0.53	148.72	89,233	3,636	4.1
40	0.71	77.77	46,663	3,292	7.1
50	0.89	38.74	23,243	2,382	10.2
60	1.07	19.23	11,537	727	6.3
4.9% Asphalt					
% of Static SCB Peak Load	R-SCB Input Load (KN)	Average Time (min)	Average SCB Load Repetitions to crack Failure	Standard Deviation	COV (%)
30	0.64	85.73	51,440	2,058	4.0
40	0.86	41.81	25,087	3,422	13.6
50	1.07	24.53	14,720	3,009	20.4
60	1.28	13.74	8,247	997	12.1
4.6% Asphalt					
% of Static SCB Peak Load	R-SCB Input Load (KN)	Average Time (min)	Average SCB Load Repetitions to crack Failure	Standard Deviation	COV (%)
30	0.46	64.05	38,430	1,810	4.7
40	0.62	24.68	14,807	2,418	16.3
50	0.77	14.19	8,513	1,441	16.9
60	0.92	7.55	4,530	134	3.0

1 KN = 224 lbf

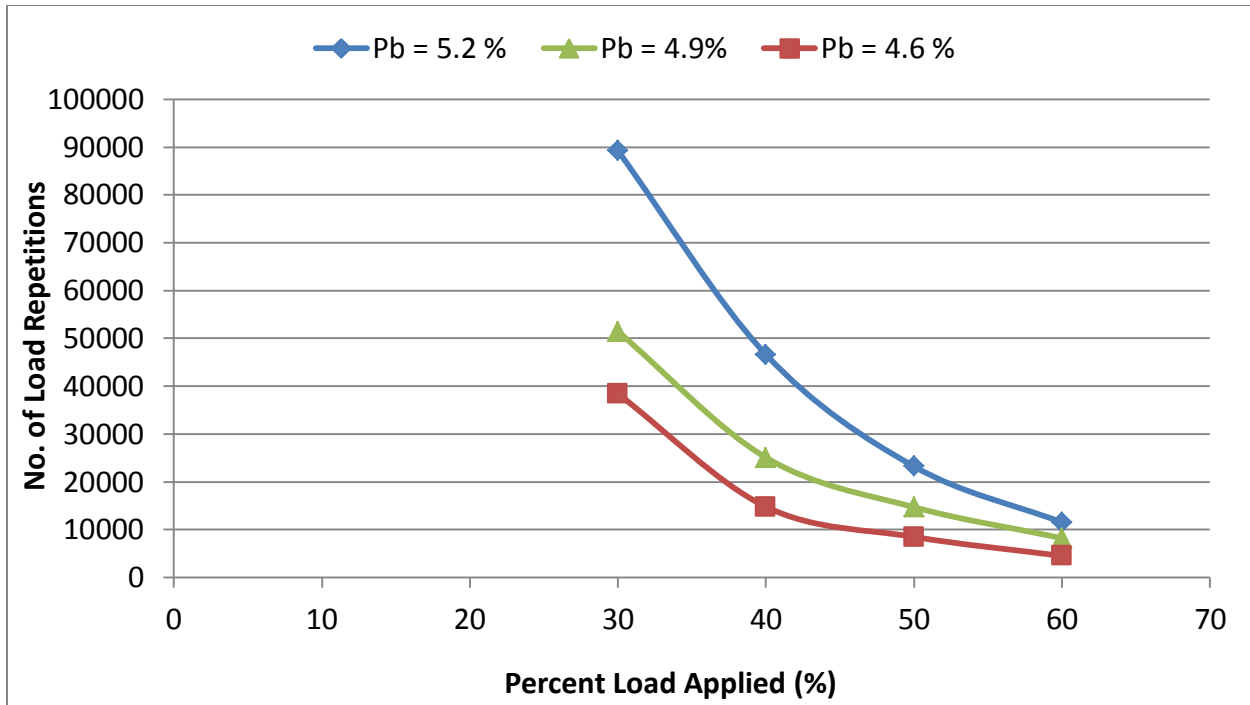


Figure 4.4 R-SCB percent load relationship curve for SM-12.5A

Figure 4.4 demonstrates that SM-12.5A mixture with 5.2% asphalt content has the best cracking resistance because it can resist the highest number of load repetitions before fracture failure when compared to the other two mixtures. Performance deteriorated with decreasing amounts of asphalt content and was similar to results of static SCB tests of SM-12.5A mixtures. In Table 4.3, performance improvement compared to the 4.6% asphalt (worst among these three) is shown. Results indicate that, “no RAP” Superpave mixture with 5.2% asphalt can resist more than twice the number of load repetitions to failure.

Table 4.3 Comparative cracking resistance improvement with increasing asphalt content

Asphalt Content (%)	Performance Improvement from mixture with 4.6% Asphalt (%)			
	30% of Static SCB Peak Load*	40% of Static SCB Peak Load*	50% of Static SCB Peak Load*	60% of Static SCB Peak Load*
5.2	132	215	173	155
4.9	34	69	73	60

*Static load to cause fracture

Table 4.4 R-SCB test results for SR-12.5A mixture with first source of RAP

20% RAP					
% of Static SCB Peak Load	R-SCB Input Load (KN)	Average Time (min)	Average SCB Load Repetitions to crack Failure	Standard Deviation	COV (%)
30	0.71	91.58	54,947	5,301	9.6
40	0.94	43.43	26,060	3,704	14.2
50	1.18	22.68	13,607	1,118	8.2
60	1.42	11.56	6,933	293	4.2
30% RAP					
% of Static SCB Peak Load	R-SCB Input Load (KN)	Average Time (min)	Average SCB Load Repetitions to crack Failure	Standard Deviation	COV (%)
30	0.90	79.22	47,533	1,249	2.6
40	1.20	41.55	24,930	901	3.6
50	1.49	18.71	11,227	572	5.1
60	1.79	8.80	5,280	305	5.8
40% RAP					
% of Static SCB Peak Load	R-SCB Input Load (KN)	Average Time (min)	Average SCB Load Repetitions to crack Failure	Standard Deviation	COV (%)
30	1.05	70.42	42,253	2,980	7.0
40	1.4	35.26	21,157	2,541	12.0
50	1.75	16.86	10,113	254	2.5
60	2.1	7.98	4,787	351	7.3

1 KN = 224 lbf

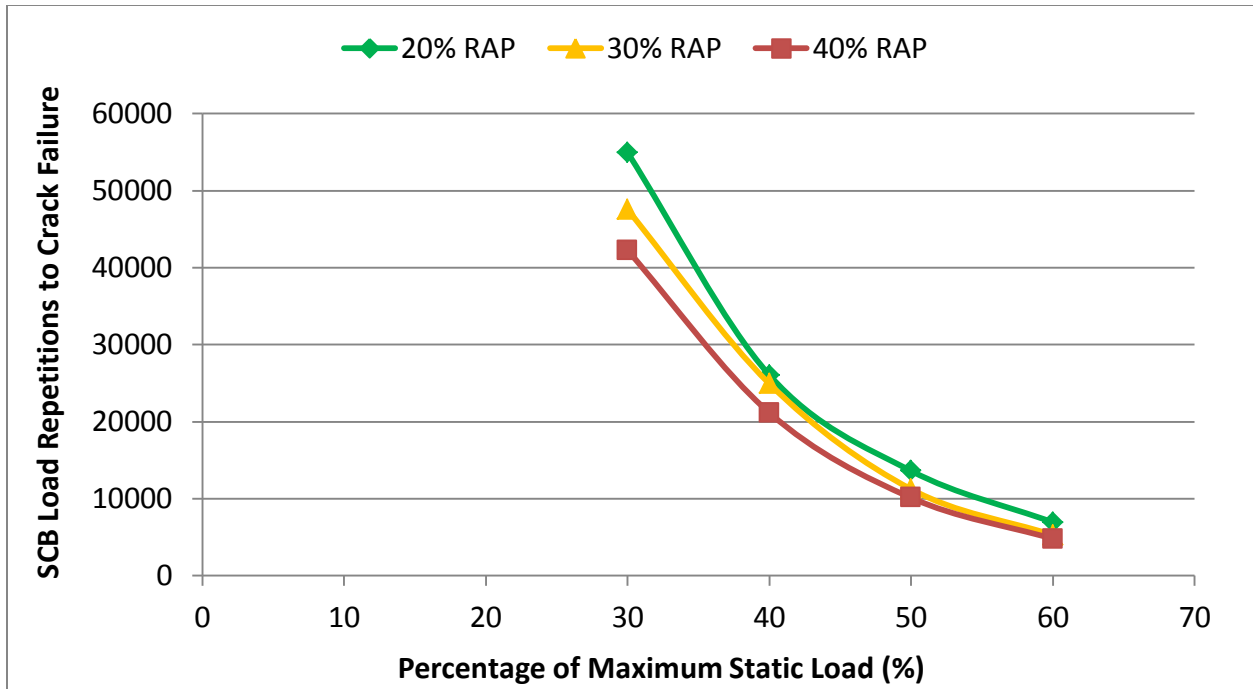


Figure 4.5 R-SCB percent load relationship curve for SR-12.5A with first source of RAP

Figure 4.5 shows that the SR-12.5A mixture with 20% RAP content for the first RAP source has the best cracking resistance. Though results for other mixtures are very close (in terms of number of cycles to failure), this mixture demonstrated the highest number of load repetitions before fracture failure compared to the other two mixtures. Performance of these mixtures deteriorated with increasing RAP content and had trends similar to results of static SCB test of the SR-12.5A mixture. Table 4.5 shows the performance improvement compared to the 40% RAP (worst among these three). Results indicate that SR-12.5A mixture with 20% RAP could resist more than 30% number of load repetitions to failure compared to the mixture with 40% RAP.

Table 4.5 Comparative cracking resistance improvement with increasing RAP content (first RAP Source)

RAP Content (%)	Performance Improvement from Mixture with 40% RAP (%)			
	30% of Static SCB Peak Load*	40% of Static SCB Peak Load*	50% of Static SCB Peak Load*	60% of Static SCB Peak Load*
20	30	23	35	45
30	13	18	11	10

*Static load to cause fracture

Table 4.6 R-SCB test results for SR-12.5A mixture with second source of RAP

20% RAP					
% of Static SCB Peak Load	R-SCB Input Load (KN)	Average Time (min)	Average SCB Load Repetitions to crack Failure	Standard Deviation	COV (%)
30	0.89	74.74	44,847	5,801	12.9
40	1.19	37.57	22,540	2,744	12.2
50	1.49	14.32	8,593	894	10.4
60	1.78	8.27	4,960	673	13.6
30% RAP					
% of Static SCB Peak Load	R-SCB Input Load (KN)	Average Time (min)	Average SCB Load Repetitions to crack Failure	Standard Deviation	COV (%)
30	0.81	49.29	29,577	2,010	6.8
40	1.08	23.55	14,130	1,349	9.6
50	1.35	11.38	6,830	721	10.6
60	1.62	6.39	3,837	340	8.8
40% RAP					
% of Static SCB Peak Load	R-SCB Input Load (KN)	Average Time (min)	Average SCB Load Repetitions to crack Failure	Standard Deviation	COV (%)
30	1.07	88.33	52,997	3,045	5.7
40	1.42	44.88	26,930	870	3.2
50	1.78	27.61	16,567	1,743	10.5
60	2.13	14.94	8,963	895	10.0

1 KN = 224 lbf

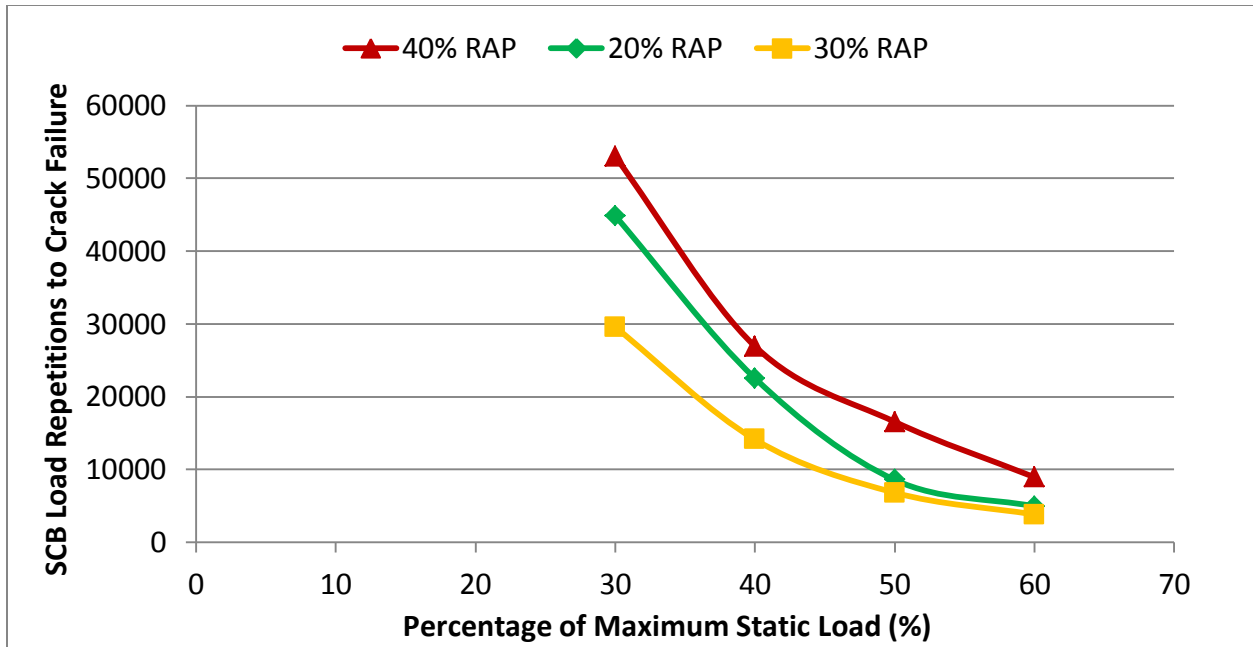


Figure 4.6 R-SCB percent load relationship curve for SR-12.5A with second source of RAP

Figure 4.6 shows that SR-12.5A mixture with 40% RAP content for the second RAP source has the best cracking resistance. This mixture carried the highest number of load repetitions before fracture failure compared to the other two mixtures. Performance of these mixtures had trends different from that of results for SR-12.5A mixtures with the first RAP source possibly because RAP from the second source was comparatively drier. Table 4.7 shows performance improvement compared to the 30% RAP (worst among these three). Results indicate that SR-12.5A mixture with 40% RAP (from the second RAP source) resisted almost twice the number of load repetitions to failure compared to the mixture with 30% RAP.

Table 4.7 Comparative cracking resistance improvement with increasing RAP content (second RAP Source)

RAP Content (%)	Performance Improvement from Mixture with 30% RAP (%)			
	30% of Static SCB Peak Load*	40% of Static SCB Peak Load*	50% of Static SCB Peak Load*	60% of Static SCB Peak Load*
40	79	91	143	134
20	52	60	26	29

*Static load to cause fracture

4.1.3 Crack Initiation and Propagation Investigation

As mentioned in Chapter 3, another set of samples prepared from SM-12.5A and SR-12.5A (both RAP sources) mixtures were used to investigate crack propagation. The clip-on gauge, attached along the notch at the bottom of each specimen, measured the crack mouth opening displacement (CMOD). Using the CMOD results, crack length and stress intensity factor, K_I , were calculated using equations 2.2 and 2.3. Crack lengths for each mixture and stress intensity factors are shown in Table 4.8.

Figures 4.7, 4.8, and 4.9 show the variation in crack length with increasing number of load repetitions. Results have two distinct parts, crack initiation and crack propagation. The crack initiation phase was relatively smaller for all mixture types. Mixtures with higher crack propensity (lesser number of load repetitions) had even smaller crack initiation phase. The crack propagation in such mixtures begins with a steep slope and fails within very few cycles.

The number of load repetitions required for crack initiation (N_i) for each of the mixtures was determined by equation 2.6. Table 4.9 tabulates the back-calculated N_i and observed N_i for each of the mixtures considered in this study.

Table 4.8 Crack lengths and stress intensity factors of mixtures

Mixture	No. of Load Repetitions Prior to Failure	Crack Length (mm)	Stress Intensity Factor (MPa·√mm)
SM-12.5A with 5.2% Asphalt	19,840	68	25
SM-12.5A with 4.9% Asphalt	14,105	61	18
SM-12.5A with 4.6% Asphalt	8,102	68	27
SR-12.5A with 20% RAP (first source)	14,720	63	18
SR-12.5A with 30% RAP (first source)	10,215	64	20
SR-12.5A with 40% RAP (first source)	7,475	57	19
SR-12.5A with 20% RAP (second source)	8,730	62	16
SR-12.5A with 30% RAP (second source)	7,500	60	14
SR-12.5A with 40% RAP (second source)	16,665	57	12

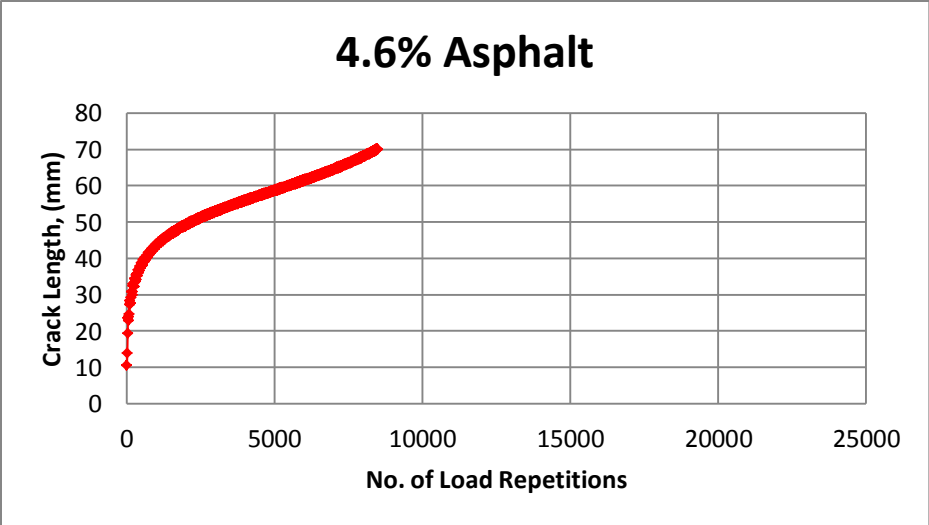
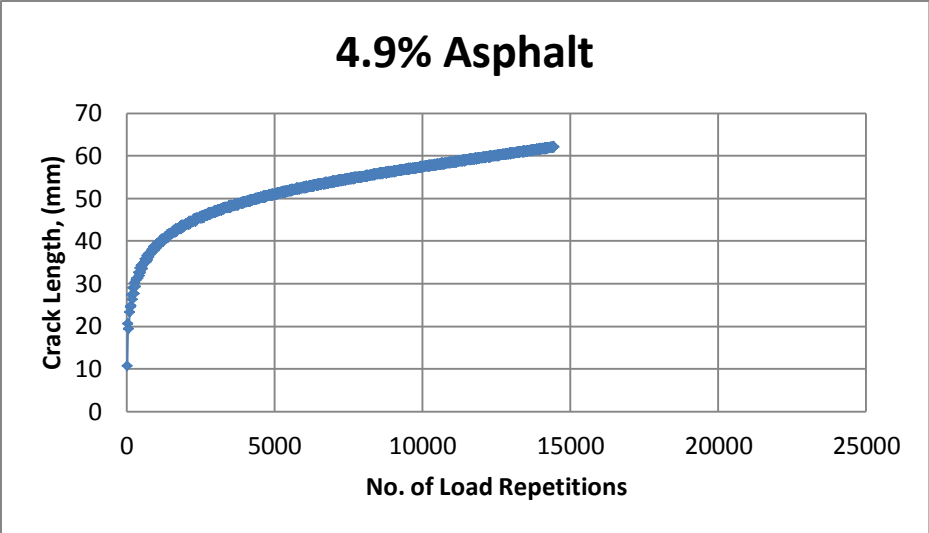
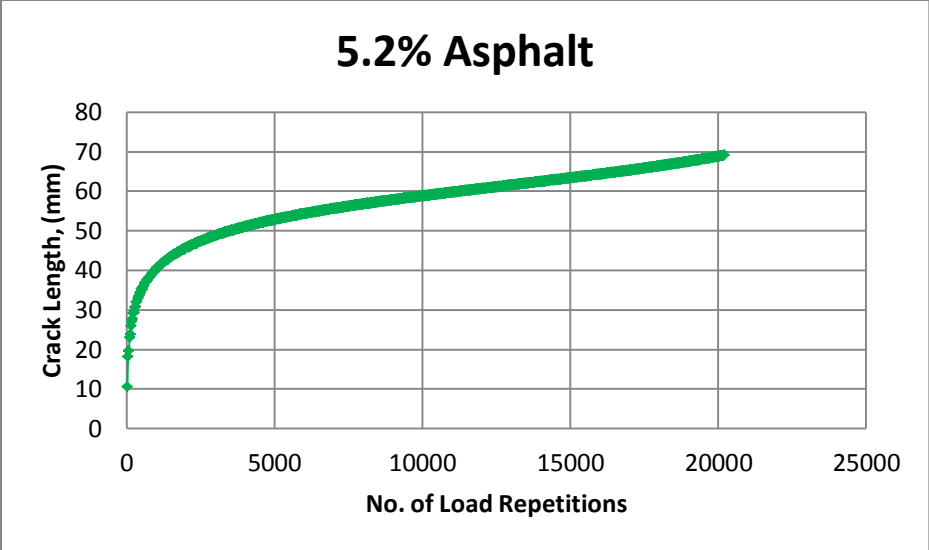


Figure 4.7 Crack length against number of load repetitions for SM-12.5A mixture

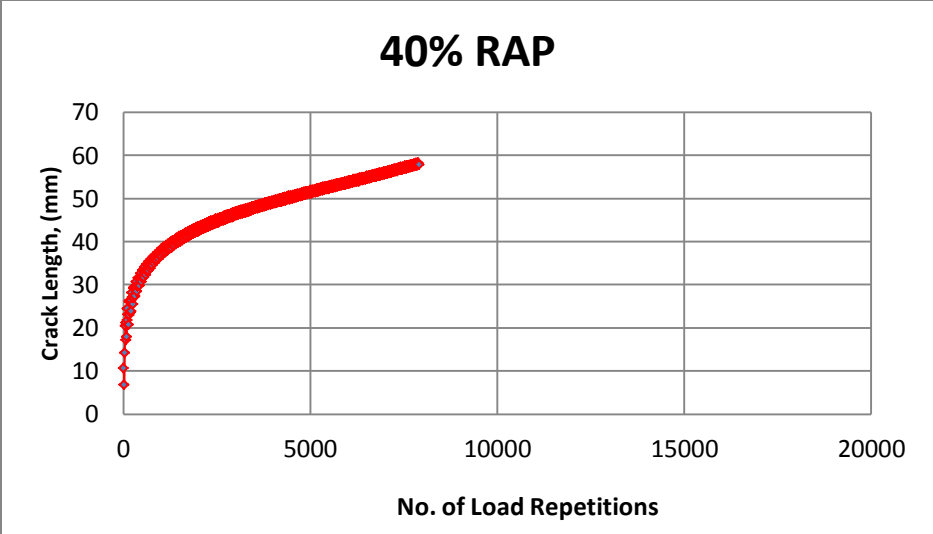
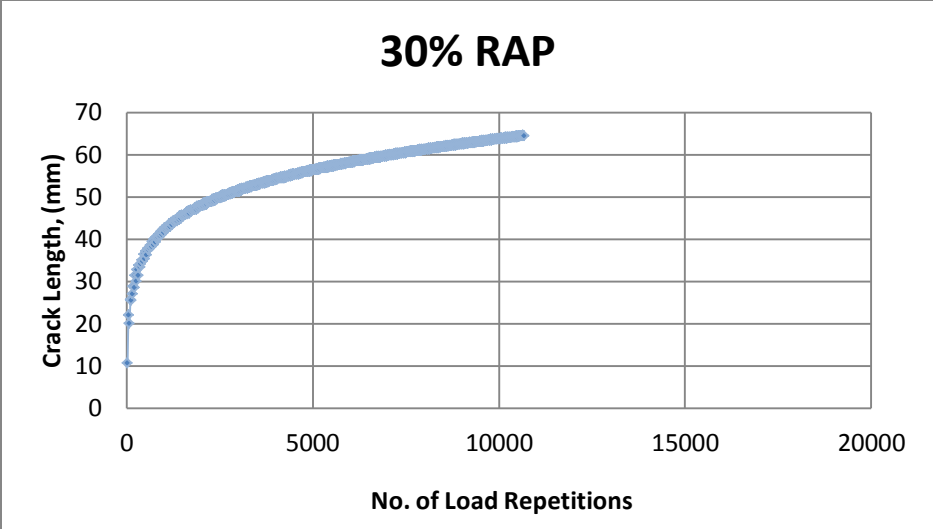
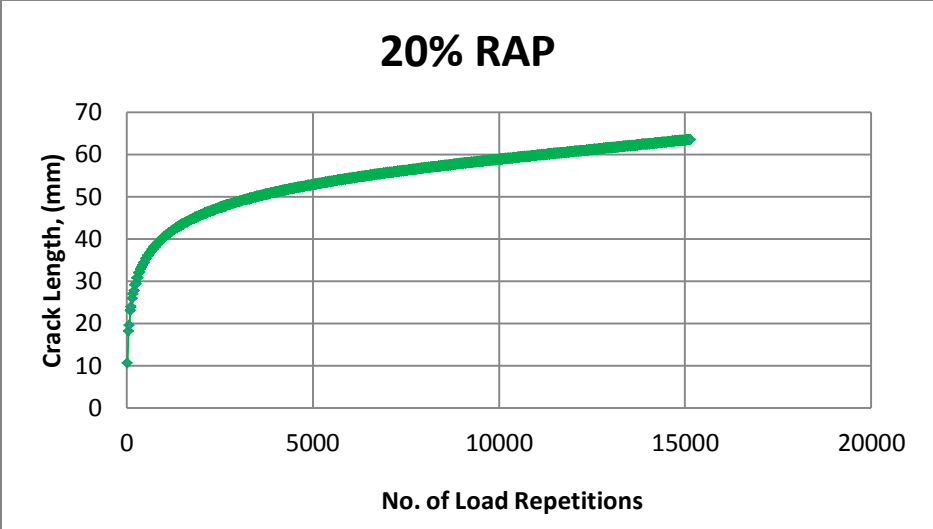


Figure 4.8 Crack length against number of load repetitions for SR-12.5A mixture (first source of RAP)

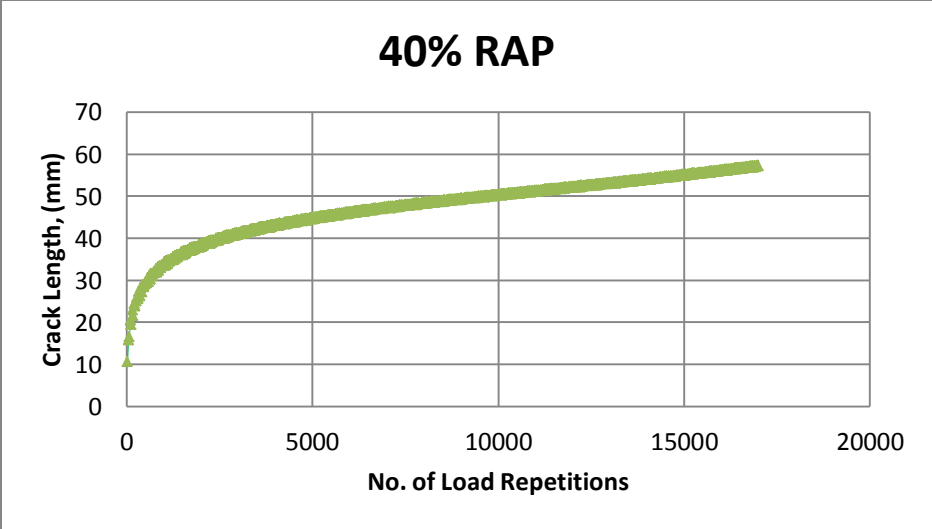
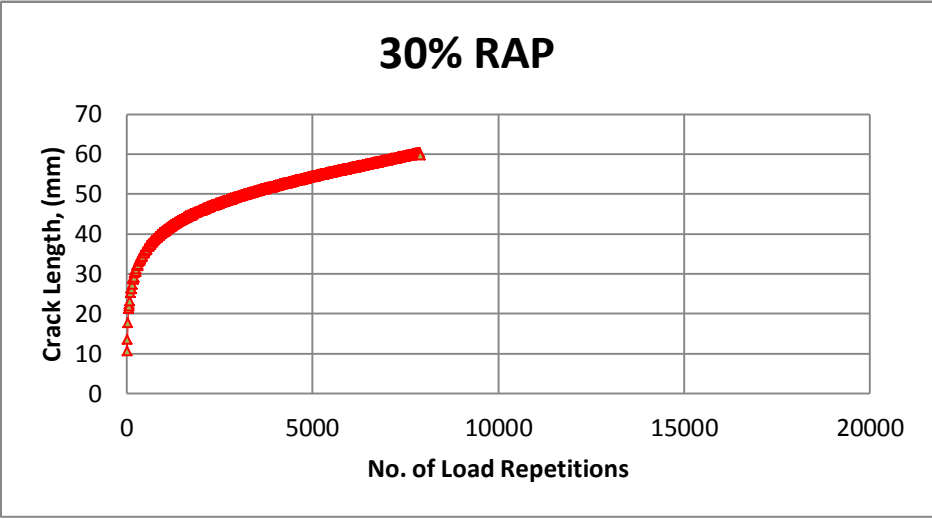
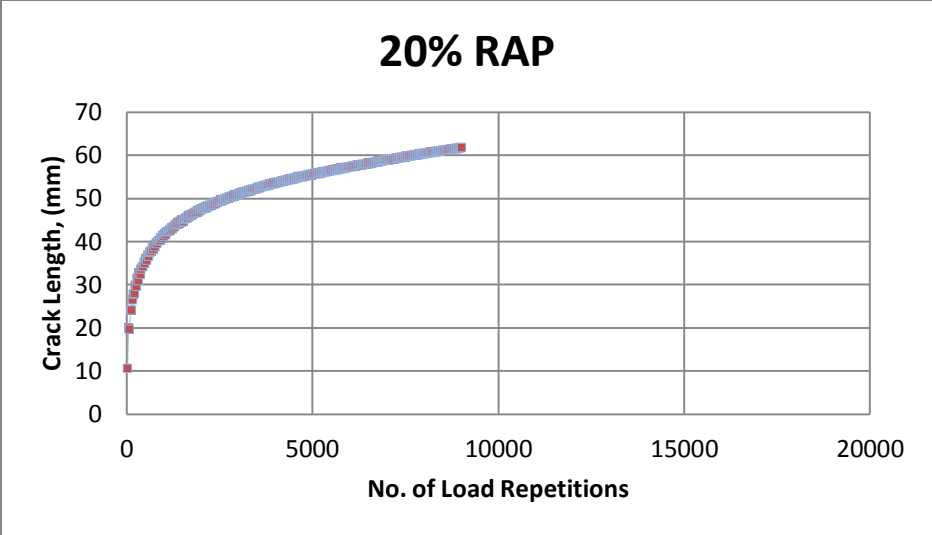


Figure 4.9 Crack length against number of load repetitions for SR-12.5A mixture (second source of RAP)

Table 4.9 Number of load repetitions for crack initiation

Mixture	Observed N_i	Predicted N_i
SM-12.5A with 5.2% Asphalt	2,000	40,876
SM-12.5A with 4.9% Asphalt	1,800	35,892
SM-12.5A with 4.6% Asphalt	2,200	30,273
SR-12.5A with 20% RAP (first source)	2,300	42,196
SR-12.5A with 30% RAP (first source)	2,100	35,272
SR-12.5A with 40% RAP (first source)	1,600	18,731
SR-12.5A with 20% RAP (second source)	1,700	23,983
SR-12.5A with 30% RAP (second source)	1,400	19,872
SR-12.5A with 40% RAP (second source)	2,400	54,392

Figure 4.10 shows the comparison of observed and predicted numbers of load repetitions for crack initiation. The plot gives a fairly good fit with $R^2 = 0.73$. Furthermore, sensitivity analysis was performed to study whether the variation in the asphalt content of mixtures and percentage of air voids in compacted specimens are affecting the mathematical model of predicted N_i for crack initiation.

Predicted N_i increases with increasing asphalt content and decreasing percentage of air voids (Lytton et al., 1993). With higher asphalt content, mixtures would be able to resist more load cycles prior to crack initiation. On the other hand, the air voids initiate crack growth. Thus, significantly higher air void in specimens would expedite the formation of micro-cracks. However, all compacted specimens used in this study had air voids within 7-8% and did not show much variation of the predicted N_i for crack initiation.

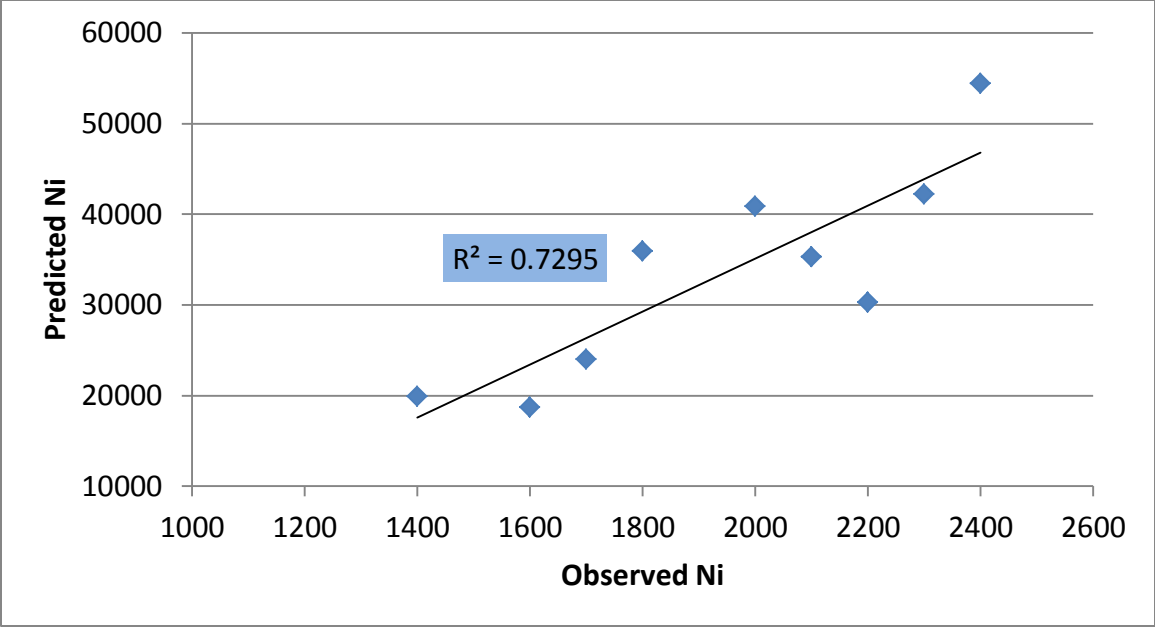


Figure 4.10 Comparison of estimated N_i and predicted N_i

4.2 Texas Overlay (OT) Test Results

OT test was the other laboratory test method performed for characterizing the cracking resistance of the Superpave mixtures. Results of standard OT tests are summarized in Tables 4.10, 4.11 and 4.12. The results in these tables represent an average of all three replicate specimens for each mix type. All specimens were confirmed to have met the target air void specification ($7 \pm 1\%$). The percentages in parentheses represent the coefficient of variation (COV) of the respective mix data set.

Table 4.10 Average OT test results for SM-12.5A mixture

Asphalt Content (%)	Air Void (%)	Average Initial Peak Load (KN)	Average No. of OT Cycles of Failure (N_{OT})*	Duration (Minutes)
5.2	7.2	2.35	1000 (0%)	167
4.9	7.3	2.90	720 (8.7%)	120
4.6	7.3	3.28	380 (10.4%)	63

*COV shown in parenthesis; 1 KN = 224 lbf

In the OT test, the cracking resistance potential of a mixture is measured and defined in terms of the number of cycles to failure, where failure is defined as 93 percent reduction in initial load. As a tentative mix screening criteria, mixes that last over 300 cycles are considered satisfactory with respect to the laboratory fatigue resistance (Walubita et al., 2004). With this criterion, in Table 4.10 the best cracking resistance is shown by the mixture with 5.2% asphalt content. All replicates of this mixture passed 1,000 cycles (maximum threshold) before reaching 93% load reduction. The mixture with 4.9% asphalt had a fairly good performance. SM mixture containing 4.6% binder had a satisfactory performance, but it still was the worst among three. Most likely, low asphalt content contributed to low cracking resistance.

Table 4.11 Average OT test results for SR-12.5A mixture for first source of RAP

RAP Content (%)	Air Void (%)	Average Initial Peak Load (KN)	Average No. of OT Cycles of Failure (N_{OT})*	Duration (Minutes)
20	7.2	2.35	805 (17.4%)	134
30	7.3	2.90	477 (24.5%)	80
40	7.1	3.28	128 (26.9%)	21

*COV shown in parenthesis; 1 KN = 224 lbf

Table 4.11 shows the OT results for the SR-12.5A mixture with the first RAP source. The mixture with 20% RAP content had the best cracking resistance among the three mixtures. The mixture containing 30% RAP had a somewhat satisfactory performance; however, SR mixture with 40% RAP was below 300 cycles. Thus, this mixture can be considered to have unsatisfactory fracture resistance.

Table 4.12 Average OT test results for SR-12.5A mixture for second source of RAP

RAP Content (%)	Air Void (%)	Average Initial Peak Load (KN)	Average No. of OT Cycles of Failure (N_{OT})*	Duration (Minutes)
20	7.1	2.66	296 (25.2%)	49
30	7.3	2.10	71 (22.7%)	12
40	7.1	3.09	435 (14.9%)	73

*COV shown in parenthesis; 1 KN = 224 lbf

Table 4.12 shows the OT results for the SR-12.5A mixture with the second RAP source. The mixture with 40% RAP content had the best cracking resistance among the three mixtures. The mixture containing 20% RAP portrayed an average number of 296 OT cycles, which was marginal when compared to the threshold value (300 cycles). SR mixture prepared with 30% RAP from the second source also performed poorly.

4.3 Statistical Analysis

4.3.1 Correlation Analysis

In this study, the statistical analysis was performed using a software package called Statistical Analysis System (SAS) ®. The purposes of correlation analysis were:

1. To discover whether there is a relationship between variables;
2. To find out the type of relationship – whether it is positive or negative;
3. To find the strength of the relationship between the two variables.

Test statistics, called the correlation coefficient r , measures the degree of association between the variables and varies between -1 and +1. The strength of relationship is determined by r values tabulated in Table 4.13.

Table 4.13 Interpretation of correlation (Mendenhall, and Sincich, 2003)

Correlation Strength	Pearson's Correlation Coefficient (r)	
	Positive	Negative
None/Negligible	0.0 to 0.3	-0.3 to 0.0
Weak	0.3 to 0.7	-0.7 to -0.3
Strong	0.7 to 1.0	-1.0 to -0.7

The association of different variables with the cracking test results (R-SCB and OT) was identified using the correlation analysis. Variables include virgin asphalt content (%), asphalt contained in RAP (%), total asphalt content (%), air voids (%), VMA (%), VFA (%), film thickness (microns), and dust proportion. Detailed volumetric data for each replicate specimen for these tests are tabulated in the appendix.

Table 4.14 Correlation matrix for SM-12.5A mixture (R-SCB test)

	Virgin Asphalt Content (%)	Air Void (%)	VMA @ N _F (%)	VFA @ N _F (%)	Film Thickness in Microns	Cycles @ 30% F _{peak}	Cycles @ 50% F _{peak}	Dust Proportion
Virgin Asphalt Content (%)	1.00	0.45 (0.22)	0.99 <.0001	0.87 (0.00)	0.98 <.0001	0.96 <.0001	0.95 <.0001	-0.63 (0.07)
Air Void (%)	0.45 (0.22)	1.00	0.41 (0.27)	0 (0.99)	0.38 (0.32)	0.28 (0.47)	0.3 (0.43)	0 (1.00)
VMA @ N_F (%)	0.99 <.0001	0.41 (0.27)	1.00	0.91 (0.00)	(0.97) <.0001	0.94 (0.00)	0.91 (0.00)	-0.61 (0.08)
VFA @ N_F (%)	0.87 (0.00)	0 (0.99)	0.91 (0.00)	1.00	0.88 (0.00)	0.9 (0.00)	0.86 (0.00)	-0.65 (0.06)
Film Thickness in Microns	0.98 <.0001	0.38 (0.32)	0.97 <.0001	0.88 (0.00)	1.00	0.99 <.0001	0.95 (0.00)	-0.76 (0.02)
Cycles @ 30% F_{peak}	0.96 <.0001	0.28 (0.47)	0.94 (0.00)	0.9 (0.00)	0.99 <.0001	1.00	0.94 (0.00)	-0.81 (0.01)
Cycles @ 50% F_{peak}	0.95 <.0001	0.3 (0.43)	0.91 (0.00)	0.86 (0.00)	0.95 (0.00)	0.94 (0.00)	1.00	-0.66 (0.05)
Dust Proportion	-0.63 (0.07)	0 (1.00)	-0.61 (0.08)	-0.65 (0.06)	-0.76 (0.02)	-0.81 (0.01)	-0.66 (0.05)	1.00

**p*-value shown in parenthesis

Table 4.14 shows the correlation coefficient values and associated *p*-values for SM-12.5A mixture in the R-SCB test. Figure 4.11 illustrates scatter plots of the variables. When drawing conclusions from the correlation table, both the *p*-value of the relationships as well as their scatter plots were taken into consideration. If *p*-value was greater than 0.05, then the conclusion could not be made that the correlation coefficient is significantly different than zero. Therefore, such relationships were not considered since the analysis might not be valid. Analysis results show that variables virgin asphalt content (0.95), VMA (0.91), and film thickness (0.95) have strong correlation with the number of cycles obtained at 50% of F_{peak} as input. Some variables had weak negative correlation, such as asphalt content and dust proportion (-0.63), VMA and dust proportion (-0.61), and cycles and dust proportion (-0.66). Film thickness and dust proportion have somewhat strong negative correlation (-0.76).

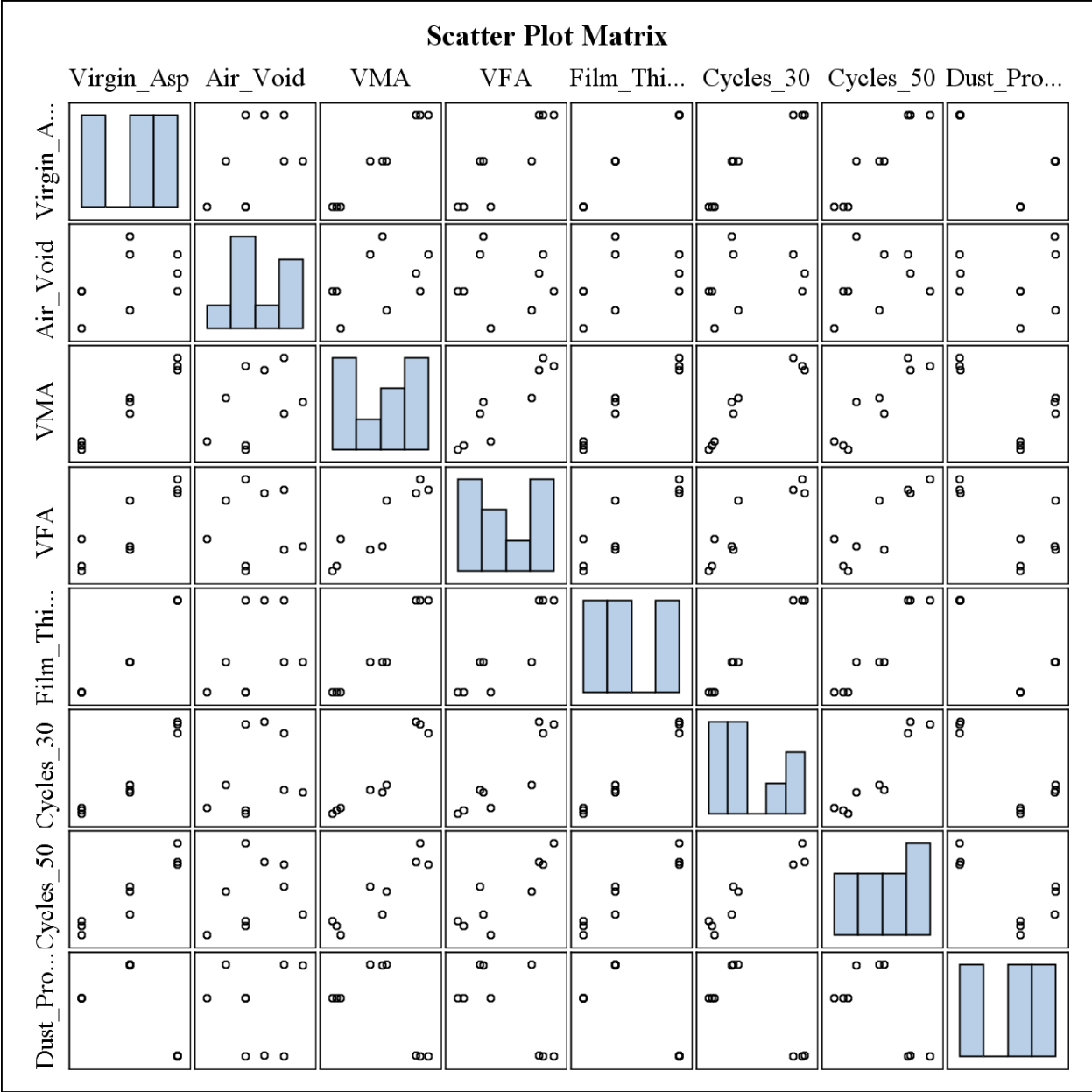


Figure 4.11 Scatter plot matrix for SM-12.5A mix (R-SCB test)

Table 4.15 Correlation matrix for SR-12.5A mixture with first RAP source (R-SCB test)

	Total Asphalt Content (%)	Virgin Asphalt (%)	Asphalt Contained in RAP (%)	Air Void (%)	VMA @ N_F (%)	VFA @ N_F (%)	Film Thickness in Microns	Cycles @ 30% Peak Load	Cycles @ 50% Peak Load	Dust Proportion
Total Asphalt Content (%)	1.00	0.87 (0.00)	-0.72 (0.03)	-0.17 (0.66)	0.68 (0.05)	0.56 (0.11)	0.76 (0.02)	0.60 (0.09)	0.56 (0.12)	-0.74 (0.02)
Virgin Asphalt (%)	0.87 (0.00)	1.00	-0.97 <.0001	-0.54 (0.14)	0.95 <.0001	0.89 (0.00)	0.98 <.0001	0.84 (0.01)	0.85 (0.00)	-0.98 <.0001
Asphalt Contained in RAP (%)	-0.72 (0.03)	-0.97 <.0001	1.00	0.66 (0.05)	-0.99 <.0001	-0.96 <.0001	-1.00 <.0001	-0.87 (0.00)	-0.91 (0.00)	1.00 <.0001
Air Void (%)	-0.17 (0.66)	-0.54 (0.14)	0.66 (0.05)	1.00	-0.66 (0.05)	-0.84 (0.00)	-0.64 (0.06)	-0.67 (0.05)	-0.62 (0.07)	0.65 (0.06)
VMA @ N_F (%)	0.68 (0.05)	0.95 <.0001	-0.99 <.0001	-0.66 (0.05)	1.00	0.96 <.0001	0.99 <.0001	0.81 (0.01)	0.88 (0.00)	-0.99 <.0001
VFA @ N_F (%)	0.56 (0.11)	0.89 (0.00)	-0.96 <.0001	-0.84 (0.00)	0.96 <.0001	1.00	0.95 (0.00)	0.84 (0.01)	0.86 (0.00)	-0.95 <.0001
Film Thickness in Microns	0.76 (0.02)	0.98 <.0001	-1.00 <.0001	-0.64 (0.06)	0.99 <.0001	0.95 (0.00)	1.00	0.87 (0.00)	0.90 (0.00)	-1.00 <.0001
Cycles @ 30% F_{peak}	0.60 (0.09)	0.84 (0.01)	-0.87 (0.00)	-0.67 (0.05)	0.81 (0.01)	0.84 (0.01)	0.87 (0.00)	1.00	(0.92)	-(0.87) (0.00)
Cycles @ 50% F_{peak}	0.56 (0.12)	0.85 (0.00)	-0.91 (0.00)	-0.62 (0.07)	0.88 (0.00)	0.86 (0.00)	0.90 (0.00)	0.92 (0.00)	1.00	-0.91 (0.00)
Dust Proportion	-0.74 (0.02)	-0.98 <.0001	1.00 <.0001	0.65 (0.06)	-0.99 <.0001	-0.95 <.0001	-1.00 <.0001	-0.87 (0.00)	-0.91 (0.00)	1.00

**p*-value shown in parenthesis

Table 4.15 shows the correlation matrix for SR-12.5A mixtures from the first RAP source. Figure 4.12 illustrates scatter plots of the variables. Variables total asphalt content and VMA (0.68) and air void and dust proportion (0.65) had weak positive correlation. Dust proportion was observed to have strong negative correlation with VMA (-0.99), film thickness (-1.00), and number of cycles at 50% of F_{peak} as input (0.91).

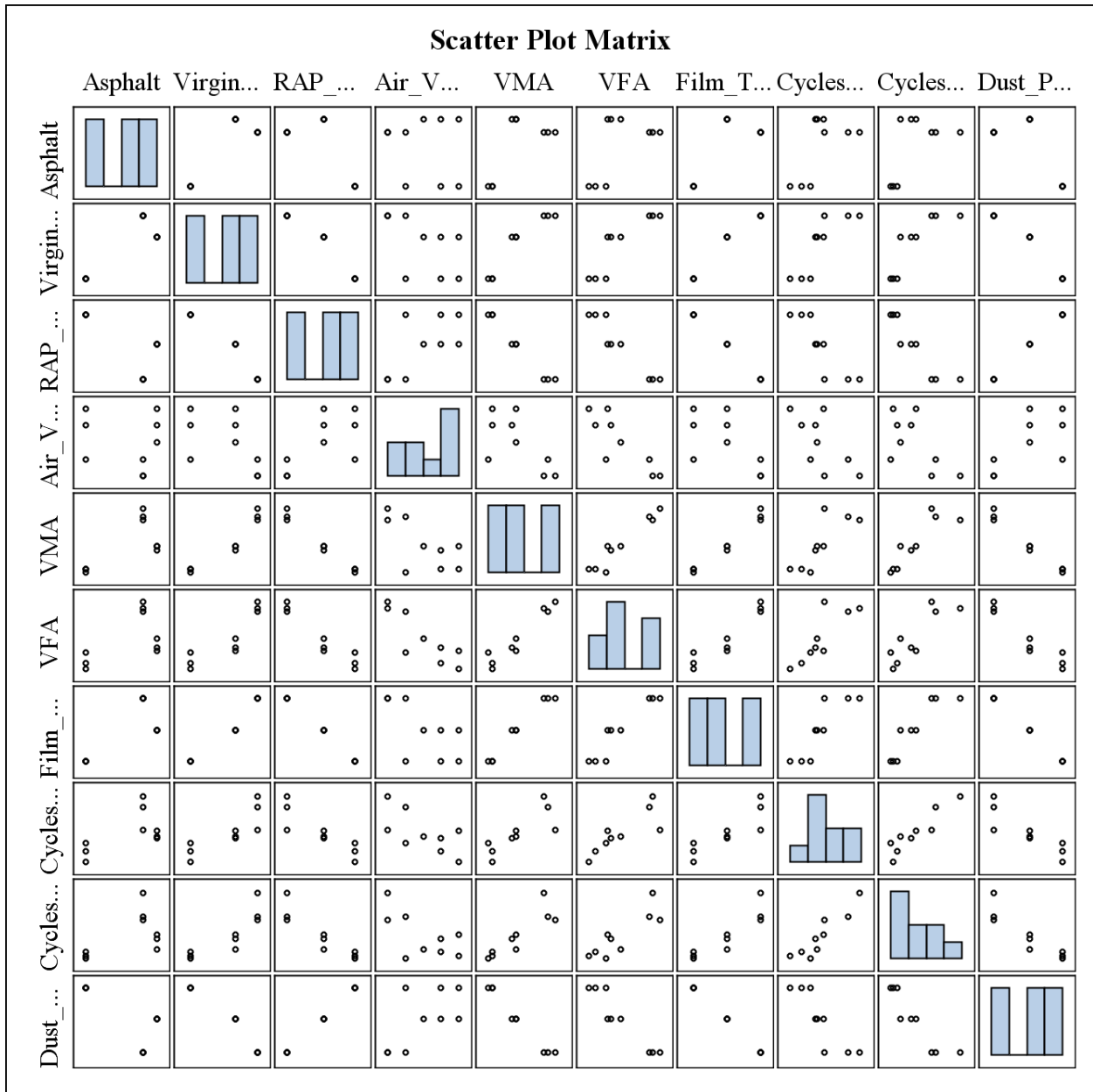


Figure 4.12 Scatter plot matrix for SR-12.5A mix with first source of RAP (R-SCB test)

Table 4.16 Correlation matrix for SR-12.5A mixture with second RAP source (R-SCB test)

	Total Asphalt Content (%)	Virgin Asphalt (%)	Asphalt Contained in RAP (%)	Air Void (%)	VMA @ N_F (%)	VFA @ N_F (%)	Film Thickness in Microns	Cycles @ 30% Peak Load	Cycles @ 50% Peak Load	Dust Proportion
Total Asphalt Content (%)	1.00	0.81 (0.01)	-0.65 (0.06)	0.63 (0.07)	0.63 (0.07)	0.13 (0.74)	-0.58 (0.10)	-0.89 (0.00)	-0.96 <.0001	-0.53 (0.14)
Virgin Asphalt (%)	0.81 (0.01)	1.00	-0.97 <.0001	0.38 (0.32)	0.96 <.0001	0.63 (0.07)	0.02 (0.97)	-0.50 (0.17)	-0.87 (0.00)	-0.93 (0.00)
Asphalt Contained in RAP (%)	-0.65 (0.06)	-0.97 <.0001	1.00	-0.25 (0.52)	-0.99 <.0001	-0.76 (0.02)	-0.24 (0.53)	0.30 (0.43)	0.75 (0.02)	0.99 <.0001
Air Void (%)	0.63 (0.07)	0.38 (0.32)	-0.25 (0.52)	1.00	0.34 (0.37)	-0.43 (0.25)	-0.54 (0.14)	-0.73 (0.02)	-0.61 (0.08)	-0.15 (0.71)
VMA @ N_F (%)	0.63 (0.07)	0.96 <.0001	-0.99 <.0001	0.34 (0.37)	1.00	0.70 (0.04)	0.25 (0.51)	-0.30 (0.43)	-0.73 (0.02)	-0.98 <.0001
VFA @ N_F (%)	0.13 (0.74)	0.63 (0.07)	-0.76 (0.02)	-0.43 (0.25)	0.70 (0.04)	1.00	0.65 (0.06)	0.27 (0.49)	-0.24 (0.54)	-0.82 (0.01)
Film Thickness in Microns	-0.58 (0.10)	0.02 (0.97)	-0.24 (0.53)	-0.54 (0.14)	0.25 (0.51)	0.65 (0.06)	1.00	0.81 (0.01)	0.43 (0.25)	-0.39 (0.30)
Cycles @ 30% F_{peak}	-0.89 (0.00)	-0.50 (0.17)	0.30 (0.43)	-0.73 (0.02)	-0.30 (0.43)	0.27 (0.49)	0.81 (0.01)	1.00	0.84 (0.00)	0.16 (0.69)
Cycles @ 50% F_{peak}	-0.96 <.0001	-0.87 (0.00)	0.75 (0.02)	-0.61 (0.08)	-0.73 (0.02)	-0.24 (0.54)	0.43 (0.25)	0.92 (0.00)	1.00	-0.91 (0.00)
Dust Proportion	-0.53 (0.14)	-0.93 (0.00)	0.99 <.0001	-0.15 (0.71)	-0.98 <.0001	-0.82 (0.01)	-0.39 (0.30)	-0.87 (0.00)	-0.91 (0.00)	1.00

**p*-value shown in parenthesis

Table 4.16 shows the correlation matrix for the SR-12.5A mixtures from the second RAP source. Figure 4.13 illustrates scatter plots of the variables. Variables VMA and number of cycles at 50% of F_{peak} (-0.73), dust proportion and VMA (-0.98), total asphalt content and number of cycles at 50% of F_{peak} as input (-0.96) have strong negative correlations. VMA and total asphalt content (0.63) have a weak positive correlation.

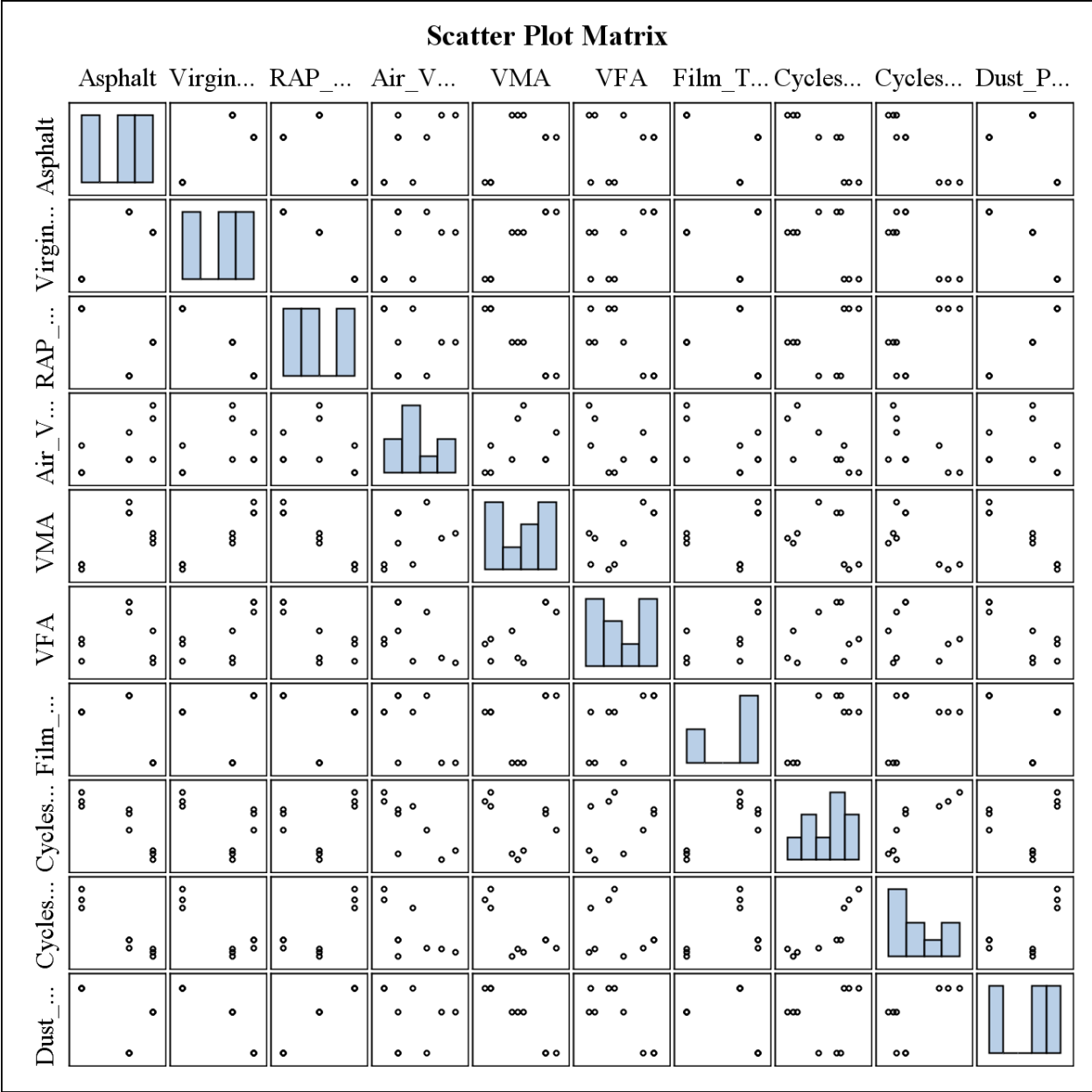


Figure 4.13 Scatter plot matrix for SR-12.5A mix for second source of RAP (R-SCB test)

Table 4.17 Correlation matrix for SM-12.5A mixture (OT test)

	Virgin Asphalt Content (%)	Air Void (%)	VMA @ N_F (%)	VFA @ N_F (%)	Film Thickness in Microns	No. of OT Cycles	Dust Proportion
Virgin Asphalt Content (%)	1.00	-0.73 (0.10)	0.97 (0.00)	0.94 (0.00)	1.00 <.0001	0.97 (0.00)	1.00 <.0001
Air Void (%)	-0.73 (0.10)	1.00	-0.76 (0.08)	-0.87 (0.02)	-0.73 (0.10)	-0.84 (0.04)	-0.73 (0.10)
VMA @ N_F (%)	0.97 (0.00)	-0.76 (0.08)	1.00	0.98 (0.00)	0.97 (0.00)	0.98 (0.00)	0.97 (0.00)
VFA @ N_F (%)	0.94 (0.00)	-0.87 (0.02)	0.98 (0.00)	1.00	0.94 (0.00)	0.99 (0.00)	0.94 (0.00)
Film Thickness in Microns	1.00 <.0001	-0.73 (0.10)	0.97 (0.00)	0.94 (0.00)	1.00	0.97 (0.00)	1.00 <.0001
No. of OT Cycles	0.97 (0.00)	-0.84 (0.04)	0.98 (0.00)	0.99 (0.00)	0.97 (0.00)	1.00	0.97 (0.00)
Dust Proportion	1.00 (0.07)	-0.73 (1.00)	0.97 (0.08)	0.94 (0.06)	1.00 (0.02)	0.97 (0.01)	1.00

**p*-value shown in parenthesis

Table 4.17 shows the correlation matrix of the OT test results of SM-12.5A mixture. Figure 4.14 illustrates the scatter plots of the variables. The number of OT cycles for 5.2% asphalt content reached the maximum threshold value (1,000) which was excluded from statistical analysis since the data was considered to be censored. Variables virgin asphalt content and VMA (0.97), virgin asphalt content and number of cycles (0.97), OT cycles and VMA (0.98), OT cycles and film thickness (0.97), and OT cycles and dust proportion (0.97) had strong positive correlation. Some variables, such as VMA and air void (-0.76), film thickness and air void (-0.73), dust proportion and air void (-0.73) apparently showed strong negative correlation, but the *p*-value for all relationships was higher than 0.05. Also, scatter plots in Figure 4.14 demonstrate that plots did not show a clear linear relationship.

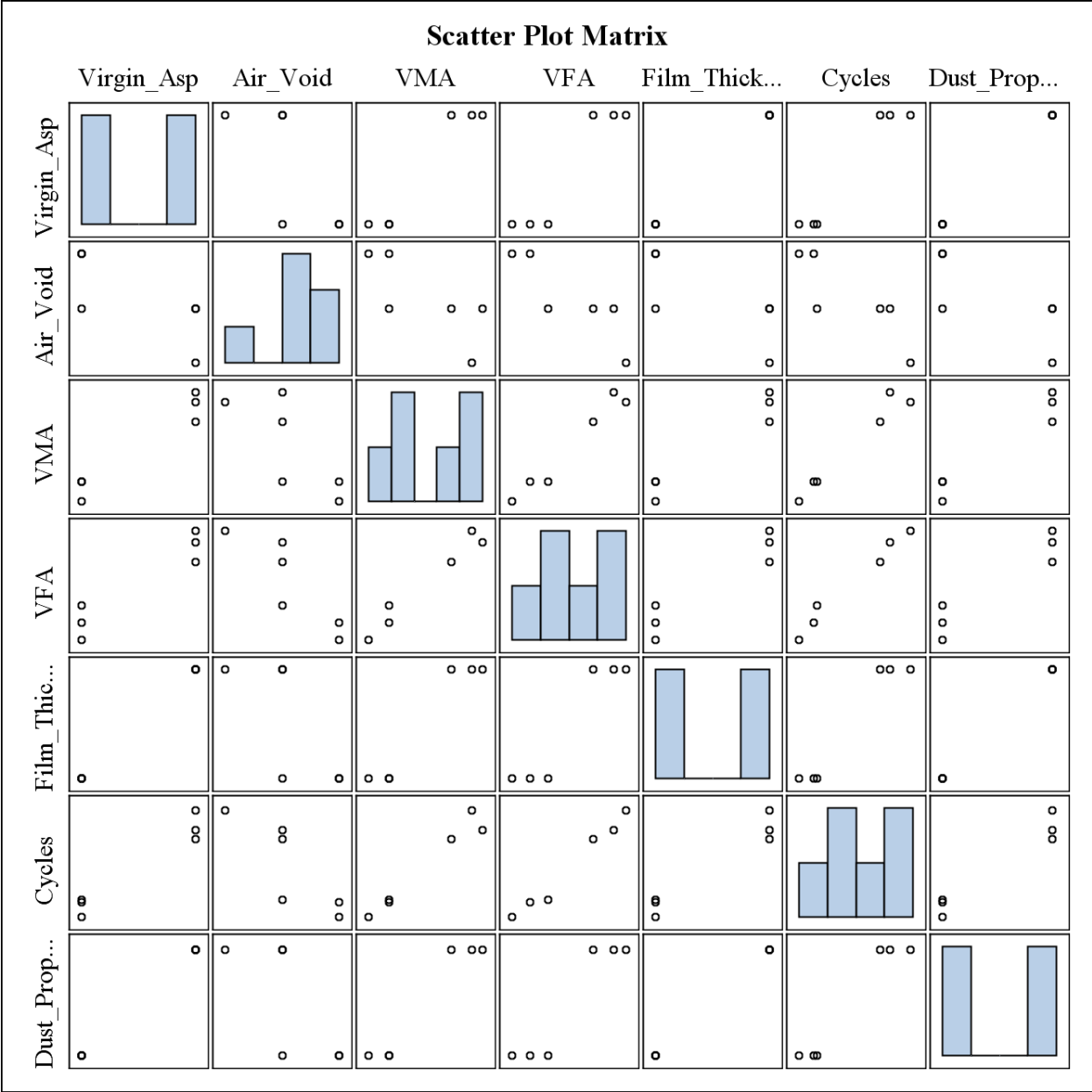


Figure 4.14 Scatter plot matrix for SM-12.5A mix (OT test)

Table 4.18 Correlation matrix for SR-12.5A mixture with first RAP source (OT test)

	Total Asphalt Content (%)	Virgin Asphalt (%)	Asphalt Contained in RAP (%)	Air Void (%)	VMA @ N_F (%)	VFA @ N_F (%)	Film Thickness in Microns	No of OT Cycles	Dust Proportion
Total Asphalt Content (%)	1.00	0.87 (0.00)	-0.72 (0.03)	0.42 (0.26)	0.75 (0.02)	0.53 (0.14)	0.88 (0.00)	0.73 (0.03)	-0.78 (0.01)
Virgin Asphalt (%)	0.87 (0.00)	1.00	-0.97 <.0001	0.20 (0.61)	0.98 <.0001	0.83 (0.01)	1.00 <.0001	0.94 (0.00)	-0.99 <.0001
Asphalt Contained in RAP (%)	-0.72 (0.03)	-0.97 <.0001	1.00	-0.07 (0.85)	-1.00 <.0001	-0.90 (0.00)	-0.96 <.0001	-0.95 <.0001	1.00 <.0001
Air Void (%)	0.42 (0.26)	0.20 (0.61)	-0.07 (0.85)	1.00	0.11 (0.78)	-0.35 (0.35)	0.22 (0.58)	0.16 (0.68)	-0.12 (0.76)
VMA @ N_F (%)	0.75 (0.02)	0.98 <.0001	-1.00 <.0001	0.11 (0.78)	1.00	0.89 (0.00)	0.97 <.0001	0.96 <.0001	-1.00 <.0001
VFA @ N_F (%)	0.53 (0.14)	0.83 (0.01)	-0.90 (0.00)	-0.35 (0.35)	0.89 (0.00)	1.00	0.82 (0.01)	0.83 (0.01)	-0.88 (0.00)
Film Thickness in Microns	0.88 (0.00)	1.00 <.0001	-0.96 <.0001	0.22 (0.58)	0.97 <.0001	0.82 (0.01)	1.00	0.93 (0.00)	-0.98 <.0001
No of OT Cycles	0.73 (0.03)	0.94 (0.00)	-0.95 <.0001	0.16 (0.68)	0.96 <.0001	0.83 (0.01)	0.93 (0.00)	1.00	-0.95 <.0001
Dust Proportion	-0.78 (0.01)	-0.99 <.0001	1.00 <.0001	-0.12 (0.76)	-1.00 <.0001	-0.88 (0.00)	-0.98 <.0001	-0.95 <.0001	1.00

*p-value shown in parenthesis

Table 4.18 shows the correlation matrix of the OT test results for the SR-12.5A mixture with the first RAP source. Figure 4.15 illustrates scatter plots between the variables. VMA (0.96), total asphalt content (0.73), and film thickness (0.93) have a strong positive correlation with OT cycles, while dust proportion (-0.95) showed a strong negative correlation.

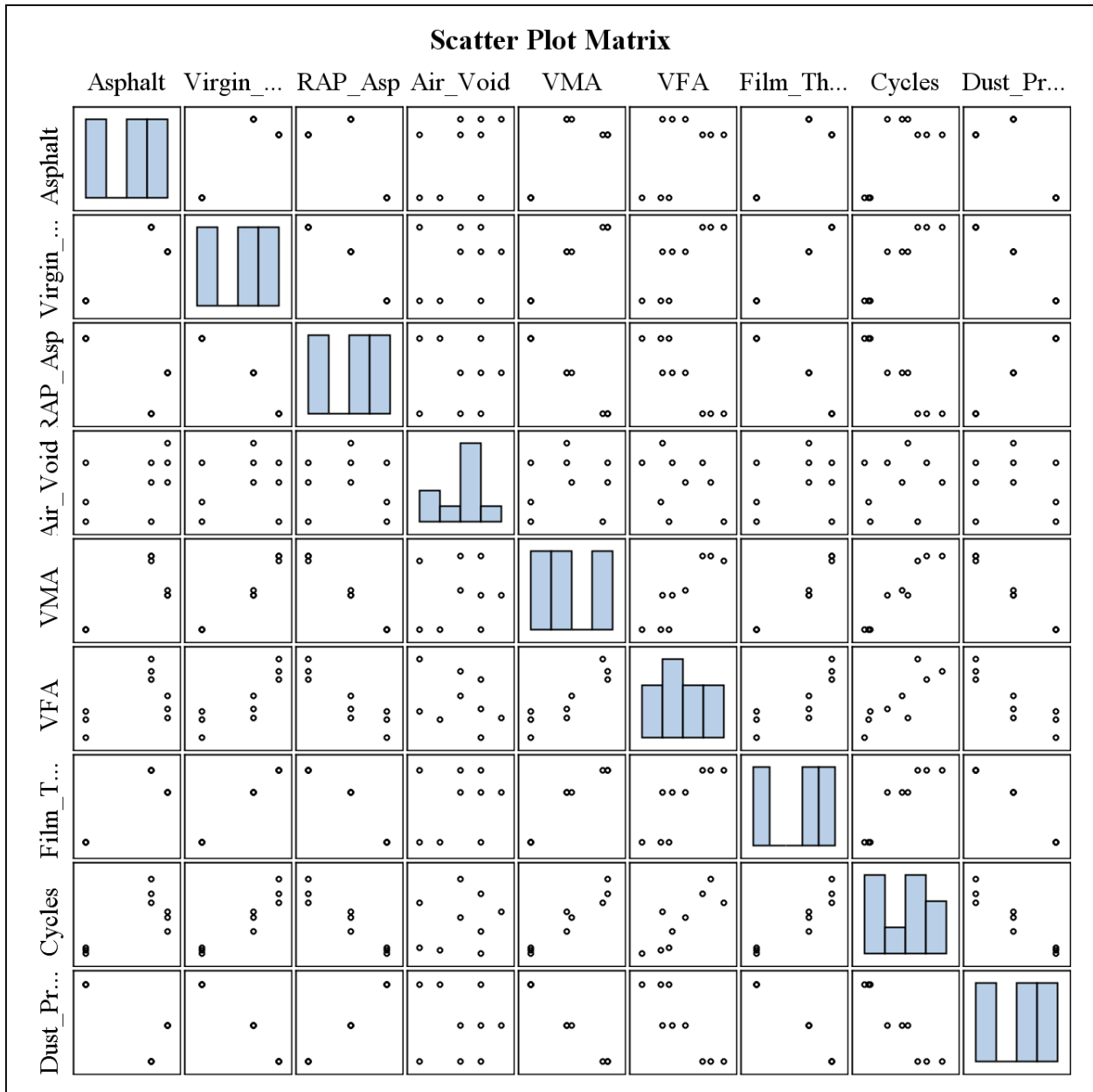


Figure 4.15 Scatter plot matrix for SR-12.5A mix with first source of RAP (OT test)

Table 4.19 Correlation matrix for SR-12.5A mixture with second RAP source (OT test)

	Total Asphalt Content (%)	Virgin Asphalt (%)	Asphalt Contained in RAP (%)	Air Void (%)	VMA @ N_F (%)	VFA @ N_F (%)	Film Thickness in Microns	No of OT Cycles	Dust Proportion
Total Asphalt Content (%)	1.00	0.81 (0.01)	-0.65 (0.06)	0.56 (0.11)	0.27 (0.48)	-0.16 (0.68)	-0.70 (0.04)	-0.90 (0.00)	-0.69 (0.04)
Virgin Asphalt (%)	0.81 (0.01)	1.00	-0.97 <.0001	0.25 (0.52)	0.78 (0.01)	0.37 (0.33)	-0.14 (0.71)	-0.55 (0.12)	-0.98 <.0001
Asphalt Contained in RAP (%)	-0.65 (0.06)	-0.97 <.0001	1.00	-0.10 (0.79)	-0.90 (0.00)	-0.53 (0.14)	-0.08 (0.83)	0.37 (0.33)	1.00 <.0001
Air Void (%)	0.56 (0.11)	0.25 (0.52)	-0.10 (0.79)	1.00	-0.25 (0.51)	-0.76 (0.02)	-0.65 (0.06)	-0.69 (0.04)	-0.13 (0.73)
VMA @ N_F (%)	0.27 (0.48)	0.78 (0.01)	-0.90 (0.00)	-0.25 (0.51)	1.00	0.82 (0.01)	0.49 (0.18)	0.03 (0.93)	-0.88 (0.00)
VFA @ N_F (%)	-0.16 (0.68)	0.37 (0.33)	-0.53 (0.14)	-0.76 (0.02)	0.82 (0.01)	1.00	0.72 (0.03)	0.44 (0.23)	-0.50 (0.17)
Film Thickness in Microns	-0.70 (0.04)	-0.14 (0.71)	-0.08 (0.83)	-0.65 (0.06)	0.49 (0.18)	0.72 (0.03)	1.00	0.84 (0.00)	-0.04 (0.92)
No of OT Cycles	-0.90 (0.00)	-0.55 (0.12)	0.37 (0.33)	-0.69 (0.04)	0.03 (0.93)	0.44 (0.23)	0.84 (0.00)	1.00	0.40 (0.28)
Dust Proportion	-0.69 (0.04)	-0.98 <.0001	1.00 <.0001	-0.13 (0.73)	-0.88 (0.00)	-0.50 (0.17)	-0.04 (0.92)	0.40 (0.28)	1.00

**p*-value shown in parenthesis

Table 4.19 shows the correlation matrix of the OT test results for the SR-12.5A mixture with the second RAP source. Figure 4.16 illustrates scatter plots between the variables. Results from the second source of RAP show strong positive correlation between OT cycles and film thickness (0.84).

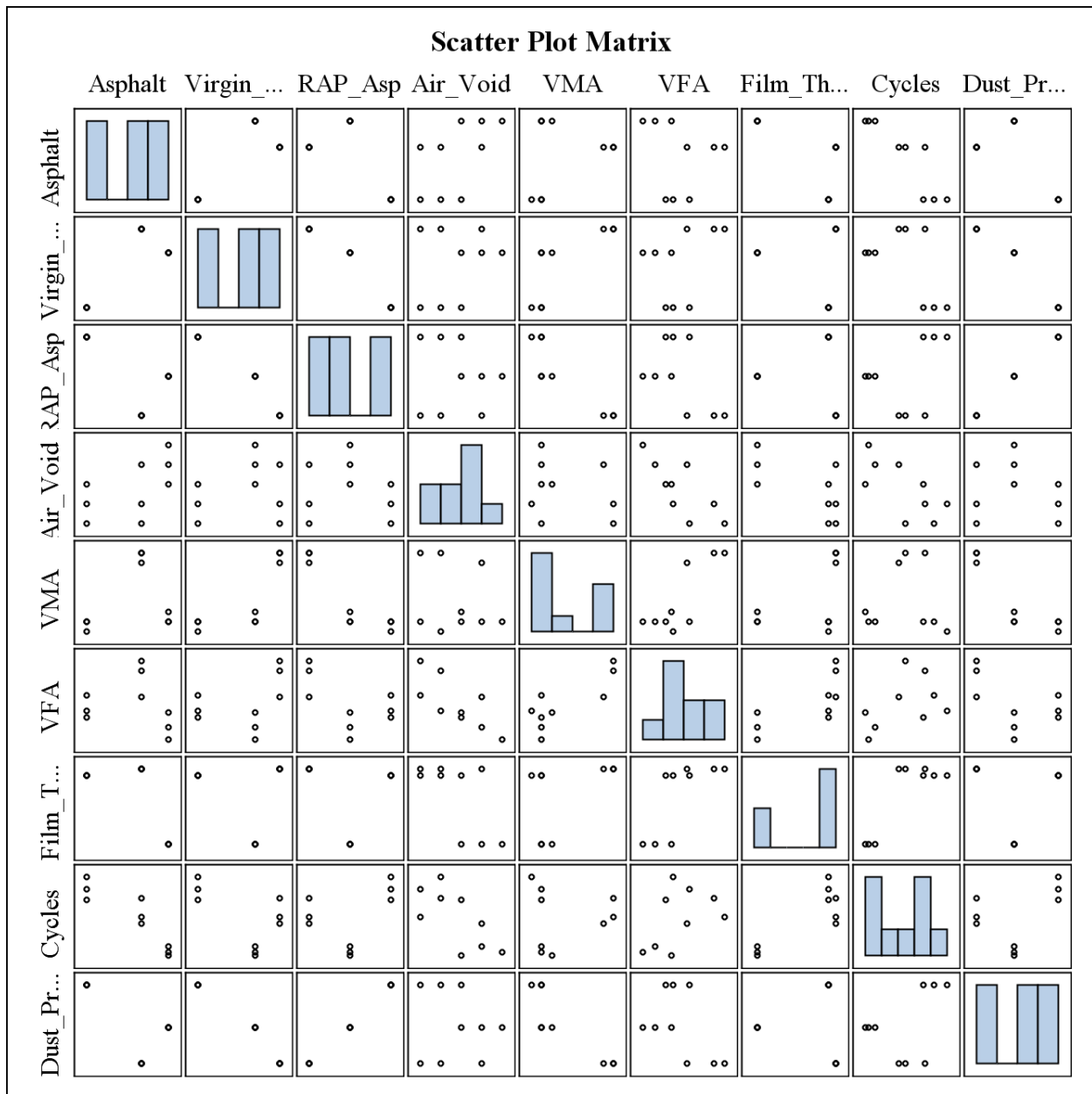


Figure 4.16 Scatter plot matrix for SR-12.5A mix with second source of RAP (OT test)

A summary of correlation analysis results of R-SCB test and OT test are given in Table 4.20, 4.21, 4.22, and 4.23.

Table 4.20 Summary of correlation analysis of R-SCB test results (SM-12.5A mixture)

Parameters showing Strong Correlation	Correlation Coefficient
Virgin Asphalt-VMA	0.98
Virgin Asphalt - Film thickness	0.98
Virgin Asphalt - Cycles @ 30% peak load	0.96
Virgin Asphalt -Cycles @ 50% peak load	0.95
VMA - Film thickness	0.97
VMA- Cycles @ 30% peak load	0.94
VMA- Cycles @ 50% peak load	0.91
Film thickness - Cycles @30% peak load	0.99
Film thickness - Cycles @50% peak load	0.95
Film thickness - Dust proportion	-0.77
Cycles @30% peak load -Dust proportion	-0.81

Table 4.21 Summary of correlation analysis of OT test results (SM-12.5A mixture)

Parameters showing Strong Correlation	Correlation Coefficient
Virgin Asphalt-Air Void	-0.72
Virgin Asphalt -VMA	0.97
Virgin Asphalt - Film thickness	1.00
Virgin Asphalt - Cycles	0.97
Virgin Asphalt -Dust Proportion	1.00
Air Void -VMA	-0.73
Air Void- Film thickness	-0.73
Air Void-Cycles	-0.84
Air Void-Dust Proportion	-0.73
VMA- Film thickness	0.97
VMA- Cycles	0.98
VMA-Dust Proportion	0.97
Film thickness - Cycles	0.97
Film thickness - Dust Proportion	1.00
Cycles -Dust Proportion	0.97

Table 4.22 Summary of correlation analysis of R-SCB test results (SR-12.5A mixture)

R-SCB test results of SR-12.5A mixture with first source of RAP	
Parameters showing Strong Correlation	Correlation Coefficient
Total Asphalt - Film thickness	-0.76
Total Asphalt -Dust proportion	-0.74
Virgin Asphalt -VMA	0.95
Virgin Asphalt - Film thickness	0.98
Virgin Asphalt - Cycles @ 30% peak load	0.84
Virgin Asphalt - Cycles @ 50% peak load	0.85
Virgin Asphalt -Dust proportion	-1.00
VMA -Film thickness	0.99
VMA - Cycles @ 30% peak load	0.81
VMA - Cycles @ 50% peak load	0.88
Film thickness - Cycles @30% peak load	0.87
Film thickness - Cycles @50% peak load	0.90
Film thickness - Dust proportion	-1.00
Cycles @30% peak load -Dust proportion	-0.87
Cycles @50% peak load -Dust proportion	-0.91
R-SCB test results of SR-12.5A mixture with second source of RAP	
Parameters showing Strong Correlation	Correlation Coefficient
Total Asphalt - Cycles @30% peak load	-0.89
Total Asphalt - Cycles @30% peak load	-0.96
Virgin Asphalt -VMA	0.96
Virgin Asphalt - Cycles @ 50% peak load	-0.87
Virgin Asphalt -Dust proportion	-0.93
VMA - Cycles @ 50% peak load	-0.73
VMA-Dust proportion	-0.98
Air Void- Cycles @30% peak load	-0.73
Film thickness- Cycles @30% peak load	0.81

Table 4.23 Summary of correlation analysis of OT test results (SR-12.5A mixture)

OT test results of SR-12.5A mixture with first source of RAP	
Parameters with Strong Correlation	Correlation Coefficient
Total Asphalt -VMA	0.75
Total Asphalt - Film thickness	0.88
Total Asphalt - Cycles	0.73
Total Asphalt -Dust Proportion	-0.78
Virgin Asphalt -VMA	0.98
Virgin Asphalt - Film thickness	1.00
Virgin Asphalt - Cycles	0.94
Virgin Asphalt -Dust Proportion	-0.99
VMA - Film thickness	0.97
VMA - Cycles	0.96
VMA – Dust Proportion	-0.99
Film thickness - Cycles	0.93
Film thickness - Dust Proportion	-0.98
Cycles -Dust Proportion	-0.95
OT test results of SR-12.5A mixture with second source of RAP	
Parameters with Strong Correlation	Correlation Coefficient
Total Asphalt -Cycles	1.00
Virgin Asphalt -VMA	0.78
Virgin asp- Film thickness	1.00
Virgin Asphalt -Dust Proportion	-0.98
VMA – Dust Proportion	-0.88
Film thickness- Cycles	0.84

4.3.2 Comparison between Means

Mean results obtained from both R-SCB (50% of $F_{\text{static SCB}}$ as input) and OT tests were compared to check if differences were significant. In addition, comparisons were performed to find a combination of minimum asphalt content and maximum RAP content based on the test results, which would be able to ensure a satisfactory cracking resistance. Initially, unequal variance was considered per treatment group. After performing the null model likelihood ratio test, results indicated that difference was not significant and was unable to show that variances are statistically different. Thus, equal variance was considered for the comparison of means. Table 4.24 show the results obtained from different normality tests of R-SCB test data. The results indicate that data are normally distributed. In addition, Figure 4.17 shows the normal probability plots for R-SCB test results. Using Tukey’s adjustment method, means from both cracking resistance tests were compared as a whole. Tukey’s method is the most powerful for all possible pairwise comparisons while controlling the type-I error rate (Kuehl, 2000). The assumptions for this test are (Kuehl, 2000):

1. The observations being tested are independent, and
2. There is equal within-group variance across the groups associated with each mean in the test (homogeneity of variance).

The adjusted p -value from the test output was compared with the level of significance (0.05). If p -value was less than or equal to 0.05, then it was considered that there were statistically significant difference between the means. Tables 4.25 and 4.27 demonstrate the multiple comparisons performed among the mean test results obtained from all mixtures considered in this study. In these tables, mixtures were split by asphalt content, RAP content, and RAP source. They were arranged according to performance test results in ascending order to get a clear view of groupings. A set of cells enclosed by border of same color denotes that those mixtures did not have any significant difference between their means. Groups were also designated at the last row in both tables.

Table 4.24 Normality test results of R-SCB test outputs

Mixture	Normality Test	p -value from Test
12.5A NMAS	Shapiro-Wilk	0.059
	Kolmogorov-Smirnov	0.065
	Anderson-Darling	0.062

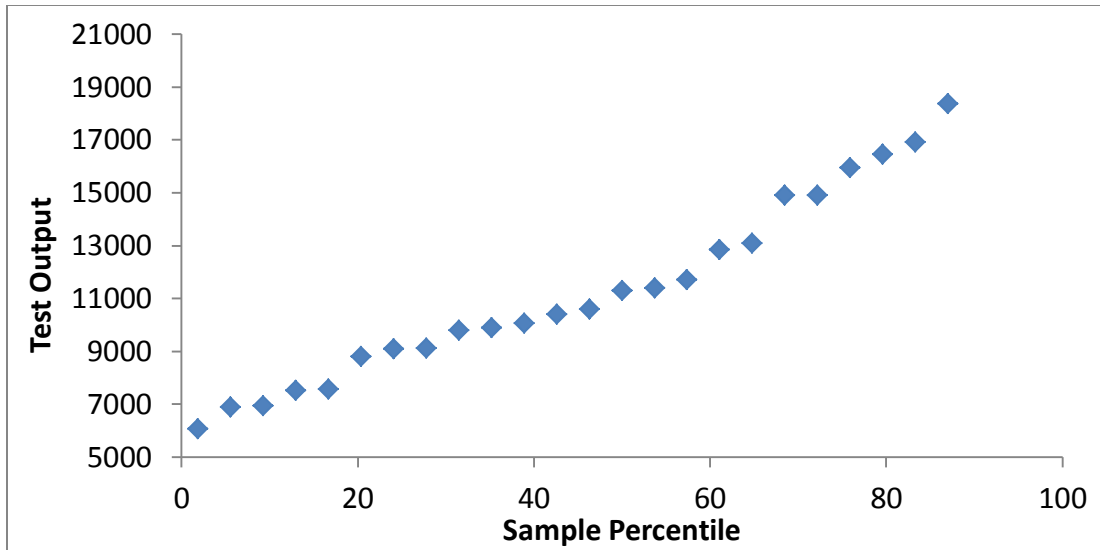


Figure 4.17 Normal probability plots for R-SCB test outputs

Though Tukey’s multiple comparisons of means for the R-SCB test results (Table 4.25) show groupings, several overlaps did not allow formation of distinctive groups. Mixtures with no RAP and 5.2% asphalt content had statistically significant different means than all other mixture types.

Table 4.25 Summary of Tukey’s multiple comparisons (R-SCB test)

Source	2	0	2	1	1	1	0	2	0
RAP %	30	0	20	40	30	20	0	40	0
Asphalt %	4.4	4.6	4.3	4.3	4.8	4.7	4.9	4.1	5.2
2_30_4.4	a								
0_0_4.6		a							
2_20_4.3			a						
1_40_4.3				ab					
1_30_4.8					abc				
1_20_4.7						bcd			
0_0_4.9							cd		
2_40_4.1								d	
0_0_5.2									e

*Mix types not connected by same letter are significantly different

The results obtained from normality tests of OT test data are shown in Table 4.26. Results indicate that data are normally distributed. In addition, Figure 4.18 shows the normal probability plots for OT test results. Table 4.27 shows the summary of the Tukey’s multiple comparisons for the OT test results. Mixture with no RAP and 5.2% binder was not included because outputs were considered censored data. Mixtures enclosed by the same colored border denote that they did not have any statistically significant difference among them. Results from the OT test showed almost clear groups. A conclusion regarding the evaluation of cracking test methods could be derived from the Tukey’s comparisons. OT test results were able to make better distinct groups among these mixtures than the R-SCB test results (less overlapping in groups). Thus, results obtained from this study apparently indicate that OT test can evaluate cracking resistance better than the R-SCB test. However, further analysis with additional mixtures can establish this observation.

Table 4.26 Normality test results of OT test outputs

Mixture	Normality Test	<i>p</i> -value from Test
12.5A NMAS	Shapiro-Wilk	>0.10
	Kolmogorov-Smirnov	>0.15
	Anderson-Darling	0.207

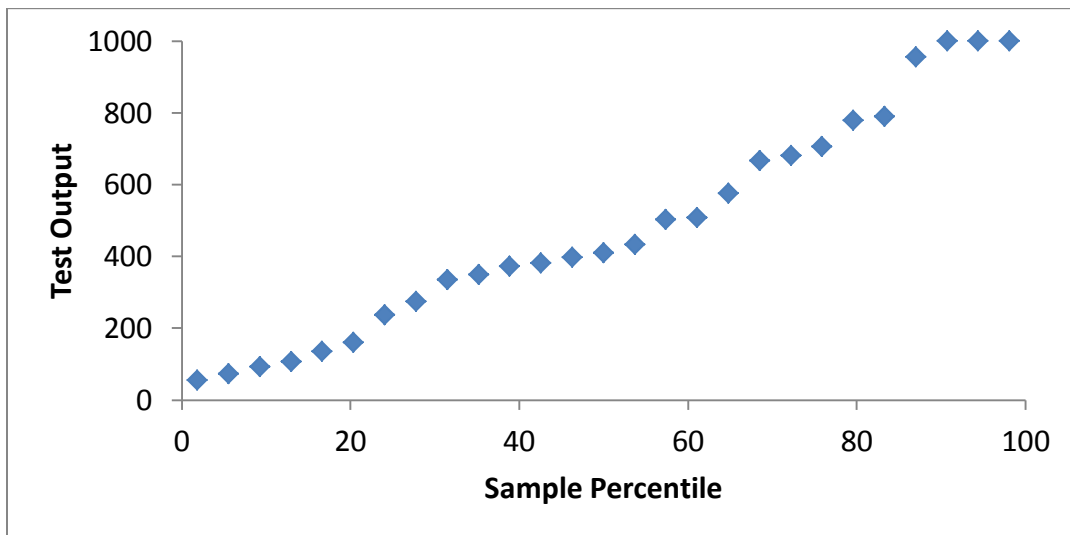


Figure 4.18 Normal probability plots for OT test outputs

Table 4.27 Summary of Tukey’s multiple comparisons (OT Test)

Source	2	1	2	0	2	1	0	1
RAP %	30	40	20	0	40	30	0	20
Asphalt %	4.4	4.3	4.3	4.6	4.1	4.8	4.9	4.7
2_30_4.4	a							
1_40_4.3		a						
2_20_4.3			ab					
0_0_4.6				b				
2_40_4.1					b			
1_30_4.8						b		
0_0_4.9							c	
1_20_4.7								c

*Mix types not connected by same letter are significantly different

Tukey's adjustment is the most powerful test that controls type I error for all possible pairwise comparisons (Kuehl, 2000). Other than performing pairwise comparison between means, Tukey's adjustment method was adopted in this study to find a combination of minimum asphalt content and maximum RAP content based on the test results while ensuring a satisfactory cracking resistance. Cracking test results of the SR-12.5A mixtures portrayed completely opposite patterns, which could be due to the intrinsic properties of various sources of RAP materials used in the mixtures. Therefore, without considering at least another source of RAP, it would not be possible to make a general conclusion about such asphalt content and RAP content combination by overall multiple comparison between the treatments.

Because of such limitations, the Bonferroni method was later used for simultaneously planned comparisons within different sources. This method controls family-wise type I error. Tables 4.28 and 4.29 show summaries of pairwise comparisons from the Bonferroni method for the R-SCB and OT tests, respectively. Results from the R-SCB test and OT tests, along with the confidence interval for means, are illustrated in the Figures 4.19 and 4.20. SM and SR mixtures are shown in ascending order of number of cycles. *p*-value obtained from the SAS outputs were compared to the Bonferroni adjusted level of significance which was the ratio of level of significance to the number of comparisons from each test ($n = 9$ for SCB test and $n = 7$ for OT test). If the obtained *p*-value was less than or equal to the Bonferroni adjusted level of

significance, then the means were considered to have statistically significant difference. Detailed SAS outputs are given in Appendix A.

Pairwise mean comparisons (R-SCB test results) within the first source of RAP indicate that there was no statistically significant difference among the mean number of cycles obtained for mixtures with 20%, 30%, and 40% RAP. Though the mixture with 20% RAP and 4.7% asphalt showed the best performance, it does not provide the maximum RAP and minimum asphalt combination. Henceforth, the mixture with 40% RAP and 4.3% asphalt can be considered to provide good cracking resistance performance under such conditions. For mixtures with second source of RAP, results were even clearer. The combination of 40% RAP content and 4.1% asphalt content had significantly different mean compared to the other two mixtures. Therefore, this mixture can provide good performance, especially when RAP from second source is used.

Table 4.28 Summary of Bonferroni method comparisons (R-SCB test)

SM-12.5A			
RAP%	0	0	0
Asphalt%	4.6	4.9	5.2
Groups*	a	b	c
SR-12.5A (RAP-1)			
RAP%	40	30	20
Asphalt%	4.3	4.8	4.7
Groups*	a	a	a
SR-12.5A (RAP-2)			
RAP%	30	20	40
Asphalt%	4.4	4.3	4.1
Groups*	a	a	b

*Mix types not connected by same letter are significantly different

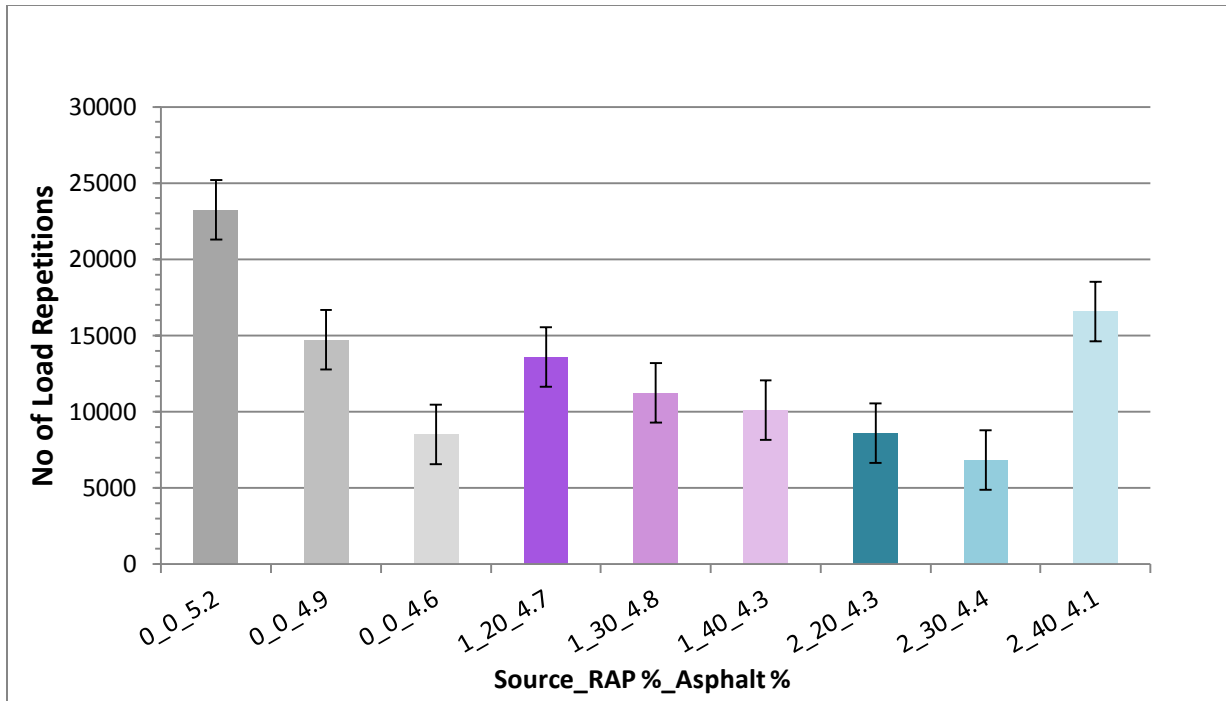


Figure 4.19 R-SCB test results with 95% confidence intervals

When analyzing the OT test results, a minimum threshold level of 300 OT cycles was used. For mixtures with the first RAP source, all means were significantly different. However, the combination of maximum RAP and minimum asphalt portrayed the poorest performance and was below the threshold level. Thus, from OT test results of SR-12.5A mixture with the first RAP source, it can be concluded that 30% RAP content and 4.8% asphalt content can provide satisfactory cracking resistance performance at the 95% confidence interval since the mean estimate of passing cycles is clearly above 300 (minimum threshold).

For mixtures with the second RAP source, test means did not show any statistically significant difference. Also, the mixture with 40% RAP and 4.1 % asphalt was able to exceed the threshold level of 300 OT cycles. Therefore, this mixture has the potential to ensure good cracking resistance when the second RAP source is used.

Table 4.29 Summary of Bonferroni method comparisons (OT test)

SM-12.5A			
RAP%	0	0	0
Asphalt%	4.6	4.9	5.2
Groups*	a	b	-
SR-12.5A (RAP-1)			
RAP%	40	30	20
Asphalt%	4.3	4.8	4.7
Groups*	a	b	c
SR-12.5A (RAP-2)			
RAP%	30	20	40
Asphalt%	4.4	4.3	4.1
Groups*	a	b	b

*Mix types not connected by same letter are significantly different

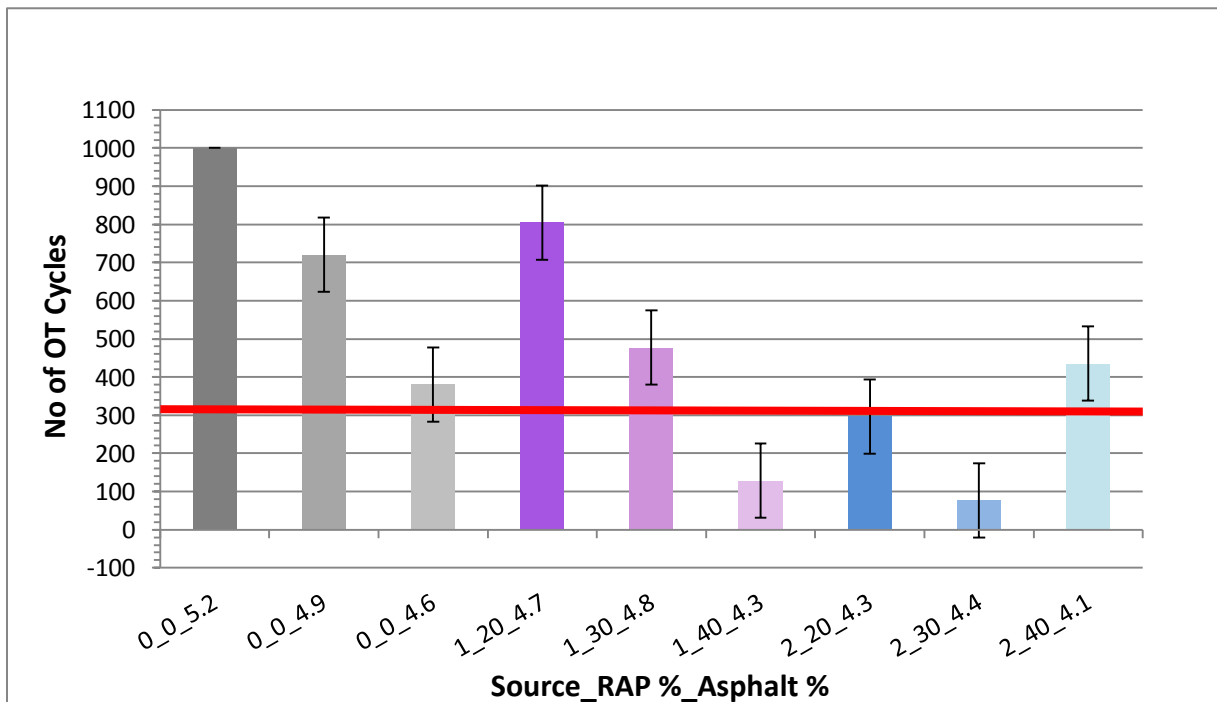


Figure 4.20 OT test results with 95% confidence intervals

Table 4.30 Virgin asphalt as a percentage of total asphalt content for both sources of RAP

First RAP Source			Second RAP Source		
Total Asphalt (%)	Virgin Asphalt (%)	Virgin Asphalt as a Percentage of Total Asphalt (%)	Total Asphalt (%)	Virgin Asphalt (%)	Virgin Asphalt as a Percentage of Total Asphalt (%)
4.7	3.6	77	4.3	3.5	81
4.8	3.1	65	4.4	3.2	73
4.3	2.1	49	4.1	2.5	61

Thus, with the results obtained from this study, conclusions can be made based on what type of RAP is used. If the RAP considered for the mixture is more binder rich, then results from the first RAP source should be considered. On the other hand, for a drier RAP, results from the second source of RAP should be taken into account. Statistical analysis suggests SR-12.5 A mixture with first RAP source have two best cracking resistant mixtures: 40% RAP with 4.3% total asphalt content (from the R-SCB test results), and 30% RAP with 4.8% asphalt content (from the OT test results). For the second RAP source, mixtures with 40% RAP and 4.1% asphalt content performed best in both cracking tests. Table 4.30 shows that percentage of virgin asphalt in the best cracking resistant mixtures from the first RAP source are 49% and 65% of total asphalt content, while the best mixture from second RAP source contains 60% virgin binder. Henceforth, it can be concluded that, based on statistical analysis, Superpave mixtures containing 30-40% RAP and virgin asphalt content between 49-65% of total asphalt should be able to provide good cracking resistance.

Chapter 5 - Conclusions and Recommendations

5.1 Conclusions

The objective of this study was to investigate the effect of varying asphalt and RAP content on cracking resistance of the Superpave mixtures. Based on the semi-circular bending test and Texas overlay test results obtained from this study, the following conclusions can be drawn:

1. Results from both static SCB test and repetitive SCB test indicate that SM-12.5A mixture with design asphalt content (5.2%), SR-12.5A mixture with 20% RAP from the first source, and 40% RAP from the second source demonstrate the best cracking resistance performance among the SM and SR mixtures, respectively.
2. Performance deteriorated with decreasing asphalt content and increasing RAP content (for the first source of RAP). However, the second source of RAP, which contained less asphalt, performed in the opposite manner.
3. While investigating the crack propagation during R-SCB test, it was observed that mixtures with higher crack propensity (less number of load repetitions) had smaller crack initiation phase.
4. Results of the OT test showed, the SM-12.5A mixture with 5.2% asphalt passed 1,000 cycles (maximum threshold) but still did not reach 93% load reduction. SR-12.5A mixture with 20% RAP and 40% RAP from first and second sources, respectively, passed the minimum level of 300 OT cycles. Thus, these mixtures are expected to show less crack propensity.
5. Statistical analysis revealed that film thickness had a strong positive correlation ($0.7 < \text{Pearson correlation coefficient} < 1.0$) with the number of load repetitions (R-SCB test) and number of OT cycles (OT test) for almost every mixture. For example, if film thickness increased, the number of cycles increased and vice versa. Thus, ensuring adequate film thickness would provide better cracking resistance.
6. Correlation analysis also indicated that Pearson correlation coefficient values for the R-SCB test outputs for both 30% of F_{SCB} as peak load and 50% of F_{SCB} as

peak load were very similar and concluded similar correlation strength, except for the SR-12.5A mixture using the second RAP source.

7. Using Tukey's method of multiple comparisons, cracking test means were compared. Though the overlay test results formed almost distinct groups, R-SCB test results showed similarity within groups. Because of such overlaps and completely opposite behaved RAP sources, it was not possible to draw a general conclusion regarding minimum asphalt and maximum RAP content, which could consequently ensure cracking resistance.
8. Tukey's comparisons also indicated that comparative results from the OT test were able to make better distinct groups among all the mixtures than R-SCB test results (less overlapping in groups). Thus, results obtained from this study indicate that OT test can evaluate cracking resistance better than R-SCB test.
9. Bonferroni's method was finally considered to draw conclusions within each source of RAP. For the second RAP source, both R-SCB and OT test suggested a combination of 4.1% asphalt content and 40 % RAP content which can provide satisfactory cracking resistance while using the least possible asphalt and maximum allowable RAP content. On the other hand, for the first source of RAP, conclusions were split between 4.8% asphalt with 30% RAP content and 4.3% asphalt with 40% RAP.
10. Superpave mixtures containing 30-40% RAP and virgin asphalt content between 49-65% of total asphalt content should be able to provide good cracking resistance.

5.2 Recommendations

Based on this study, the following recommendations are made:

1. This study was limited to only two sources of RAP. Further investigation with a few additional sources of RAP is required in order to make a general conclusion as to least possible asphalt content and highest RAP content allowable in Superpave mixtures without compromising the cracking resistance.

2. Further research is required to correlate the cracking test results with the actual field data.
3. Semi-circular bending test is not yet standardized; thus, further research using this test method is required by varying notch depth in the specimen and testing under different temperatures.
4. Finite element analysis can be conducted to further investigate the crack initiation and propagation during the R-SCB test.

References

- AASHTO T 283. (2007). "Resistance of Compacted Asphalt Mixtures to Moisture-Induced Damage," Standard Specification, American Association of State Highway and Transportation Officials, Washington, DC.
- Asphalt Institute. (1995). "Mix Design Method for Asphalt Concrete and Other Hot-Mix Types," MS-2, Asphalt Institute, Lexington, Kentucky.
- Asphalt Institute. (2007). "The Asphalt Handbook," MS-4, 7th Edition, Asphalt Institute, Lexington, Kentucky.
- Broek, D. (1987). "Elementary Engineering Fracture Mechanics," 4th Edition, Martinus Nijhoff Publishers, Dordrecht, the Netherlands.
- Brown, E., P. Kandhal, F., Roberts, D., Lee, Y., and Kennedy, T. W. (2009). "Hot Mix Asphalt Materials, Mixture Design, and Construction," NAPA Research and Education Foundation, Lanham, Maryland.
- Brown, S. F., and Scholz, T. V. (2000). "Development of Laboratory Protocols for the Aging of Asphalt Mixtures," In Proceedings of 2nd Eurasphalt and Eurobitume Congress, Barcelona, Spain, Vol. 1, pp. 83-90.
- Campan, W., Smith, J., Erickson, L., and Mertz, L. (1959). "The Relationships between Voids, Surface Area, Film Thickness and Stability in Bituminous Paving Mixtures," Proceedings of Association of Asphalt Paving Technologists, pp. 149-178.
- Carvalho, R.L, Shirazi, H., Ayres, M. Jr., and Selezneva, O. (2010). "Performance of Recycled Hot-Mix Asphalt Overlays in Rehabilitation of Flexible Pavements," In Transportation Research Record: Journal of the Transportation Research Board, Transportation Research Board of the National Academics, Washington, D.C, No. 2155, pp. 55-62.
- Chong, K. P., and Kuruppu, M. D. (1984). "New Specimen for Fracture Toughness Determination for Rock and Other Materials," International Journal of Fracture, No. 26, pp. 59-62.
- Copeland, A. (2011). "Reclaimed Asphalt Pavement in Asphalt Mixtures: State of the Practice," Report No. FHWA-HRT-11-021, Federal Highway Administration, McLean, Virginia.
- Coree, B., and Hislop, W. P. (1999). "The Difficult Nature of Minimum Voids in Mineral Aggregate: Historical Perspective," In Transportation Research Record: Journal of Transportation Research Board, Transportation Research Board of the National Academics, Washington, D.C., No. 1681, pp. 148-156.
- CROW. (2006). "The Next Step in Specifying Asphalt Mixes," Final report of CROW task group Finite Element Analysis.

- FHWA. (2008). "Highway Statistics 2008," Federal Highway Administration, U.S. Department of Transportation. <http://www.fhwa.dot.gov/policyinformation/statistics/2008/hm12.cfm> Accessed on May 25th 2013.
- Goode, J. F., and Lufsey, L. A. (1965). "Voids, Permeability, Film Thickness vs. Asphalt Hardening," Proceedings of Association of Asphalt Paving Technologists, Vol. 34.
- Hinrichsen, J. A., and Heggen, J. (1996). "Minimum Voids in Mineral Aggregate in Hot-Mix Asphalt Based on Gradation and Volumetric Properties," In Transportation Research Record: Journal of the Transportation Research Board, Transportation Research Board of the National Academics, Washington, D.C., No.1545, pp. 75-79.
- Hossain, M., Maag, R. G., and Fager, G. (2010). "Handbook of Superpave Volumetric Asphalt Mixture Design and Analysis." Superpave Certification Training Manual, Kansas State University, Manhattan, Kansas.
- Hu, S., Zhou, F., and Scullion, T. (2011). "Factors That Affect Cracking Performance in Hot-Mix Asphalt Mix Design," In Transportation Research Record: Journal of the Transportation Research Board, Transportation Research Board of the National Academics, Washington, D.C., No. 2210, pp. 37-46.
- Hu, X., Zhou, F., Hu, S., and Scullion, T. (2011). "Development of New Overlay Tester-Based Crack Sealant Adhesion Test and Associated Specification," In Transportation Research Record: Journal of the Transportation Research Board, Transportation Research Board of the National Academics, Washington, D.C., No. 0598, pp. 1-14.
- Huang, B., X. Shu, and Y. Tang, (2005). "Comparison of Semicircular Bending and Indirect Tensile Strength Tests for HMA Mixtures," American Society of Civil Engineers Geotechnical Special Publication, Issue 130-142, pp. 177-188.
- Huang, B., Shu, X., and Vukosavljevic, D. (2011). "Laboratory Investigation of Cracking Resistance of Hot-Mix Asphalt Field Mixtures Containing Screened Reclaimed Asphalt Pavement," American Society of Civil Engineers Journal of Materials in Civil Engineering, Vol. 23, No. 11, pp. 1535-1543.
- Huang, L., Cao, K., and Zeng, M. (2009). "Evaluation of Semicircular Bending Test for Determining Tensile Strength and Stiffness Modulus of Asphalt Mixtures." Journal of Testing and Evaluation, West Conshohocken, Pennsylvania, Vol. 37, pp. 122-128.
- Kandhal, P. S., and Chakraborty, S. (1996). "Effect of Asphalt Film Thickness on Short and Long-Term Aging of Asphalt Paving Mixtures," In Transportation Research Record: Journal of the Transportation Research Board, Transportation Research Board of the National Academics, Washington, D.C., No. 1535, pp. 83-90.
- Kandhal, P. S., and Cross, S. (1993). "Effect of Aggregate Gradation on Measured Asphalt Content," In Transportation Research Record: Journal of the Transportation Research Board, Transportation Research Board of the National Academics, Washington, D.C., No. 1417, pp. 21-28.

- Kandhal, P. S., Foo, K. Y., and Mallick, R. B. (1998). "A Critical Review of VMA Requirements in Superpave," In Transportation Research Record: Journal of the Transportation Research Board, Transportation Research Board of the National Academics, Washington, D.C., No. 1609, pp. 21-27.
- Kim, R. and H. Wen, (2002). "Fracture Energy from Indirect Tension Testing," Journal of the Association of Asphalt Paving Technologists, Vol. 71, pp. 779-793.
- Krans, R. L., Tolman, F., and Van de Ven, M. F. C. (1996). "Semi-Circular Bending Test: A Practical Crack Growth Test Using Asphalt Concrete," Third International RILEM Conference, Reflecting Cracking in Pavements, Spon Press, U.K., pp. 123-133.
- Kuehl, R. O. (2000). "Design of Experiments: Statistical Principles of Research Design and Analysis," 2nd Edition, Duxbury Press, California.
- Kumar, A., and Goetz, W. H. (1977). "Asphalt Hardening as Affected by Film Thickness, Voids and Permeability in Asphaltic Mixtures," Proceedings of Association of Asphalt Paving Technologists, San Antonio, Texas, pp. 571-605.
- Li, X., and Marasteanu, M. (2004). "Evaluation of the Low Temperature Fracture Resistance of Asphalt Mixtures using the Semi Circular Bend Test," Journal of the Association of Asphalt Paving Technologists, Vol. 73, pp. 401-426.
- Li, X., Williams, C., Marasteanu, M. O., Clyne, T. R., and Johnson, E. (2009). "Investigation of In-Place Asphalt Film Thickness and Performance of Hot-Mix Asphalt Mixtures," In American Society of Civil Engineers Journal of Materials in Civil Engineering, Vol. 2, ASCE 0899-1561, pp. 262-270.
- Lytton, R. L., Uzan, J., Fernando, E. G., Roque, R., Hiltunen, D., and Stoffels, S. M. (1993). "Development and Validation of Performance Prediction Models and Specifications for Asphalt Binders and Paving Mixtures," Report No. SHRP-A-357, Strategic Highway Research Program, National Research Council, Washington, D.C.
- MAPA (2010). "Asphalt Pavement Recycling Facts." <<http://moasphalt.org/facts/environmental/facts.htm>> (accessed on Jan. 11, 2013).
- Matthews, J. M., Monismith, C. L. and Craus, J. (1993). "Investigation of Laboratory Fatigue Testing Procedures for Asphalt Aggregate Mixtures," Journal of Transportation Engineering, Vol. 119, pp. 634-654.
- McDaniel, R., Soleymani, H., and Shah, A. (2002). "Use of Reclaimed Asphalt Pavement (RAP) Under Superpave Specifications: A Regional Pooled Fund Project," Report No. FHWA/IN/JTRP-2002/6. Purdue University, West Lafayette, Indiana.
- McLeod, N. W. (1956). "Relationships between Density, Bitumen Content, and Voids Properties of Compacted Bituminous Paving Mixtures," In Highway Research Board, Proceedings of Thirty-Fifth Annual Meeting, Washington, D. C., pp. 327-404.

- Mendenhall, W., and Sincich, T. (2003). "A Second Course in Statistics: Regression Analysis," 6th Edition, Prentice Hall, New Jersey.
- Mobasher, B., Mamlouk, M. S., and Lin, H. M. (1997). "Evaluation of Crack Propagation Properties of Asphalt Mixtures," *Journal of Transportation Engineering*, Vol. 123, No. 5, pp. 405-413.
- Monismith, C. L., Finn, F. N., and Vallerga, B. A. (1989). "A Comprehensive Asphalt Concrete Mixture Design System," *Asphalt Concrete Mix Design: Development of More Rational Approaches*, W. Gartner, Jr., Ed., American Society for Testing and Materials, Philadelphia, ASTM STP 1041, pp. 39-71.
- Mull, M. A., Stuart, K., and Yehia, A. (2002). "Fracture Resistance Characterization of Chemically Modified Crumb Rubber Asphalt Pavement," *Journal of Materials Science*, Vol. 37, No. 3, pp. 557-566.
- NAPA. (2013). "Asphalt Pavement Overview," <http://www.asphaltpavement.org/index.php?option=com_content&view=article&id=14&Itemid=34> (accessed on May 17, 2013).
- Pérez, J. F., Valdés, G., Miró, R., Martínez, A., & Botella, R. (2010). "Fénix Test," In *Transportation Research Record: Journal of the Transportation Research Board*, Transportation Research Board of the National Academics, Washington, D.C., No. 2181(1), pp. 36-43.
- Purcell, E. M., and Cross, S. A. (2001). "Effects of Aggregate Angularity on VMA and Rutting of KDOT Superpave Level 1 Mixes," Kansas Department of Transportation, Topeka, Kansas.
- Roberts, F. L., Kandhal, P. S., Brown, E. R., Lee, D., and Kennedy, T. W. (1996). "Hot Mix Asphalt Materials, Mixture Design and Construction," National Asphalt Pavement Association Research and Education Foundation, 2nd Edition, Lanham, Maryland.
- Ruth, B. E., Roque, R., and Nukunya, B. (2002). "Aggregate Gradation Characterization Factors and Their Relationships to Fracture Energy and Failure Strain of Asphalt Mixtures," *Journal of the Association of Asphalt Paving Technologists*, Vol. 71, pp. 310-344.
- Sabahfar, N. (2012). "Use of High-Volume Reclaimed Asphalt Pavement (RAP) for Asphalt Pavement Rehabilitation," Master's Thesis, Department of Civil Engineering, Kansas State University, Manhattan, Kansas.
- Shu, X., Huang, B., and Vukosavljevic, D. (2008). "Laboratory Evaluation of Fatigue Characteristics of Recycled Asphalt Mixture," *Construction and Building Materials*, Vol. 22(7), pp. 1323-1330.
- State Testing Procedures, Tex-226-F. (2004) "Indirect Tensile Strength Test," Standard Specification, Texas Department of Transportation, Austin, Texas.

- State Testing Procedures, Tex-248-F. (2009). "Overlay Test," Standard Specification, Texas Department of Transportation, Austin, Texas.
- van Rooijen, R. C., and de Bondt, A. H. (2008). "Crack Propagation Performance Evaluation of Asphaltic Mixes Using a New Procedure Based on Cyclic Semi-Circular Bending Tests," Proceedings, 6th RILEM International Conference on Cracking in Pavements, Chicago, Illinois, pp. 437-446.
- Von Holdt, C. and Scullion, T. (2005). "Methods of Reducing Joint Reflection Cracking: Field Performance Studies," Technical Research Report FHWA/TX-06/0-4517-3, Texas Transportation Institute, College Station, Texas.
- Walubita, L. F. (2006). "Comparison of Fatigue Analysis Approaches For Predicting Fatigue Lives Of Hot-Mix Asphalt Concrete (HMAC) Mixtures," Ph.D. Dissertation, Department of Civil Engineering, The Texas A&M University, College Station, Texas.
- Walubita, L. F., Faruk, A. N., Alvarez, A. E., and Scullion, T. (2013). "The Overlay Tester (OT): Using the Fracture Energy Index Concept to Analyze the OT Monotonic Loading Test Data," Construction and Building Materials, Vol. 40, pp. 802-811.
- Walubita, L. F., Hugo, F., and Epps Martin, A. (2002). "Indirect Tensile Fatigue Performance of Asphalt after MMLS3 Trafficking under Different Environmental Conditions," Journal of the South African Institution of Civil Engineering, Vol. 44, No. 2, pp. 2-11.
- Walubita, L. F., Martin, A. E., Jung, S. H., Glover, C. J., Chowdhury, A. E., Park, S., and Lytton, R. L. (2004). "Preliminary Fatigue Analysis of A Common TxDOT Hot Mix Asphalt Concrete Mixture," Technical Research Report FHWA/TX-05/0-4468-1, Texas Transportation Institute, College Station, Texas.
- Walubita, L. F., Umashankar, V., Hu, X., Jamison, B., Zhou, F., Scullion, T., Martin, A. E., and Dessouky, S. (2010). "New Generation Mix-Designs: Laboratory Testing and Construction of the APT Test Sections," Report No. FHWA/TX-10/0-6132-1, Texas Transportation Institute, College Station, Texas.
- Wen, H. (2003). "Investigation of Effects of Testing Methods on Characterization of Asphalt Concrete," Journal of Testing and Evaluation, Vol. 31, No. 6, pp. 1-7.
- Witczak, M. W., Kaloush, K., Pellinen, T., El-Basyouny, M., and Quintus, H. Von. (2002). "Simple Performance Test for Superpave Mix Design," Transportation Research Board, National Research Council, Washington, DC., NCHRP 465.
- Wu, Z., Mohammad, L. N., Wang, L. B., and Mull, M. A. (2005). "Fracture Resistance Characterization of Superpave Mixtures Using the Semi-Circular Bending Test," Journal of American Society for Testing and Materials International, Vol. 2, pp. 135-149.
- Zhou, F., Hu, S., and Scullion, T. (2007). "Development and Verification of the Overlay Tester Based Fatigue Cracking Prediction Approach," Technical Research Report FHWA/TX-07/9-1502-01-8, Texas Transportation Institute, College Station, Texas.

Zhou, F., Hu, S., Chen, D., and Scullion, T. (2007). "Overlay Tester: Simple Performance Test for Fatigue Cracking." In Transportation Research Record: Journal of the Transportation Research Board, Transportation Research Board of the National Academics, Washington, D.C., No. 2001, pp. 1-8.

<<http://www.pavementinteractive.org>> (accessed on May 15, 2013).

<<http://www.wjgraves.com>> (accessed on July 18, 2013).

Appendix A - Volumetric Properties and Cracking Test Results

Table A.1 R-SCB test results for SM-12.5A (5.2% asphalt content)

Test #	% of Peak Load	R-SCB Input load (KN)	Time to Crack Failure (min)	Average Time (min)	SCB Load Repetitions to Crack Failure	Average SCB Load Repetitions to crack Failure	Standard Deviation	COV (%)
1	30	0.53	150.93	148.72	90560	89,233	3,636	4.1
2			141.87		85120			
3			153.37		92020			
1	40	0.71	79.48	77.77	47690	46,663	3,292	7.1
2			71.63		42980			
3			82.20		49320			
1	50	0.89	43.30	38.74	25980	23,243	2,382	10.3
2			36.05		21630			
3			36.87		22120			
1	60	1.07	18.30	19.23	10980	11,537	727	6.3
2			20.60		12360			
3			18.78		11270			

Table A.2 R-SCB test results for SM-12.5A (4.9% asphalt content)

Test #	% of Peak Load	R-SCB Input load (KN)	Time to Crack Failure (min)	Average Time (min)	SCB Load Repetitions to Crack Failure	Average SCB Load Repetitions to crack Failure	Standard Deviation	COV (%)
1	30	0.64	82.75	85.73	49650	51,440	2,058	4.0
2			89.48		53690			
3			84.97		50980			
1	40	0.86	41.15	41.81	24690	25,087	3,422	13.6
2			36.47		21880			
3			47.82		28690			
1	50	1.07	18.82	24.53	11290	14,720	3,009	20.4
2			26.58		15950			
3			28.20		16920			
1	60	1.28	14.10	13.74	8460	8,247	997	12.1
2			15.20		9120			
3			11.93		7160			

Table A.3 R-SCB test results for SM-12.5A (4.6% asphalt content)

Test #	% of Peak Load	R-SCB Input load (KN)	Time to Crack Failure (min)	Average Time (min)	SCB Load Repetitions to Crack Failure	Average SCB Load Repetitions to crack Failure	Standard Deviation	COV (%)
1	30	0.46	66.87	64.05	40120	38,430	1,810	4.7
2			60.87		36520			
3			64.42		38650			
1	40	0.62	24.10	24.68	14460	14,807	2,418	16.3
2			28.97		17380			
3			20.97		12580			
1	50	0.77	11.58	14.19	6950	8,513	1,441	16.9
2			16.32		9790			
3			14.67		8800			
1	60	0.92	7.48	7.55	4490	4,530	134	3.0
2			7.37		4420			
3			7.80		4680			

Table A.4 R-SCB test results for SR-12.5A (20% RAP content from first RAP source)

Test #	% of Peak Load	R-SCB Input load (KN)	Time to Crack Failure (min)	Average Time (min)	SCB Load Repetitions to Crack Failure	Average SCB Load Repetitions to crack Failure	Standard Deviation	COV (%)
1	30	0.71	99.25	91.58	59550	54,947	5,301	9.7
2			81.92		49150			
3			93.57		56140			
1	40	0.94	49.27	43.43	29560	26,060	3,704	14.2
2			44.07		26440			
3			36.97		22180			
1	50	1.18	24.82	22.68	14890	13,607	1,118	8.2
2			21.40		12840			
3			21.82		13090			
1	60	1.42	12.08	11.56	7250	6,933	293	4.2
2			11.12		6670			
3			11.47		6880			

Table A.5 R-SCB test results for SR-12.5A (30% RAP content from first RAP source)

Test #	% of Peak Load	R-SCB Input load (KN)	Time to Crack Failure (min)	Average Time (min)	SCB Load Repetitions to Crack Failure	Average SCB Load Repetitions to crack Failure	Standard Deviation	COV (%)
1	30	0.90	78.58	79.22	47150	47,533	1,249	2.6
2			81.55		48930			
3			77.53		46520			
1	40	1.20	42.48	41.55	25490	24,930	901	3.6
2			42.35		25410			
3			39.82		23890			
1	50	1.49	17.65	18.71	10590	11,227	572	5.1
2			19.50		11700			
3			18.98		11390			
1	60	1.79	8.82	8.80	5290	5,280	305	5.8
2			8.28		4970			
3			9.30		5580			

Table A.6 R-SCB test results for SR-12.5A (40% RAP content from first RAP source)

Test #	% of Peak Load	R-SCB Input load (KN)	Time to Crack Failure (min)	Average Time (min)	SCB Load Repetitions to Crack Failure	Average SCB Load Repetitions to crack Failure	Standard Deviation	COV (%)
1	30	1.05	75.20	70.42	45120	42,253	2,980	7.1
2			70.78		42470			
3			65.28		39170			
1	40	1.4	38.50	35.26	23100	21,157	2,541	12.0
2			36.82		22090			
3			30.47		18280			
1	50	1.75	16.48	16.86	9890	10,113	254	2.5
2			17.32		10390			
3			16.77		10060			
1	60	2.1	8.53	7.98	5120	4,787	351	7.3
2			7.37		4420			
3			8.03		4820			

Table A.7 R-SCB test results for SR-12.5A (20% RAP content from second RAP source)

Test #	% of Peak Load	R-SCB Input load (KN)	Time to Crack Failure (min)	Average Time (min)	SCB Load Repetitions to Crack Failure	Average SCB Load Repetitions to crack Failure	Standard Deviation	COV (%)
1	30	0.89	81.68	74.74	49010	44,847	5,801	12.9
2			78.85		47310			
3			63.70		38220			
1	40	1.19	40.97	37.57	24580	22,540	2,744	12.2
2			39.37		23620			
3			32.37		19420			
1	50	1.49	15.17	14.32	9100	8,593	894	10.4
2			15.20		9120			
3			12.60		7560			
1	60	1.78	9.45	8.27	5670	4,960	673	13.6
2			7.22		4330			
3			8.13		4880			

Table A.8 R-SCB test results for SR-12.5A (30% RAP content from second RAP source)

Test #	% of Peak Load	R-SCB Input load (KN)	Time to Crack Failure (min)	Average Time (min)	SCB Load Repetitions to Crack Failure	Average SCB Load Repetitions to crack Failure	Standard Deviation	COV (%)
1	30	0.81	52.33	49.29	31400	29,577	2,010	6.8
2			45.70		27420			
3			49.85		29910			
1	40	1.08	21.13	23.55	12680	14,130	1,349	9.6
2			25.58		15350			
3			23.93		14360			
1	50	1.35	11.48	11.38	6890	6,830	721	10.6
2			12.53		7520			
3			10.13		6080			
1	60	1.62	6.97	6.39	4180	3,837	340	8.9
2			5.83		3500			
3			6.38		3830			

Table A.9 R-SCB test results for SR-12.5A (40% RAP content from second RAP source)

Test #	% of Peak Load	R-SCB Input load (KN)	Time to Crack Failure (min)	Average Time (min)	SCB Load Repetitions to Crack Failure	Average SCB Load Repetitions to crack Failure	Standard Deviation	COV (%)
1	30	1.07	83.97	88.33	50380	52,997	3,045	5.8
2			93.90		56340			
3			87.12		52270			
1	40	1.42	45.20	44.88	27120	26,930	870	3.2
2			46.15		27690			
3			43.30		25980			
1	50	1.78	24.82	27.61	14890	16,567	1,743	10.5
2			30.62		18370			
3			27.40		16440			
1	60	2.13	16.63	14.94	9980	8,963	895	9.9
2			14.37		8620			
3			13.82		8290			

Table A.10 Volumetric properties of R-SCB test specimens (SM-12.5A)

Specimen ID	Asphalt Content (%)	RAP (%)	No of SCB Cycles @ 30% peak load	No of SCB Cycles @ 50% peak load	Air Void (%)	VMA (%)	VFA (%)	Film Thickness (Microns)	Dust Proportion
B-5.2-1	5.2	0	90,560	25,980	7.3	18.3	60.1	10.2	0.87
B-5.2-2	5.2	0	85,120	21,630	7.5	18.5	59.5	10.2	0.87
B-5.2-3	5.2	0	92,020	22,120	7.4	18.2	59.3	10.2	0.88
B-4.9-1	4.9	0	49,650	11,290	7.6	17.4	56.3	8.4	1.73
B-4.9-2	4.9	0	53,690	15,950	7.2	17.5	58.9	8.4	1.74
B-4.9-3	4.9	0	50,980	16,920	7.5	17.1	56.1	8.4	1.74
B-4.6-1	4.6	0	40,120	6,950	7.1	16.4	56.7	7.5	1.42
B-4.6-2	4.6	0	36,520	9,790	7.3	16.2	54.9	7.5	1.42
B-4.6-3	4.6	0	38,650	8,800	7.3	16.3	55.2	7.5	1.42

Table A.11 Volumetric properties of R-SCB test specimens (SR-12.5A, first source of RAP)

Specimen ID	Asphalt Content (%)	RAP (%)	No of SCB Cycles @ 30% peak load	No of SCB Cycles @ 50% peak load	Air Void (%)	VMA (%)	VFA (%)	Film Thickness (Microns)	Dust Proportion
B-20-1	4.7	20	59,550	14,890	7.2	17.1	57.9	7.7	1.32
B-20-2	4.7	20	49,150	12,840	7.2	17.4	58.6	7.7	1.32
B-20-3	4.7	20	56,140	13,090	7.3	17.2	57.6	7.7	1.32
B-30-1	4.8	30	47,150	10,590	7.4	16.4	54.9	6.9	1.59
B-30-2	4.8	30	48,930	11,700	7.6	16.4	53.7	6.9	1.59
B-30-3	4.8	30	46,520	11,390	7.5	16.3	54.0	6.9	1.59
B-40-1	4.3	40	45,120	9,890	7.3	15.7	53.5	6.1	1.84
B-40-2	4.3	40	42,470	10,390	7.5	15.8	52.5	6.1	1.84
B-40-3	4.3	40	39,170	10,060	7.6	15.8	51.9	6.1	1.84

Table A.12 Volumetric properties of R-SCB test specimens (SR-12.5A, second source of RAP)

Specimen ID	Asphalt Content (%)	RAP (%)	No of SCB Cycles @ 30% peak load	No of SCB Cycles @ 50% peak load	Air Void (%)	VMA (%)	VFA (%)	Film Thickness (Microns)	Dust Proportion
B-20'-1	4.3	20	49,010	9,100	7.2	16.3	55.8	6.7	1.81
B-20'-2	4.3	20	47,310	9,120	7.2	16.3	55.8	6.7	1.81
B-20'-3	4.3	20	40,120	7,560	7.4	16.5	55.2	6.7	1.81
B-30'-1	4.4	30	31,400	6,890	7.6	15.9	52.2	5.9	1.88
B-30'-2	4.4	30	27,420	7,520	7.5	15.8	52.5	5.9	1.88
B-30'-3	4.4	30	29,910	6,080	7.2	15.7	54.1	5.9	1.88
B-40'-1	4.1	40	50,380	14,890	7.3	15.3	52.3	6.5	1.92
B-40'-2	4.1	40	56,340	18,370	7.1	15.3	53.6	6.5	1.92
B-40'-3	4.1	40	52,270	16,440	7.1	15.2	53.3	6.5	1.92

Table A.13 OT test results for SM-12.5A

Asphalt Content (%)	Air Void (%)	Initial Peak Load (KN)	Average Initial Peak Load (KN)	No. of OT Cycles of Failure (N _{OT})	Average No. of OT Cycles of Failure (N _{OT})	Duration (Minutes)	Standard Deviation	COV (%)
5.2	7.3	1.965	1.973	1000	1,000	167	0	0.0
	7.4	1.886		1000				
	7.2	2.068		1000				
4.9	7.3	2.799	2.90	667	720	120	62	8.7
	7.3	2.987		705				
	7.2	2.903		789				
4.6	7.4	3.432	3.28	335	380	63	39	10.4
	7.3	3.219		409				
	7.4	3.186		397				

Table A.14 Volumetric properties of OT test specimens (SM-12.5A)

Specimen ID	Asphalt Content (%)	RAP (%)	No of OT Cycles	Air Void (%)	VMA (%)	VFA (%)	Film Thickness (Microns)	Dust Proportion
A-5.2-1	5.2	0	1,000	7.3	18.4	60.3	10.5	0.84
A-5.2-2	5.2	0	1,000	7.4	18.1	59.1	10.5	0.84
A-5.2-3	5.2	0	1,000	7.2	18.3	60.7	10.5	0.84
A-4.9-1	4.9	0	667	7.3	17.1	57.3	7.9	1.69
A-4.9-2	4.9	0	705	7.3	17.4	58.0	7.9	1.69
A-4.9-3	4.9	0	789	7.2	17.3	58.4	7.9	1.69
A-4.6-1	4.6	0	335	7.4	16.3	54.6	6.9	1.40
A-4.6-2	4.6	0	409	7.3	16.5	55.8	6.9	1.40
A-4.6-3	4.6	0	397	7.4	16.5	55.2	6.9	1.40

Table A.15 OT test results for SR-12.5A (first source of RAP)

RAP Content (%)	Air Void (%)	Initial Peak Load (KN)	Average Initial Peak Load (KN)	No. of OT Cycles of Failure (N_{OT})	Average No. of OT Cycles of Failure (N_{OT})	Duration (Minutes)	Standard Deviation	COV (%)
20	7.2	2.341	2.35	956	805	134	139	17.3
	7.3	2.418		778				
	7.0	2.296		680				
30	7.3	2.799	2.90	348	477	80	116	24.5
	7.4	2.987		576				
	7.2	2.903		507				
40	7.3	3.432	3.28	91	128	21	34	26.9
	7.1	3.219		134				
	7.0	3.186		159				

Table A.16 Volumetric properties of OT test specimens (SR-12.5A, first source of RAP)

Specimen ID	Asphalt Content (%)	RAP (%)	No of OT Cycles	Air Void (%)	VMA (%)	VFA (%)	Film Thickness (Microns)	Dust Proportion
A-20-1	4.7	20	956	7.2	16.9	57.4	8.4	1.28
A-20-2	4.7	20	778	7.3	16.9	56.8	8.4	1.28
A-20-3	4.7	20	680	7.0	16.8	58.3	8.4	1.28
A-30-1	4.8	30	348	7.3	16.1	54.7	7.7	1.52
A-30-2	4.8	30	576	7.4	16.1	54.0	7.7	1.52
A-30-3	4.8	30	507	7.2	16.2	55.6	7.7	1.52
A-40-1	4.3	40	91	7.3	15.4	52.6	6.1	1.79
A-40-2	4.3	40	134	7.1	15.4	53.9	6.1	1.79
A-40-3	4.3	40	159	7.0	15.4	54.5	6.1	1.79

Table A.17 OT test results for SR-12.5A (second source of RAP)

RAP Content (%)	Air Void (%)	Initial Peak Load (KN)	Average Initial Peak Load (KN)	No. of OT Cycles of Failure (N _{OT})	Average No. of OT Cycles of Failure (N _{OT})	Duration (Minutes)	Standard Deviation	COV (%)
20	7.3	2.615	2.66	236	296	49	74	25.2
	7.1	2.769		380				
	7.0	2.599		273				
30	7.2	1.917	2.10	54	71	12	16	22.7
	7.4	2.069		72				
	7.3	2.318		86				
40	7.2	2.989	3.09	372	435	73	65	14.9
	7.0	3.098		432				
	7.1	3.185		502				

Table A.18 Volumetric properties of OT test specimens (SR-12.5A, second source of RAP)

Specimen ID	Asphalt Content (%)	RAP (%)	No of OT Cycles	Air Void (%)	VMA (%)	VFA (%)	Film Thickness (Microns)	Dust Proportion
A-20'-1	4.3	20	236	7.3	16.0	54.4	6.9	1.76
A-20'-2	4.3	20	380	7.1	16.1	55.9	6.9	1.76
A-20'-3	4.3	20	273	7.0	16.1	56.5	6.9	1.76
A-30'-1	4.4	30	54	7.2	15.5	53.5	5.8	1.82
A-30'-2	4.4	30	72	7.4	15.4	51.9	5.8	1.82
A-30'-3	4.4	30	106	7.3	15.4	52.6	5.8	1.82
A-40'-1	4.1	40	372	7.2	15.4	53.2	6.8	1.89
A-40'-2	4.1	40	432	7.0	15.4	54.5	6.8	1.89
A-40'-3	4.1	40	502	7.1	15.3	53.6	6.8	1.89

Table A.19 Tukey's multiple comparison of R-SCB test results

Differences of Least Squares Means											
Trt	Trt	Estimate	Standard Error	DF	t Value	Pr > t	Adjustment	Adj P	Alpha	Lower	Upper
0_0_4.6	0_0_4.9	-6206.67	1300.12	18	-4.77	0.0002	Tukey	0.0037	0.05	-8938.11	-3475.22
0_0_4.6	0_0_5.2	-14730	1300.12	18	-11.33	<.0001	Tukey	<.0001	0.05	-17461	-11999
0_0_4.6	1_20_4.7	-5093.33	1300.12	18	-3.92	0.0010	Tukey	0.0219	0.05	-7824.78	-2361.89
0_0_4.6	1_30_4.8	-2713.33	1300.12	18	-2.09	0.0514	Tukey	0.5099	0.05	-5444.78	18.1127
0_0_4.6	1_40_4.3	-1600.00	1300.12	18	-1.23	0.2343	Tukey	0.9386	0.05	-4331.45	1131.45
0_0_4.6	2_20_4.3	-80.0000	1300.12	18	-0.06	0.9516	Tukey	1.0000	0.05	-2811.45	2651.45
0_0_4.6	2_30_4.4	1683.33	1300.12	18	1.29	0.2118	Tukey	0.9204	0.05	-1048.11	4414.78
0_0_4.6	2_40_4.1	-8053.33	1300.12	18	-6.19	<.0001	Tukey	0.0002	0.05	-10785	-5321.89
0_0_4.9	0_0_5.2	-8523.33	1300.12	18	-6.56	<.0001	Tukey	0.0001	0.05	-11255	-5791.89
0_0_4.9	1_20_4.7	1113.33	1300.12	18	0.86	0.4031	Tukey	0.9928	0.05	-1618.11	3844.78
0_0_4.9	1_30_4.8	3493.33	1300.12	18	2.69	0.0151	Tukey	0.2195	0.05	761.89	6224.78
0_0_4.9	1_40_4.3	4606.67	1300.12	18	3.54	0.0023	Tukey	0.0463	0.05	1875.22	7338.11
0_0_4.9	2_20_4.3	6126.67	1300.12	18	4.71	0.0002	Tukey	0.0043	0.05	3395.22	8858.11
0_0_4.9	2_30_4.4	7890.00	1300.12	18	6.07	<.0001	Tukey	0.0003	0.05	5158.55	10621
0_0_4.9	2_40_4.1	-1846.67	1300.12	18	-1.42	0.1726	Tukey	0.8758	0.05	-4578.11	884.78
0_0_5.2	1_20_4.7	9636.67	1300.12	18	7.41	<.0001	Tukey	<.0001	0.05	6905.22	12368
0_0_5.2	1_30_4.8	12017	1300.12	18	9.24	<.0001	Tukey	<.0001	0.05	9285.22	14748
0_0_5.2	1_40_4.3	13130	1300.12	18	10.10	<.0001	Tukey	<.0001	0.05	10399	15861
0_0_5.2	2_20_4.3	14650	1300.12	18	11.27	<.0001	Tukey	<.0001	0.05	11919	17381
0_0_5.2	2_30_4.4	16413	1300.12	18	12.62	<.0001	Tukey	<.0001	0.05	13682	19145
0_0_5.2	2_40_4.1	6676.67	1300.12	18	5.14	<.0001	Tukey	0.0018	0.05	3945.22	9408.11
1_20_4.7	1_30_4.8	2380.00	1300.12	18	1.83	0.0838	Tukey	0.6637	0.05	-351.45	5111.45
1_20_4.7	1_40_4.3	3493.33	1300.12	18	2.69	0.0151	Tukey	0.2195	0.05	761.89	6224.78
1_20_4.7	2_20_4.3	5013.33	1300.12	18	3.86	0.0012	Tukey	0.0248	0.05	2281.89	7744.78
1_20_4.7	2_30_4.4	6776.67	1300.12	18	5.21	<.0001	Tukey	0.0015	0.05	4045.22	9508.11
1_20_4.7	2_40_4.1	-2960.00	1300.12	18	-2.28	0.0352	Tukey	0.4029	0.05	-5691.45	-228.55
1_30_4.8	1_40_4.3	1113.33	1300.12	18	0.86	0.4031	Tukey	0.9928	0.05	-1618.11	3844.78
1_30_4.8	2_20_4.3	2633.33	1300.12	18	2.03	0.0579	Tukey	0.5465	0.05	-98.1127	5364.78
1_30_4.8	2_30_4.4	4396.67	1300.12	18	3.38	0.0033	Tukey	0.0634	0.05	1665.22	7128.11
1_30_4.8	2_40_4.1	-5340.00	1300.12	18	-4.11	0.0007	Tukey	0.0149	0.05	-8071.45	-2608.55
1_40_4.3	2_20_4.3	1520.00	1300.12	18	1.17	0.2576	Tukey	0.9534	0.05	-1211.45	4251.45
1_40_4.3	2_30_4.4	3283.33	1300.12	18	2.53	0.0212	Tukey	0.2828	0.05	551.89	6014.78

Differences of Least Squares Means											
Trt	Trt	Estimate	Standard Error	DF	t Value	Pr > t	Adjustment	Adj P	Alpha	Lower	Upper
1_40_4.3	2_40_4.1	-6453.33	1300.12	18	-4.96	0.0001	Tukey	0.0025	0.05	-9184.78	-3721.89
2_20_4.3	2_30_4.4	1763.33	1300.12	18	1.36	0.1918	Tukey	0.9000	0.05	-968.11	4494.78
2_20_4.3	2_40_4.1	-7973.33	1300.12	18	-6.13	<.0001	Tukey	0.0002	0.05	-10705	-5241.89
2_30_4.4	2_40_4.1	-9736.67	1300.12	18	-7.49	<.0001	Tukey	<.0001	0.05	-12468	-7005.22

Table A.20 Bonferroni's pairwise comparison of R-SCB test results

Estimates					
Label	Estimate	Standard Error	DF	t Value	Pr > t
Virgin Aggregate: 5.2% Asphalt vs. 4.9% Asphalt	-6206.67	1300.12	18	-4.77	0.0002
Virgin Aggregate: 5.2% Asphalt vs. 4.6% Asphalt	-14730	1300.12	18	-11.33	<.0001
Virgin Aggregate: 4.9% Asphalt vs. 4.6% Asphalt	-8523.33	1300.12	18	-6.56	<.0001
RAP Source #1: 20% RAP & 4.7% Asphalt vs. 30% RAP & 4.8% Asphalt	2380.00	1300.12	18	1.83	0.0838
RAP Source #1: 20% RAP & 4.7% Asphalt vs. 40% RAP & 4.3% Asphalt	3493.33	1300.12	18	2.69	0.0151
RAP Source #1: 30% RAP & 4.8% Asphalt vs. 40% RAP & 4.3% Asphalt	1113.33	1300.12	18	0.86	0.4031
RAP Source #2: 20% RAP & 4.3% Asphalt vs. 30% RAP & 4.4% Asphalt	1763.33	1300.12	18	1.36	0.1918
RAP Source #2: 20% RAP & 4.3% Asphalt vs. 40% RAP & 4.1% Asphalt	-7973.33	1300.12	18	-6.13	<.0001
RAP Source #2: 30% RAP & 4.4% Asphalt vs. 40% RAP & 4.1% Asphalt	-9736.67	1300.12	18	-7.49	<.0001

Table A.21 Tukey's multiple comparison of OT test results

Differences of Least Squares Means											
Trt	Trt	Estimate	Standard Error	DF	t Value	Pr > t	Adjustment	Adj P	Alpha	Lower	Upper
0_0_4.6	0_0_4.9	-340.00	64.8260	16	-5.24	<.0001	Tukey	0.0016	0.05	-477.43	-202.57
0_0_4.6	1_20_4.7	-424.33	64.8260	16	-6.55	<.0001	Tukey	0.0001	0.05	-561.76	-286.91
0_0_4.6	1_30_4.8	-96.6667	64.8260	16	-1.49	0.1554	Tukey	0.8014	0.05	-234.09	40.7584
0_0_4.6	1_40_4.3	252.33	64.8260	16	3.89	0.0013	Tukey	0.0220	0.05	114.91	389.76
0_0_4.6	2_20_4.3	84.0000	64.8260	16	1.30	0.2134	Tukey	0.8877	0.05	-53.4251	221.43
0_0_4.6	2_30_4.4	303.00	64.8260	16	4.67	0.0003	Tukey	0.0048	0.05	165.57	440.43
0_0_4.6	2_40_4.1	-55.0000	64.8260	16	-0.85	0.4087	Tukey	0.9869	0.05	-192.43	82.4251
0_0_4.9	1_20_4.7	-84.3333	64.8260	16	-1.30	0.2117	Tukey	0.8858	0.05	-221.76	53.0918
0_0_4.9	1_30_4.8	243.33	64.8260	16	3.75	0.0017	Tukey	0.0288	0.05	105.91	380.76
0_0_4.9	1_40_4.3	592.33	64.8260	16	9.14	<.0001	Tukey	<.0001	0.05	454.91	729.76
0_0_4.9	2_20_4.3	424.00	64.8260	16	6.54	<.0001	Tukey	0.0001	0.05	286.57	561.43
0_0_4.9	2_30_4.4	643.00	64.8260	16	9.92	<.0001	Tukey	<.0001	0.05	505.57	780.43
0_0_4.9	2_40_4.1	285.00	64.8260	16	4.40	0.0005	Tukey	0.0083	0.05	147.57	422.43
1_20_4.7	1_30_4.8	327.67	64.8260	16	5.05	0.0001	Tukey	0.0023	0.05	190.24	465.09
1_20_4.7	1_40_4.3	676.67	64.8260	16	10.44	<.0001	Tukey	<.0001	0.05	539.24	814.09
1_20_4.7	2_20_4.3	508.33	64.8260	16	7.84	<.0001	Tukey	<.0001	0.05	370.91	645.76
1_20_4.7	2_30_4.4	727.33	64.8260	16	11.22	<.0001	Tukey	<.0001	0.05	589.91	864.76
1_20_4.7	2_40_4.1	369.33	64.8260	16	5.70	<.0001	Tukey	0.0007	0.05	231.91	506.76
1_30_4.8	1_40_4.3	349.00	64.8260	16	5.38	<.0001	Tukey	0.0012	0.05	211.57	486.43
1_30_4.8	2_20_4.3	180.67	64.8260	16	2.79	0.0132	Tukey	0.1664	0.05	43.2416	318.09
1_30_4.8	2_30_4.4	399.67	64.8260	16	6.17	<.0001	Tukey	0.0003	0.05	262.24	537.09
1_30_4.8	2_40_4.1	41.6667	64.8260	16	0.64	0.5295	Tukey	0.9975	0.05	-95.7584	179.09
1_40_4.3	2_20_4.3	-168.33	64.8260	16	-2.60	0.0195	Tukey	0.2261	0.05	-305.76	-30.9082
1_40_4.3	2_30_4.4	50.6667	64.8260	16	0.78	0.4459	Tukey	0.9918	0.05	-86.7584	188.09
1_40_4.3	2_40_4.1	-307.33	64.8260	16	-4.74	0.0002	Tukey	0.0042	0.05	-444.76	-169.91
2_20_4.3	2_30_4.4	219.00	64.8260	16	3.38	0.0038	Tukey	0.0585	0.05	81.5749	356.43
2_20_4.3	2_40_4.1	-139.00	64.8260	16	-2.14	0.0477	Tukey	0.4299	0.05	-276.43	-1.5749
2_30_4.4	2_40_4.1	-358.00	64.8260	16	-5.52	<.0001	Tukey	0.0009	0.05	-495.43	-220.57

Table A.22 Bonferroni's pairwise comparison of OT test results

Estimates					
Label	Estimate	Standard Error	DF	t Value	Pr > t
Virgin Aggregate: 4.9% Asphalt vs. 4.6% Asphalt	-340.00	64.8260	16	-5.24	<.0001
RAP Source #1: 20% RAP & 4.7% Asphalt vs. 30% RAP & 4.8% Asphalt	327.67	64.8260	16	5.05	0.0001
RAP Source #1: 20% RAP & 4.7% Asphalt vs. 40% RAP & 4.3% Asphalt	676.67	64.8260	16	10.44	<.0001
RAP Source #1: 30% RAP & 4.8% Asphalt vs. 40% RAP & 4.3% Asphalt	349.00	64.8260	16	5.38	<.0001
RAP Source #2: 20% RAP & 4.3% Asphalt vs. 30% RAP & 4.4% Asphalt	219.00	64.8260	16	3.38	0.0038
RAP Source #2: 20% RAP & 4.3% Asphalt vs. 40% RAP & 4.1% Asphalt	-139.00	64.8260	16	-2.14	0.0477
RAP Source #2: 30% RAP & 4.4% Asphalt vs. 40% RAP & 4.1% Asphalt	-358.00	64.8260	16	-5.52	<.0001